Janus-head ligands
in heterobimetallic
complexes

Dissertation zur Erlangung des
mathematisch-naturwissenschaftlichen Doktorgrades
"Doctor rerum naturalium"
der Georg-August-Universität Göttingen

vorgelegt von
Dipl.-Chem. Christian Kling
aus Hannover

Göttingen 2010

D7

Referent: Prof. Dr. Dietmar Stalke

Korreferent: Prof. Dr. George M. Sheldrick

Tag der Mündlichen Prüfung: 29.09.2010

Die vorliegende Arbeit wurde in der Zeit von Januar 2007 bis August 2010 am Institut für Anorganische Chemie der Georg-August-Universität zu Göttingen unter der Leitung von Prof. Dr. Dietmar Stalke angefertigt.

Contents

Chapter I   Introduction

Chapter II   Noval metal complex of di(*2*-pyridyl)amide

Chapter V   **Iron complexes of di(*2*-benzothiazolyl)phosphane**

Chapter VI   **Hetreobimetallic complexes of di(*2*-benzothiazolyl)phosphane**

Chapter VII — Crystallographic section

Chapter VIII Conclusion and Outlook

1 Introduction

Among the current main targets in inorganic chemical research are synthesis and stabilization of unusual metal oxidation states, coordination in general, and the mimicry of biological relevant metal centers. Metal organic compounds are usually used as auxiliaries or reagents in organic chemistry, while modern inorganic chemistry mainly focuses on the metal core of the employed complexes in order to gain insights into catalytic properties, fine tuning thereof, and catalytic mechanisms. Due to the identification of heterobimetallic active centers and observation of cooperative effects, formation and structure determination of natural active centers and heterobimetallic complexes gained increasing attention. Thus, ligand design became an important field of research aiming on the development of efficient, profitable, and sustainable catalysts for chemical transformations.

1.1 Historical backround

Catalysis derives from the greek verb καταλυειν (katàlyein) meaning "to untie", "to annul" or "to pick up". The oldest evidence of human benefits in catalysis goes back to the Sumerian from Mesopotamia at 6000 B.C. turning sugar into alcohol by fermentation. One of the first processes preparing an important bulk chemical is the lead chamber process to prepare sulfuric acid. It is originally known from the medieval times, but in 1748 *John Roebuck* introduced this process to industry in Birmingham/England setting a basis for the industrial revolution.[1] Sulfuric acid is still one of the most important bulk chemicals. A nations sulfuric acid production is still a good indicator for its industrial strength.[2] Most of it is used to produce fertilizers directly as ammonium sulfate or indirectly in the production of phosphoric acid. By now the way of producing sulfuric acid was supplanted by the contact process, but the lead chamber process is still used in fuel gas cleaning and the desulphurisation of CO_2 for final storage. Another commercially very successful early use of catalysis is the lighter/lamp by *Johann Wolfgang Döbereiner* using the reaction of hydrogen gas on a platinum sponge.[3,4]
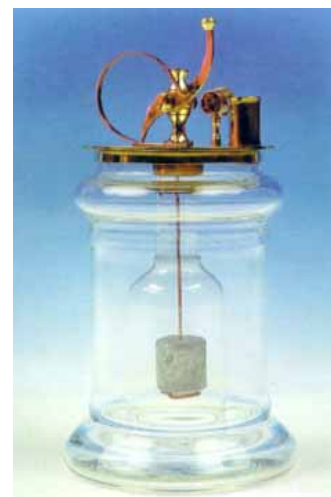
Figure 1: *Döbereiner* lamp.

In 1835 *Jöns Jakob Berzelius* recognized the need of another reagent beside the reactants in a catalyzed reaction. The modern definition of catalysis is from *Wilhelm Ostwald:*

> „*Ein Katalysator ist ein Stoff, der die Geschwindigkeit einer chemischen Reaktion erhöht, ohne selbst dabei verbraucht zu werden und ohne die endgültige Lage des thermodynamischen Gleichgewichts dieser Reaktion zu verändern.*"[5]
>
> *(in english: a catalyst is a compound accelerating a chemical reaction without being consumed and not changing the thermodynamical equilibrium of the reaction)*

Honoring his work *Ostwald* was awarded with the Nobelprize in chemistry in 1909. Table 1 shows a list of all Nobelprizewinners in the field of catalysis, ascribing the importance of this research area during all decades.

Table 1: List of Nobel-prize-winners in the field of catalysis.

Year	Laureate	Rationale
1909	Wilhelm Ostwald	"[for] his work on catalysis and for his investigations into the fundamental principles governing chemical equilibria and rates of reaction"
1912	Paul Sabatier	"for his method of hydrogenating organic compounds in the presence of finely disintegrated metals"
1918	Fritz Haber	"for the synthesis of ammonia from its elements"
1932	Irving Langmuir	"for his discoveries and investigations in surface chemistry"
1946	James Bachteller Sumner	"for his discovery that enzymes can be crystallized"
1963	Karl Ziegler, Giulio Natta	"for their discoveries in the field of the chemistry and technology of high polymers"
1975	John W. Cornforth	"for his work on the stereochemistry of enzyme-catalyzed reactions"
2001	William S. Knowles, Ryoji Noyori	"for their work on chirally catalysed hydrogenation reactions"
	Barry Sharpless	"for his work on chirally catalysed oxidation reactions"
2005	Yves Chauvin, Robert Grubbs, Richard R. Schrock	"for the development of the metathesis method in organic synthesis"
2007	Gerhard Ertl	"for his studies of chemical processes on solid surfaces"

1.2 Status quo

For the modern society catalysis gained ecological and economical significance and for the value creation chain of the chemical industry. Beside the production and distribution of catalysts their optimization towards energy and resource input gained significant economical importance. Looking exemplarily at the production of ammonia, this becomes self-evident:

Ammonia as a bulk chemical is the main source for most nitrogen containing chemical products, such as urea-resin and fertilizers. Since the nutrition of the world population mainly depends on based fertilizers, 83 % of ammonia are converted to these, mainly to urea or ammonium-nitrate, -phosphate and -sulfate. To achieve the conversion from the elements to ammonia according to the *Haber-Bosch* process more than 1 % of man-made energy is consumed.[6] Economical and ecological impacts on the world energy budget can easily be derived even by little optimizations within these necessary processes.

In more than 85 % of all synthesized chemical products at least one catalyzed step is presumed. Thus green chemistry became one of the buzz words underlining the public perception of modern chemistry. To achieve these expectations catalysis is inalienable.

1.3 Differentiation in catalysis

1.3.1 Heterogeneous catalysis

The exhaust gas after treatment of a modern car is probably the best known heterogeneous catalyst.[7] Technically, it is the oldest and simultaneously quantitatively and on a turnover basis most important form of industrial catalysis. By definition, the reactant and the catalyst are in different phases. In most cases the catalyst is a solid and the reactant liquid or gaseous. The reaction takes place on the surfaces of the catalyst. Control of interactions on the surface and fine-tuning of these are hardly possible. The advantages of this form are the straight forward separation of the catalyst from the product, the thermal stability and the low costs.

1.3.2 Homogenous catalysis

In a strict sense, homogenous catalysis is the oldest form, since all acid- and enzyme-catalyzed reactions are included within this definition. The habitual language use usually considers reactions at metal complexes. Due to the ligand-metal contact

direct influence on the catalytically active centre is possible. It is possible to transfer stereochemical information from the ligand to the desired product within the catalysis cycle. This makes the homogenous catalysis a very powerful tool, especially in the production of fine chemicals and pharmaceuticals. Tailoring new ligands and tuning their characteristics in obeying oligomerization, stabilizing unusual oxidation states as well as metal complexes with defined coordination number, geometry, solubility and reactivity is one of the main research topics.[8] A major disadvantage of the homogenous catalysis it the often complicated removal of the catalyst in order to obtain pure product.[9]

1.3.3 Design and request on ligands

Metal atoms are linked to the ligand by a dative bond; therefore the ligand is an electron-pair donator. Water, ammonia or phosphanes are elementary ligands, providing a lone pair to donate in an unoccupied coordination site of the metal atom. All these basic ligands do not show any steric demand or information. Modifications towards alcohols, asymmetric ethers, or sterically demanding amines or phosphanes are literature-known and have a huge influence on the resulting metal complex. Through the eyes of a chemist the arrangement of multiple donor atoms in one single ligand is favorable. Entropic effects make these ligands preferable due to higher turnover and stability. The term chelate was first applied in 1920 by *Sir Morgan* and *Mr. Drew*, who stated:

> *"The adjective chelate, derived from the great claw or chele (Greek: χηλη) of the lobster or other crustaceans, is suggested for the caliper like groups which function as two associating units and fasten to the central atom so as to produce heterocyclic rings."[10]*

Putting up on this effect, many multi-dentate ligands and metal complexes thereof have been prepared and analyzed over the last few decades. All these ligands have a bridge between the donor atoms in common. Modifying this bridge in length, kind, and flexibility opens up a wide range to new ligands and is a great toolbox for fine tuning within a given metal-donor system:

- *Length*: depending on the length of the bridge selectivity towards the metal atom occurs. Famous examples for this are crown ethers and cryptands.
- *Steric demand*: adequate groups can stabilize e.g. internal metal-metal bonds and protect them from unintended reaction.[11]

- *Chiral information*: appropriate residues within the bridge or asymmetric substitution can transfer their information to the product or provide an substrate specificity useful in chiral resolution.

- *Solubility*: by hydrophobic respectively hydrophilic residues to the bridge the solubility in a given solvent can be adjusted or neglected. This is very useful for the recovery of the catalyst.

By combining different hetero atoms within one ligand chelating the same metal atom different metal-ligand bonds are formed. Differences in the strength of the bond can be forecasted by the HSAB concept by *Pearson*. Such ligands are also called hemilabile or hybrid ligands. The name was originally for (P,N)- and (P,O)-ligands used by *Rauchfuss et al.*, but the phenomenon was reported before by *Braunstein et al.*, who later on extended the idea to binuclear systems.[12-15]

Due to the different metal-ligand bonds the weaker bond can be cleaved while the other bond stays unaffected. This plays an important role within the catalytical cycle, since now the catalyst is activated and able to bind the substrate (see Scheme 1). Meanwhile the ligand stays fixed to the metal atom and its information is transferred. After transformation of the substrate in the catalytical cycle the product is released by a reductive elimination. This step is promoted by the free intramolecular coordination site for entropic reasons and due to pre-organization resulting in a quicker and more efficient catalysis.
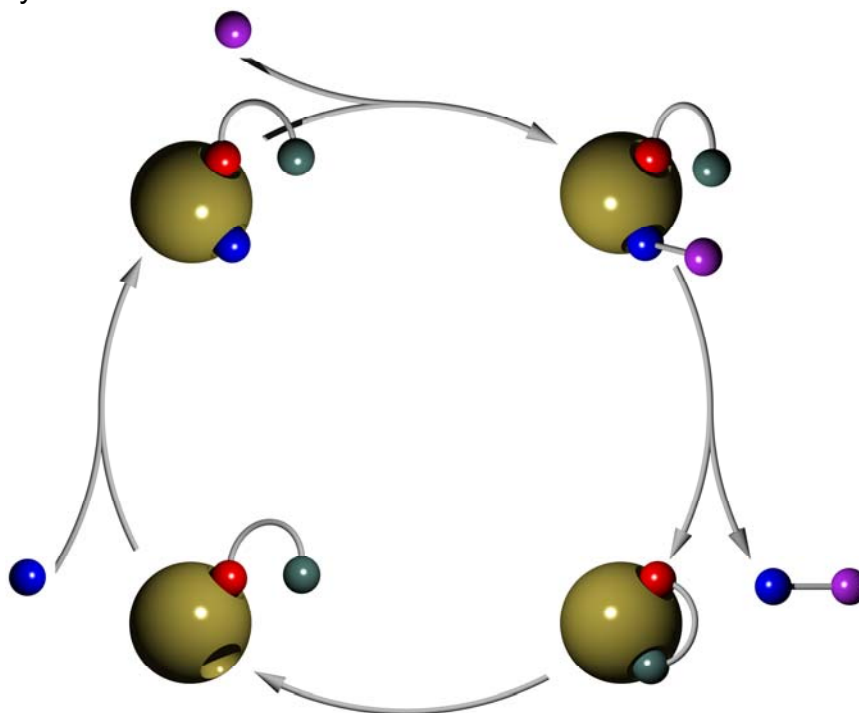
Scheme 1: hemilable ligand within the catalysis cycle.

One of the widest used hemilabile ligand is a nickelphosphane-complex in the *Shell Higher Olefin Process* (SHOP).[16] It produces higher linear olefins *via* ethene oligomerization and olefin metathesis.
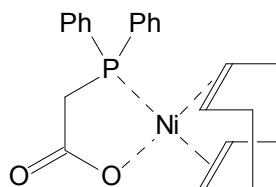
Scheme 2: common industrial metal complexes in the SHOP-process.

In the past heteroaromatics as shown in Scheme 3 were widely used in coordination and bioinorganic chemistry. The electronic and steric properties enabled these ligands to coordinate many metals, but their fixed geometry kept them inflexible.
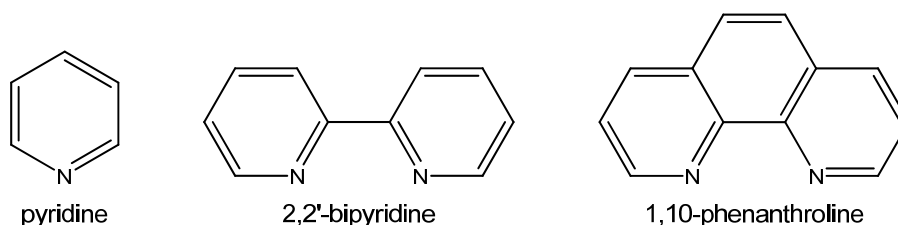
Scheme 3: Nitrogen based heteroaromatics.

Either by bridging heteroaromatic rings or by centralizing the heteroaromatic ring this problem is avoided. Since the end of the last century pincer ligands came to the fore. Usually these kind of ligands consist of a central heteroaromatic five- or six-membered ring substituted in 2,5- respectively 2,6-position. The side chains contain further donor atoms like nitrogen or phosphorous and are commonly bilaterally equal. Scheme 4 shows the typical layout of pincer ligands.

X_1= C, N, O, S, ... X_2= NR_2, PR_3, OR, SR, ...   n= 0,1, 2, ...
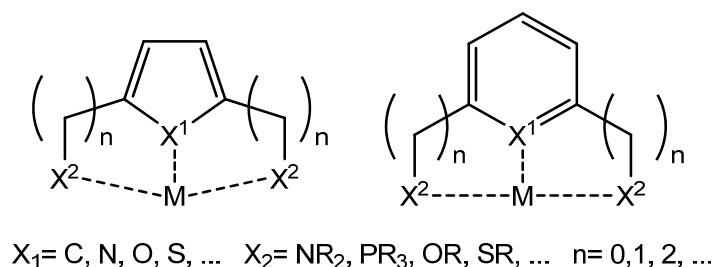
Scheme 4: typical layout of pincer ligands.

These ligands are abbreviated by three letters, with the first and last letter pointing out the donor atom of the side chain while the middle one points out the heteroatom

of the central aromatic. Following this nomenclature bis(diphenylphosphano)pyridine is a so called PNP-ligand. Pincer ligands show wide use in modern organic reactions, such as *Heck* reactions,[17,18] *Suzuki-Miyaura* Couplings,[19] dehydrogenation of alkanes,[20,21] hydrogen transfer,[22] aldolic condensations[23,24] or asymmetric allylic alkylation.[19]

1.3.4 Bimetallic complexes

Exploring and comparing different catalytic cycles shows the applied metal complex is indeed a precursor to the catalytically active side. A co-catalyst is often needed to influence the activity and selectivity in a positive way. Examples are methylaluminoxane (MAO) in the olefin polymerization and hydroiodic acid in the *Monsanto* process.

Di(cyclopentadienyl)dimethyl zirconium and trimethylaluminium each on its own or as a mixture show no or only very poor catalytic activity in polymerization reactions of olefins. Hydrolyzing the trimethylaluminium to the well established MAO in advance[25-32] turns the mixture to a very active species.[26,33]

Even though there is neither a defined formula nor structure of MAO, the huge effort in research within this field is not astonishing.[26-31]

Therefore modern bimetallic catalysts only take a fractional amount of MAO.[31,34]

One has to discriminate intermolecular and intramolecular bimetallic interactions. The first always requires a well defined mixture of at least two different metal complexes to form the catalytically active heterobimetallic species with one metal activating the electrophile, the other activating the nucleophile. When using an intramolecular heterobimetallic complex these features are combined in just one single complex.[31,35-37]

Beside olefin polymerization there are many reactions catalyzed by at least two metal atoms known, such as CO insertion by rhodium/iron complexes and the activation of carbon-halide bonds.[38,39] Examples of for the presence of two metal atoms in the active center are well known in biological systems, too. Instances for this are the carbon monoxide dehydrogenase/Acetyl-CoA synthetases,[40-42] purple acid phosphatases[43]and superoxide dismutases.[44]

1.3.5 Designing a new ligand for heterobimetallic complexes

There are two different ways of designing a ligand for heterobimetallic complexes. On the one hand it is possible to link a coordinated metal to a second metal fragment by bridging atom such as oxygen.[45] On the other hand an adapted ligand can connect two different metal atoms with a defined geometry. This leads to the idea of the *Janus-head* ligands. In Roman mythology, *Janus* (or *Ianus*) was the god of gates, doors, doorways, beginnings and endings. He is most often depicted as having two faces or heads, facing in opposite directions. These heads

Figure 2: Bust of *Janus*

were rumored to look both into the future and the past. This idea of a two-faced ligand can be found in different approaches. One possibility is the linkage of donor sides to a given backbone.[46] The idea is very prominent in electron-transfer studies.[47-49] Another approach are di(pyridyl)phosphanes acting as *N,N-* or *N,P-* chelating ligand or even as an exclusive P-donating ligand.[50,51] More flexibility can be achieved by exchange pyridyl- with picolyl-residues. Thus the ligand not only gains flexibility but also a new donorside by deprotonating the methylenbridge.[52-55] Another approach is a linkage of donorsides to a given back bone.[46] Different approaches to achieve a *Janus-head* ligand from the *Stalke* workgroup are shown in Scheme 5.
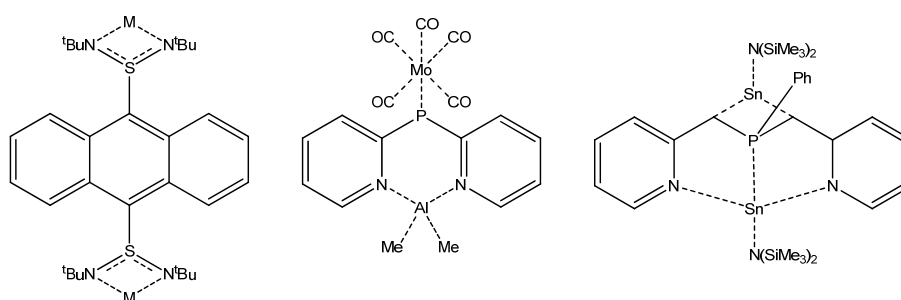
Scheme 5: aproaches to *Janus*-head ligands by the *Stalke* group

Inspired by the pyridine- and picoline-based ligands *Stey* developed a new ligand using benzothiazole as hetereoaromatic.[56-58] Benzothiazole is a more stable and cheaper derivative of thiazole and has an additional sulfur atom to the pyridine-like nitrogen atom. It is an electron-rich heteroaromatic with π-electron excess mainly located at the nitrogen atom. The two heteroaromatics are linked by a divalent phosphorous atom. The resulting ligand has up to eight lone pairs available for

coordination of a metal fragment. Due to its diverse hetero-atoms and the free rotation within the P-C bond it procures coordination sides in many different hardness and geometry grades. It can act as an *N,N-*, *N,P-*, *N,S-*, *S,P-* or only *P*-donor. Additionally a haptotropic coordination is possible.

Stey showed the potential of the ligand in mono-metal complexes with lithium, aluminum, caesium, zinc, cadmium, tin and iron. Bimetallic examples with tungsten as well as a heterobimetallic one with molybdenum and lithium were shown in addition. All examples were characterized structurally by X-ray diffraction and mostly by nuclear magnetic resonance (NMR) spectroscopy.

2 Scope

This work is based on the studies of *Stey*.[56-59] First a reproduction of the synthesis and purification of the ligand was essential. Furthermore the maximum amount per run has to be identified and if possible improved in order to provide pure enough ligand for further experiments.

Yet unsolved is the storage due to the low stability even at –40°C in an inert gas atmosphere. Thus a transformation to a better storable form is desirable. Ideally this is either reversible without any loss or already a step towards new metal complexes. New metal complexes should emphasize the versatile characters of the ligand and show the assumed coordination motifs, such as a coordination of metal fragments by the phosphorus atom. This can either be underlined by the anticipated phosphanidic character and/or in (hetero)bimetallic complexes. Eligible are metals with known catalytic activity and especially a combination thereof.

From the pure ligand and its metal complexes single crystals are targeted in a high quality for experimental charge density studies based on a high resolution X-ray diffraction experiments. These crystals must have a very high quality ideally without any disorder to obtain significant data.

At this stage the ligand has a planar bend structure. Substituents in the *4,4'*-positions would provide more steric demand and might stabilize new complexes. Therefore similar approaches to modified ligands are parts of this thesis.

Additionally complexes on the basis of commercially available di(*2*-pyridyl)amine will be examined in order to get better insights in the coordination motifs. Utilizing this ligand might also provide a better reaction control as a new tool in fine tuning the reactivity. Improvements of preparation in good yield and high purities as well as their complete analytic data are inalienable for further use.

3 Literatrure
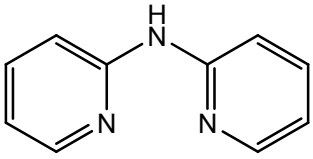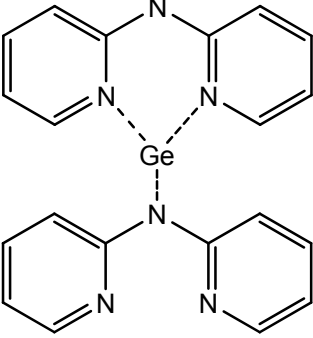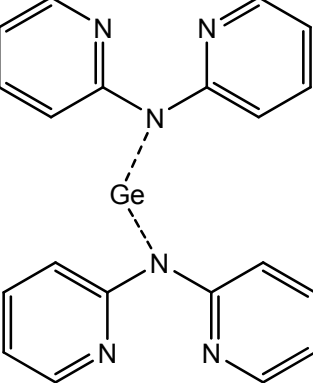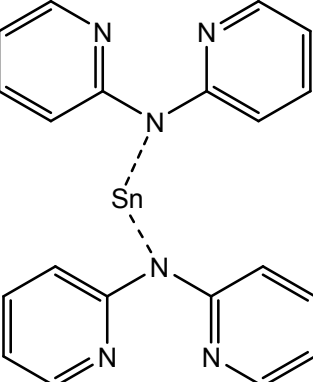
[1] H. Ost, *Lehrbuch der technischen Chemie*, Verlag von Robert Oppenheimer, Berlin, **1890**.

[2] P. J. Chenier, *Survey of Industrial Chemistry*, John Wiley & Sons, New York, **1987**, p. 45-57.

[3] J. W. Döbereiner, *Über neu entdeckte höchst merkwürdige Eigenschaften des Platins und die pneumatisch-capillare Thätigkeit gesprungener Gläser: ein Beitrag zur Corpuscularphilosophie*, Schmid, Jena, **1823**.

[4] J. Schiff, *Briefwechsel zwischen Johann Wolfgang von Goethe und Johann Wolfgang Döbereiner (1810-1830)*, **1914**, p. 78.

[5] W. Ostwald, *Z. Phys. Chem. (Leipzig)* **1894**, *15*, 706-709.

[6] M. Appl, *Ammonia* in *Ullmann's Encyclopedia of Industrial Chemistry* (Ed. B. Elvers), Wiley-VCH, Weinheim, **2006**.

[7] J. M. Thomas, W. J. Thomas, *Introduction to the Principles of Heterogeneous Catalysis*, Academic Press, London, **1967**.

[8] B. Cornils, W. A. Herrmann, *Applied Homogenous Catalysis with Organometallic Compounds*, VCH, Weinheim, **1996**.

[9] H. Werner, *Landmarks in Organo-Transition Metal Chemistry - A Personal View*, Springer Verlag, Heidelberg, **2009**.

[10] G. T. Morgan, H. D. K. Drew, *J. Chem. Soc., Trans.* **1920**, *117*, 1456-1465.

[11] S. P. Green, C. Jones, A. Stasch, *Science* **2007**, *318*, 1754-1758.

[12] P. Braunstein, D. Matt, F. Mathey, D. Thavard, *J. Chem. Research (S)* **1978**, 232.

[13] J. C. Jeffrey, T. B. Rauchfuss, *Inorg. Chem.* **1979**, *18*, 2658-2666.

[14] P. Braunstein, M. Knorr, C. Stern, *Coord. Chem. Rev.* **1998**, *903*, 178-180.

[15] P. Braunstein, F. Naud, *Angew. Chem.* **2001**, *113*, 702-722; *Angew. Chem. Int. Ed.* **2001**, *40*, 680-700.

[16] K. Weissermel, H.-J. Arpe, *Industrial Organic Chemistry*, Wiley-VCH, Weinheim, **1997**.

[17] M. Beller, A. Zapf, *Synlett* **1998**, *7*, 792-794.

[18] D. E. Bergbreiter, P. L. Osburn, Y.-S. Liu, *J. Am. Chem. Soc.* **1999**, *121*, 9531-9538.

[19] D. Zim, A. S. Gruber, G. Ebeling, J. Dupont, A. L. Monteiro, *Org. Lett.* **2000**, *2*, 281-2884.
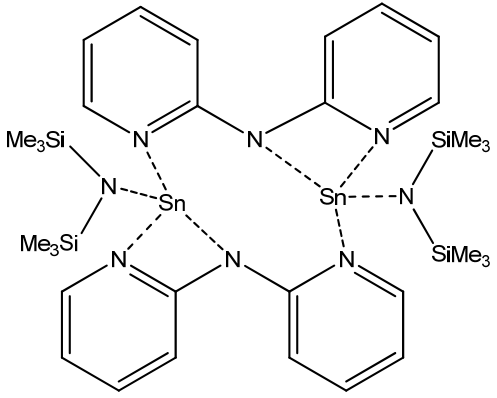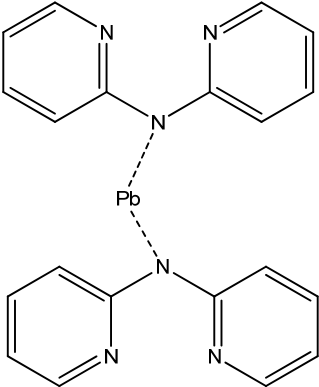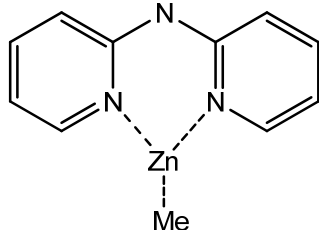
[20] M. Gupta, C. Hagen, W. C. Kaska, R. E. Cramer, C. M. Jensen, *J. Am. Chem. Soc.* **1997**, *119*, 840-841.

[21] S. Niu, M. B. Hall, *J. Am. Chem. Soc.* **1999**, *121*, 3992-3999.

[22] P. Dani, T. Karlen, R. A. Gossage, S. Glasdiali, G. van Koten, *Angew. Chem.* **2000**, *39*, 743-745; *Angew. Chem. Int. Ed.* **2000**, *112*, 759-761.

[23] J. M. Longmire, X. Zhang, *Organometallics* **1998**, *17*, 4374-4379.

[24] M. T. Stark, G. Jones, C. Richards, *Organometallics* **2000**, *19*, 1282-1291.

[25] K. P. Bryliakov, N. V. Semikolenova, D. V. Yudaev, V. A. Zakharov, H. H. Brintzinger, M. Ystenes, E. Rytter, E. P. Talsi, *J. Organomet. Chem.* **2003**, *683*, 92-102.

[26] A. Andresen, H.-G. Cordes, J. Herwig, W. Kaminsky, A. Merck, R. Mottweiler, J. Pein, H. Sinn, H.-J. Vollmer, *Angew. Chem.* **1976**, *88*, 689-690; *Angew. Chem. Int. Ed. Engl.* **1976**, *15*, 630-631.

[27] J. Storre, A. Klemp, H. W. Roesky, H.-G. Schmidt, M. Noltemeyer, R. Fleischer, D. Stalke, *J. Am. Chem. Soc.* **1996**, *118*, 1380-1386.

[28] J. Storre, C. Schnitter, H. W. Roesky, H.-G. Schmidt, M. Noltemeyer, R. Fleischer, D. Stalke, *J. Am. Chem. Soc.* **1997**, *119*, 7505-7513.

[29] M. R. Mason, J. M. Smith, S. G. Bott, A. R. Barron, *J. Am. Chem. Soc.* **1993**, *115*, 4971-4984.

[30] M. Watanabi, N. McMahon, J. Harlan, A. R. Barron, *Organometallics* **2001**, *20*, 460-467.

[31] G. Bai, S. Singh, H. W. Roesky, M. Noltemeyer, H.-G. Schmidt, *J. Am. Chem. Soc.* **2005**, *127*, 3449-3455.

[32] J. R. Zoeller, V. H. Agreda, S. L. Cook, N. L. Lafferty, S. W. Polichnowski, P. D. Pond, *Catal. Today* **1992**, *13*, 73-91.

[33] H. Sinn, W. Kaminsky, H.-J. Vollmer, W. Rüdiger, *Angew. Chem.* **1980**, *92*, 396-402; *Angew. Chem. Int. Ed. Engl.* **1980**, *19*, 390-393.

[34] C. Fernández-Cortabitarte, F. García, J. V. Morey, M. McPartlin, S. Singh, A. E. H. Wheatley, D. S. Wright, *Angew. Chem.* **2007**, *119*, 5521-5524; *Angew. Chem. Int. Ed.* **2007**, *46*, 5425-5428.

[35] M. Shibasaki, H. Sasai, T. Arai, *Angew. Chem.* **1997**, *109*, 1290-1311; *Angew. Chem. Int. Ed. Engl.* **1997**, *36*, 1235-1256.

[36] S. Handa, K. Nagawa, Y. Sohtome, S. Matsunaga, M. Shibasaki, *Angew. Chem.* **2008**, *120*, 3274-3277; *Angew. Chem. Int. Ed.* **2008**, *47*, 3230-3233.

[37]   C. A. de Parrodi, P. J. Walsh, *Angew. Chem.* **2009**, *121*, 4773-4776; *Angew. Chem. Int. Ed.* **2009**, *48*, 4679-4682.

[38]   A. Fukuoka, M. Ichikawa, J. A. Hriljac, D. F. Shriver, *Inorg. Chem.* **1987**, *26*, 3643-3645.

[39]   D. Prim, B. Andrioletti, F. R.-M. Rose-Munch, E. Rose, F. Couty, *Tetrahedron* **2004**, *60*, 3325-3347.

[40]   S. W. Ragsdale, M. Kumar, *Chem. Rev.* **1996**, *96*, 2515-2540.

[41]   T. I. Doukov, T. M. Iverson, J. Seravalli, S. W. Ragsdale, C. L. Drennan, *Science* **2002**, *298*, 567-572.

[42]   C. Darnault, A. Volbeda, E. J. Kim, P. Legrand, X. Vernede, P. A. Lindahl, J. C. Fontecilla-Camps, *Nature Struct. Biol.* **2003**, *10*, 271-279.

[43]   N. Sträter, T. Klabunde, P. Tucker, H. Witzel, B. Krebs, *Science* **1995**, *268*, 1489-1492.

[44]   J. A. Tainer, E. D. Getzoff, J. S. Richardson, D. C. Richardson, *Nature* **1983**, *306*, 284-286.

[45]   G. B. Nikiforov, H. W. Roesky, T. Schulz, D. Stalke, M. Witt, *Inorg. Chem.* **2008**, *47*, 6435-6443.

[46]   T. Schulz, Ph.D. thesis, Universität Göttingen (Germany), **2010**.

[47]   B. S. Brunschwig, C. Creutz, N. Sutin, *Chem. Soc. Rev.* **2002**, *31*, 168-184.

[48]   C. N. Carlson, C. J. Kuehl, R. E. Da Re, J. M. Veauthier, E. J. Schelter, A. E. Milligan, B. L. Scott, E. D. Bauer, J. D. Thompson, D. E. Morris, K. D. John, *J. Am. Chem. Soc.* **2006**, *128*, 7230-7241.

[49]   O. S. Wenger, *Coord. Chem. Rev.* **2009**, *253*, 1439-1457.

[50]   M. Pfeiffer, T. Stey, H. Jehle, B. Klüpfel, W. Malisch, D. Stalke, V. Chandrasekhar, *Chem. Commun.* **2001**, *4*, 337-338.

[51]   I. Objartel, H. Ott, D. Stalke, *Z. Anorg. Allg. Chem.* **2008**, *634*, 2373-2379.

[52]   A. Murso, D. Stalke, *Dalton Trans.* **2004**, 2563-2569.

[53]   A. Murso, M. Straka, M. Kaupp, R. Bertermann, D. Stalke, *Organometallics* **2005**, *24*, 3576-3578.

[54]   S. Wingerter, M. Pfeiffer, A. Murso, C. Lustig, T. Stey, V. Chandrasekhar, D. Stalke, *J. Am. Chem. Soc.* **2001**, *123*, 1381-1388.

[55]   I. Objartel, N. A. Pott, M. John, D. Stalke, *Organometallics* **2010**, DOI: 10.1021/om1005885.

[56]   T. Stey, M. Pfeiffer, J. Henn, S. K. Pandey, D. Stalke, *Chem. Eur. J.* **2007**, *13*, 3636-3642.

[57]   T. Stey, J. Henn, D. Stalke, *Chem. Commun.* **2007**, 413-415.

[58]   T. Stey, D. Stalke, *Z. Anorg. Allg. Chem.* **2005**, *651*, 2931-2936.

[59]   T. Stey, Ph.D. thesis, Universität Würzburg (Germany), **2004**.

1 List of compounds

name	number	Lewis formula
Di(2-pyridyl)amine	1	
Bis(di(2-pyridyl)amido)germanium	2	
Bis(di(2-pyridyl)amido)germanium	3	
Bis(di(2-pyridyl)amido)tin(II)	4	

(Di(*2*-pyridyl)amido)tin (hexamethyldisilazane)	**5**	
Bis(di(2-pyridyl)amido)lead(II)	**6**	
(Di(2-pyridyl)amido)(methyl)zinc	**7**	

2 Introduction

Metal amides are being used in numerous applications as reaction intermediates or as catalysts in chemical reactions. Typically this includes the fabrication of pharmaceuticals, cosmetics, fragrances and flavors, polymers, and biodiesel fuel. Metal amides are frequently used as strong non-nucleophilic bases. Advantages of metal amides are a higher base strength, a better solubility in hydrocarbons and convenient handling compared to its alcoholates and hydride equivalents. Furthermore, amido derivatives of selective elements have shown promising potential as single source precursors for *chemical vapor deposition* (CVD).[1-3]

Over the last years many anionic ligands with *N*-heteroaromatic rings have been in the focus of research by *Stalke et al.*[4-6] such as di(2-pyridyl)methyl,[7,8] -phosphanide and -arsenides[9,10] as well as tripyrazolylgermanates and -stannates.[11,12] *Kempe et al.* focused their research complexes on aminopyridinato ligands in catalysis.[13-17]

Due to the similar structural motif and their similar coordination behavior these ligands very are comparable even if they formally form carbanions, phosphanides or arsenides. The negative charge is located within the heteroaromatics mainly at the nitrogen atom in all reported structures. *A priori*, one can image three different coordination modes (see Scheme 1).
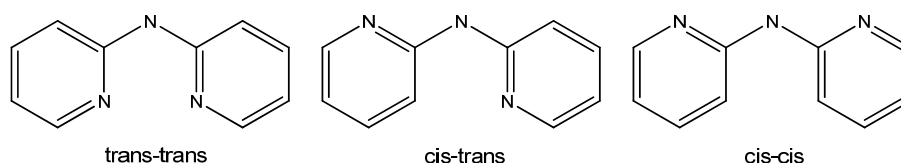
Scheme 1: conceivable coordination modes of di(2-pyridyl)amide.

Scheme 2 shows all these coordination modes reported until now in different complexes of aluminium, late transition elements, titanium and tantalum.[18-20]
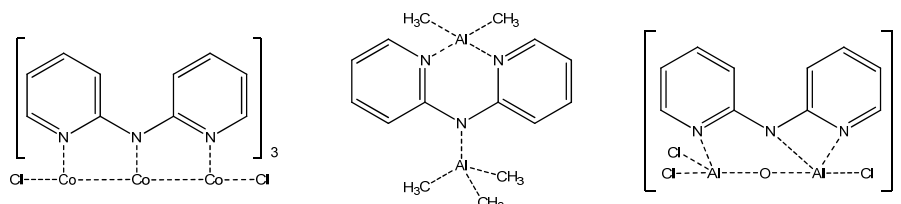
Scheme 2: reported coordination modes of di(2-pyridyl)amides.

Surprisingly, examples of main group complexes are limited.[21-23] Only one germanium(II)chloride complex and a couple of tin(IV)complexes have been reported as group 14 examples until now.[24]

3 Synthesis and structure

3.1 General procedure for group 14 metals

Following standard lab practice for metalation of amines, the organometallic reactants were added drop wise to a solution of di(*2*-pyridyl)amine(**1**) in dry toluene at -78°C in a first step. While optimizing the reaction conditions, different temperatures were screened showing the same yield at increased reaction time when performing the metalation at room temperature. Therefore, all reactions can easily be performed without any cooling.

Most of the complexes of group 14 metals were prepared in the same way. After dissolving the di(*2*-pyridyl)amine in toluene inside the dry box, *n*-butyllithium was added dropwise *via* syringe using *Schlenk* techniques. After stirring for 15 minutes the desired group 14 metal was added in a 2:1 ratio as a halide salt performing a salt elimination reaction. After the reaction was completed the precipitating lithiumhalide was removed by filtration. Concentrating the filtrate and storage at room temperature resulted in crystals suitable for single crystal X-ray diffraction experiments.

3.2 Bis(di(*2*-pyridyl)amido)germanium (2) and (3)

Following the general procedure, bis(di(*2*-pyridyl)amido)germanium was prepared by lithiation and salt elimination in a second step. *Gushwa* and *Richards* used methyllithium and dissolved germaniumdichloride to prepare (di(*2*-pyridyl)amido)-germaniumchloride at -78°C. Regrettably, they were unable to get crystals or any analytical data of bis(di(*2*-pyridyl)amido)germanium with their procedure. Solid $GeCl_2$·dioxane and driving the reaction at room temperature led to the success.[24]
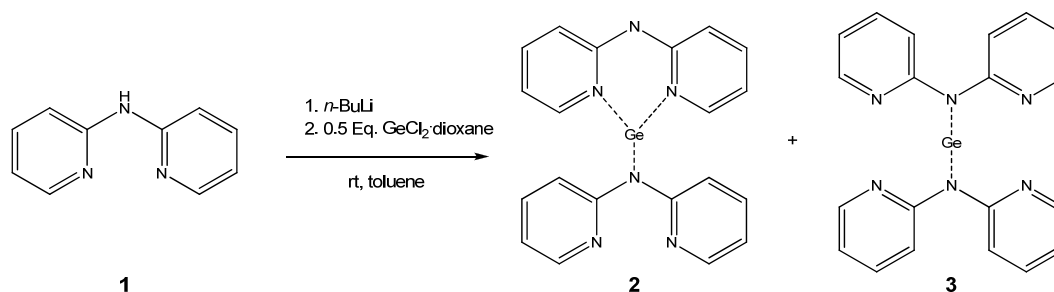
Scheme 3: reaction of (di(*2*-pyridyl)amide with $GeCl_2$·dioxane to **2** and **3**.

Crystallization of the filtrate led to pale yellow single crystals within three days. Bis(di(2-pyridyl)amido)germanium (**2**) crystallizes in the orthorhombic space group

Pbca. The germanium atom is coordinated by two di(*2*-pyridyl)amides each in a different manner.
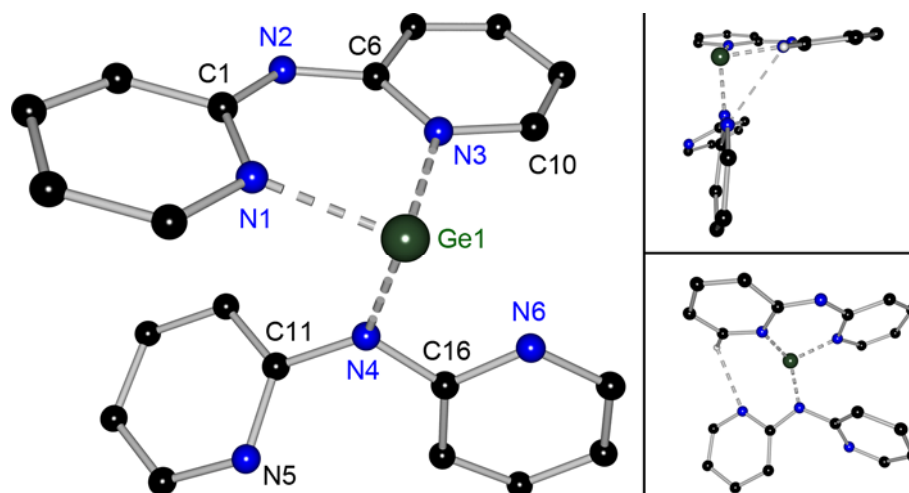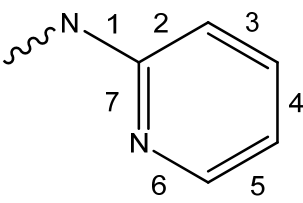
Figure 1: Solid state structure of bis(di(*2*-pyridyl)amido)germanium (**2**).

Hydrogen atoms are omitted for clarity.

Table 1: Selected bond lengths [pm] and angles [°] for **2**.

Ge1–N1	202.4(2)		
Ge1–N2	201.9(2)	N1–Ge1–N3	87.68(9)
Ge1–N4	198.5(2)	N1–Ge1–N4	91.49(8)
		N3–Ge1–N4	96.70(8)
N2–C1	134.6(4)		
N2–C6	134.3(3)	C1–N2–C6	125.4(2)
N4–C11	141.2(3)	C11–N4–C16	120.7(2)
N4–C16	137.7(3)	Uncoord. arom. Twist	61.9

The coordination motif reasambles the one of (di(*2*-pyridyl)amido)germaniumchloride reported by *Gushwa* and *Richards*.[24] One amide moiety is nearly planar (12.1° out of plane) and chelates the germanium atom with both nitrogen atoms in the *trans-trans* fashion (scheme 1) of its heteroaromatic rings. The second amide moiety coordinates the germanium atom with the bridging nitrogen atom exclusively, resembling in the *cis-trans* conformation. Likewise, it coordinates perpendicularly towards the (di(*2*-pyridyl)amido)germanium plane, clearly indicating the lone-pair character at the germanium atom.

Table 2: Comparison of bond length [pm] within di(2-pydridyl)amide in **2**, PyH (A)[25] and Py$_2$NH(B).[26,27]

Source	Conformer	1	2	3	4	5	6	7
A			139.4	139.2	139.2	139.4	133.8	133.8
B	*cis-trans*	138.0	139.5	137.0	137.0	136.5	134.0	133.5
2	*trans-trans* (N1)	134.6	141.0	136.3	140.4	135.6	136.5	137.2
2	*trans-trans* (N3)	134.2	143.3	135.5	139.8	135.7	135.5	137.6
2	*cis-trans* (N5)	141.2	138.9	138.3	137.6	138.0	134.6	134.5
2	*cis-trans* (N6)	137.7	140.9	137.6	138.7	137.7	133.6	134.2

The first amide moiety (N1–N3, C1–10) is arranged pseudo-mirror-inverted along the N2–Ge1 axis. Therefore, all analogous bond lengths in the pyridyl rings match within their standard deviations in a *trans-trans* conformation. The best planes of the rings are tilted against each other by 10.9°. The germanium atom is 22.7 pm out of the N,N,N-plane. Both N–C$_{ipso}$ bonds are shortened through coordination. Their included angle of 125.4° is reduced by 5.7° compared to the free di(2-pyridyl)amine. Bond lengths and angles hint to N2 being sp^2-hybridized. The charge is delocalized within the pyridyl rings, partially localized in double bonds in the *3-* and *5-*positions, leaving a formally positive N2 with shortend bonds due to electrostatic interactions. Additionally, the equal charge distribution is underlined be the symmetric appearance of the ligand.

The other amide moiety (N4–N6, C11–C20) shows great differences between both pyridyl rings beside the *cis-trans* conformation. The best planes of both heteroaromatic rings are twisted by 61.9° while the C11–N4–C16 angle is 120.6°. The N5 containing pyridyl ring shows the longer C–N bond to the bridging nitrogen atom N4 compared to both the free di(2-pyridyl)amine and the second pyridyl ring containing N6. The N5 heads away from the germanium atom. All bonds are slightly elongated compared to the free di(2-pyridyl)amine except the little shortened C11–C12 bond.

The other pyridyl ring including N6 shows a shortened bond towards the bridging N4. A Ge1–N6 bond is unlikely due to a distance of 264.3 pm which would be one of the longest Ge–N bonds reported to the *Cambridge Crystallographers Data Centre*

(CCDC) as Scheme 4 clearly shows. Hence, a differentiation caused by coordination as reported in comparable aluminum complexes cannot be taken in to account.[23]
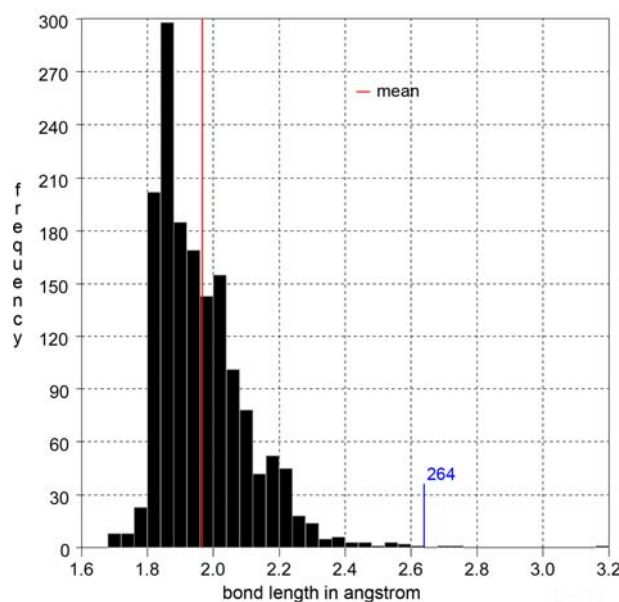
Scheme 4: frequency of bond lengths reported to the CCDC.

The bridging nitrogen atom N4 is bonded to the two pyridyl rings and the central germanium atom. An angle of 120.6° is enclosed at N4 between the heteroaromatic *ipso*-carbon atom bonds. Overall the angles sum up to 357.4°. The elongation of the C16–C17 and the C18–C19 bonds is obvious as well. Both bonds are longer than the other remaining C–C bonds within this pyridyl ring. Summing up the found changes within the molecule, it leads to the interpretation shown in Scheme 5.
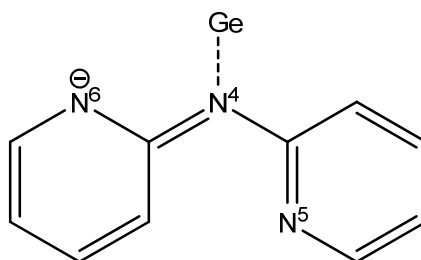
Scheme 5: canonical form that contributes most to explain the bonding in **2.**

N4–C16 has a more pronounced double bond character then N4–C11. Additionally, the N*pyridyl*–C bonds are slightly shorter in the pyridyl ring containing N6. This hints to predominant charge localization at N6 and correspondently increased double bond character at the shorter C17–C18 and C19–C20 bond. Furthermore, one of the lone pairs at N6 points towards H10 providing a pre-organization as shown in Figure 1. The other pyridyl ring including N4 bends heavily out of plane to avoid steric strain.

The geometry at the germanium atom is slightly distorted trigonal pyramidal with a lone pair occupying the vacant space.

Interestingly, the NMR shows two different sets of signals. The minor set easily can be assigned to the determined structure by its splitting and confirmed by HH-COSY spectra. Only eight different corresponding signals can be identified. This implies equality of both pyridyl rings within each di(*2*-pyridyl)amide ligand.

The phenomenon was earlier reported by *Raston et al.* unable to distinguish between the different nitrogen atoms.[28] This has been explained by studies and the theoretical calculations by *Stalke et al.*[23] They determined an energetic difference of only 7.4 kJ/mol between the *trans-trans* and the *cis-trans* conformers. The *cis-cis* and the *trans-trans* conformers only differ by 1.4 kJ/mol. Hence the dynamic behavior can be explained by a rearrangement process.

The major set of signals is based on a symmetric di(*2*-pyridyl)amino compound with only four chemically different protons. Their shift excludes di(*2*-pyridyl)amine as well as di(*2*-pyridyl)amidogermaniumchloride reported by *Gushwa* and *Richards*. As it is similar to the bis(di(*2*-pyridyl)amido)tin (**4**) a similar structure is assumed for compound **3**. In solution a 1:1 ratio of compound **2** to compound **3** was detected.

3.3 Bis(di(2-pyridyl)amido)tin (4)

It seems astonishing that no tin(II) complex of di(*2*-pyridyl)amine has been reported so far, although there are a couple of tin(IV) complexes. Thus di(*2*-pyridyl)amine was used according to the general procedure (see Scheme 6).
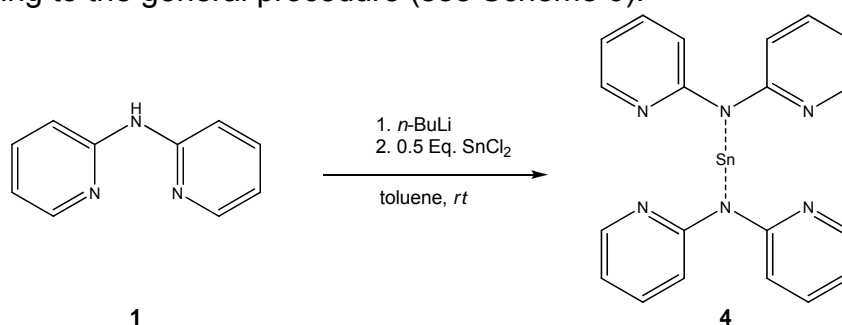
Scheme 6: preparation of bis(di(*2*-pyridyl)amido)tin (**4**).

Suitable single-crystals for an X-ray diffraction experiment were obtained within three days.
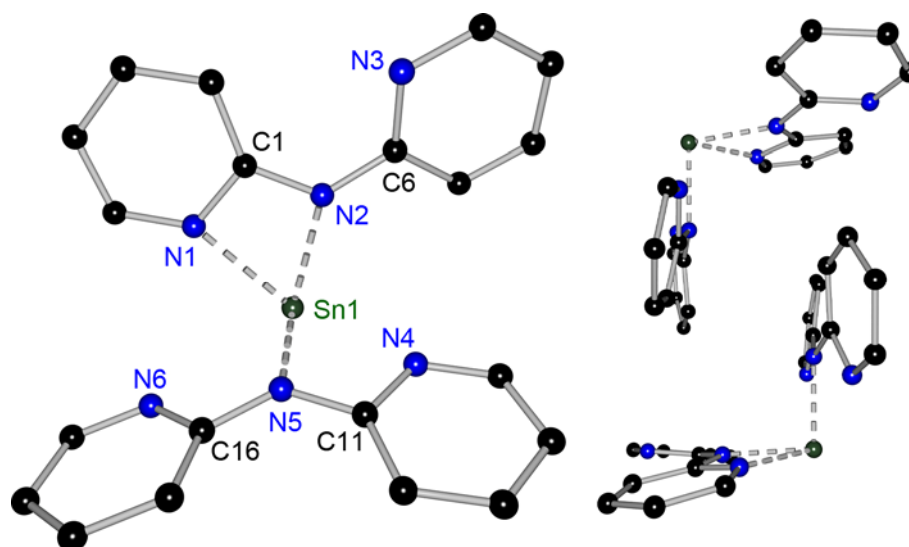
Figure 2: Solid state structure of bis(di(2-pyridyl)amido)tin (**4**). Hydrogen

atoms are omitted for clarity.

Table 3: Selected bond lengths [pm] and angles [°] for **4**.
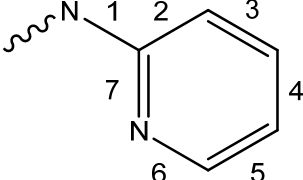
Sn1–N1	233.2(2)	N1–Sn1–N5	89.28(7)
Sn1–N2	223.2(2)	N2–Sn1–N5	96.83(7)
Sn1–N4	256.6(2)	N1–C1–N2	108.40(19)
Sn1–N5	215.0(2)	N4–C11–N5	109.45(19)
N2–C1	136.2(3)	C1–N2–C6	126.37(19)
N2–C6	138.5(3)	C11–N5–C16	130.16(19)
N5–C11	137.1(3)	N2–C6–C7	118.1(2)
N5–C16	137.4(3)	N6–C16–N5	111.67(19)

Bis(di(2-pyridyl)amido)tin (**4**) crystallizes in the monoclic space group $P2_1/n$ with one monomer per asymmetric unit. The tin atom is coordinated by two di(2-pyridyl)-amides. One of these is a *cis-trans* conformer (N1–N3, C1–C10) while the other has a *cis-cis* conformation (N4–N6, C11–C20).

Within the *cis-cis* configurated ligand all analogous bonds are identical within their standard deviation. The best planes of the heteroaromatic are twisted by 20.1°. The tin atom is 27.5 pm above the plane of the pyridyl ring containing N4 and 19.5 pm beneath the plane of the pyridyl ring containing N6. The Sn1–N5 bond length is 215.0 pm and has an angle of 161.4° to the C11–N5–C16 plane. The $C_{ipso}N_{bridge}C'_{ipso}$-bond angle for an uncoordinated di(2-pyridyl)amine of 131.1° is slightly lowered to 130.2° for C11–N5–C16 angle. The overall angular sum at N5 is 357.2°. Based on these facts, the central nitrogen N5 is assumed to be

sp^2-hybridized. The remaining p-orbital is perpendicular to the 3 σ-bonds and couples to the π–system of both heteroaromatic rings. Therefore the charge is completely delocalized within the ligand.

Table 4: Comparison of bond lengths within di(2-pydridyl)amine in **4**, PyH (A)[25] and Py$_2$NH(B).[26,27]

Source	Conformer	1	2	3	4	5	6	7
A			139.4	139.2	139.2	139.4	133.8	133.8
B	*cis-trans*	138.0	139.5	137.0	137.0	136.5	134.0	133.5
4	*cis-cis* (N4)	137.1	140.9	137.1	138.4	138.1	133.7	135.5
4	*cis-cis* (N6)	137.4	140.6	137.8	138.0	138.3	133.5	135.2
4	*cis-trans*(N1)	136.5	141.0	137.6	139.9	137.2	133.6	136.2
4	*cis-trans*(N3)	138.5	140.4	137.0	139.2	137.7	134.4	134.3

Scheme 7 shows the frequency of Sn–N bond lengths reported to the CCDC. The N4-Sn1 (256.8 pm) distance is within the range of reported bond lengths while the N6–Sn1 distance (302.3 pm) is at the outer limit. Since there is no significant difference between both pyridyl rings, a N6–Sn1 bond is not to be assumed.
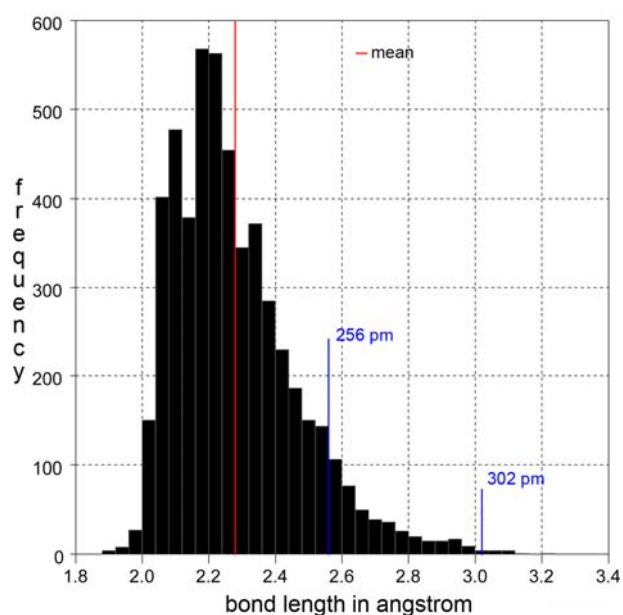
Scheme 7: frequency of Sn–N bond length reported to the CCDC.

In contrast, the heteroaromatic rings of the *cis-trans* conformer show differences. The best planes of the heteroaromatic rings are twisted by 18.0°. The pyridyl ring containing N1 is involved in the coordination. Changes in bond length have the same tendency as in the *cis-cis* conformer even though a bit more pronounced. The tin atom is 20.3 pm out of the best plane of the coordinating pyridyl ring and 15.6 pm above the N1–C1–N2 plane. The Sn1–N bond lengths are 223.2 pm towards N2 and 233.2 pm towards N1 respectively. The angle between the two pyridyl rings at N2 with 126.4° is smaller than the analogous at N5. Within the other pyridyl ring containing N3, most bonds are slightly elongated compared to the uncoordinated amine. This heteroaromatic ring with the related nitrogen lone pair points away from the tin atom. Therefore, it cannot take part in any coordination. The bridging nitrogen atom N2 is sp^2-hybridized like N5 and its perpendicular p-orbital couples into the aromatic systems of both pyridyl rings. Yet slight charge localization at the coordinating heteroaromatic ring is assumed, as the more pronounced bond length changes show. This is underlined by the elongation of the Sn1–N2 bond compared to its analogous Sn1–N5 bond since the localization of the charge in the pyridyl ring causes a charge depletion at the bridging nitrogen atom N2 and thereof a elongation of the bond.

In contrast to compound **2** with a very pronounced localization of the negative charge at one pyridyl ring nitrogen atom, this cannot be proven based on this X-ray data. Again the different coordination modes of the same ligand within one complex are noticeably. As mentioned earlier, low rotation barrier as well as the observable π-stacking and H-(π-density) interactions in the crystal might have influence during the crystallization.

On the basis of this X-ray diffraction experiment a definite charge allocation is not possible although the changes in bond length and angles give good hints. Only a charge density study on the basis of a high-resolution X-ray experiment and multipole model refinement may give further insights on the charge distribution.

In contrast to compound **2**, the complex **4** does not show a splitting of the signals in the NMR experiments. In solution, the ligand must be symmetric showing only four signals in the ^{1}H-NMR spectra at room temperature. This matches with the studies on [Al{(NPy)Py)}₃].[23] ^{15}N-NMR spectroscopy shows two different signals which differ considerably with respect to their chemical shifts because of their magnetically non equivalent environment. The signals can be allocated similar to the neutral ligand, but their change compared to the neutral ligand differs significantly. While the signal of

the pyridyl ring nitrogen atom only shifts down by ~2 ppm the bridging nitrogen atom shifts down by more than 35 ppm compared to the neutral ligand. These downfield shifts indicate a loss of shielding. This fact can be easily explained by the charge transfer towards the coordinated tin atom. This effect is even more distinct at the bridging nitrogen atom.

3.4 (Di(*2*-pyridyl)amido)tin(hexamethyldisilazane) (5)

In an alternative experiment heading towards a tin(II) complex of di(2-pyridyl)amide a reaction with bis(hexamethyldisilazane)tin was performed. The amine was mixed in the argon dry box with the amide and toluene was added.
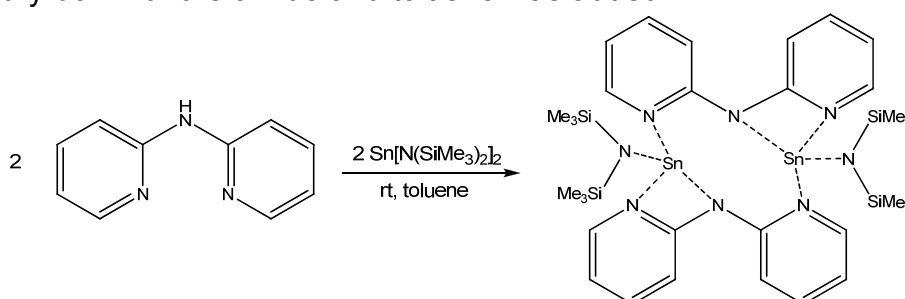
Scheme 8: preparation of (di(*2*-pyridyl)amido)tin(hexamethyldisilazane) (**5**).

After removal of all volatile material, the residue was re-dissolved in toluene and crystallization of a concentrated solution afforded crystals for a single crystal X-ray diffraction experiment after 2 weeks.
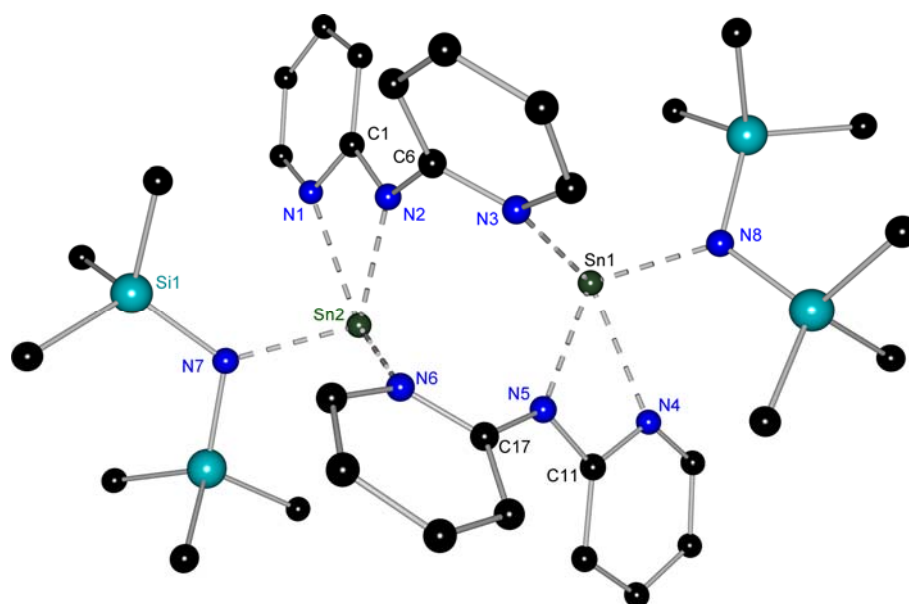
Figure 3: solid state structure of (di(*2*-pyridyl)amido)tin(hexamethyldisilazane)

(**5**). Hydrogen atoms are omitted for clarity.

Table 5: Selected bond lengths [pm] and angles [°] for (di(*2*-pyridyl)amido)tin(hexamethyldisilazane) (**5**).

Sn1–N3	2.547(3)		
Sn1–N4	246.2(3)	N1–Sn2–N2	55.95(9)
Sn1–N5	227.0(3)	N1–Sn2–N6	132.30(9)
Sn1–N8	213.8(3)	N3–Sn2–N8	85.75(10)
Sn2–N1	249.0(3)	N4–Sn1–N5	56.17(9)
Sn2–N2	224.4(4)	N4–Sn1–N8	89.13(19)
Sn2–N6	248.8(3)	N6–Sn1–N7	85.20(10)
Sn2–N7	214.9(3)	C1–N2–C6	124.1(3)
N2–C1	135.8(4)	C11–N5–C17	124.3(3)
N2–C6	137.8(4)	Twist py(N1)–py(N3)	52.3
N5–C11	136.8(4)	Twist py(N4)–py(N6)	52.9
N5–C17	137.6(4)		

(Di(*2*-pyridyl)amido)tin(hexamethyldisilazane) (**5**) crystallizes in the triclinic space group $P\bar{1}$ as a dimer in the asymmetric unit.

Within the di(*2*-pyridyl)amide ligand the two pyridyl rings can be distinguished since one of them binds to the same tin atom as the bridging nitrogen atom does, and the other binds to the second tin atom providing the dimeric link. This difference becomes obvious looking at the N–C$_{ipso}$ bond length. Towards the pyridyl ring coordinating the same tin atom it is 136.3 pm on average. In contrast the other N–C$_{ipso}$ bonds average to 137.7 pm.

Each tin atom is asymmetrically coordinated by two nitrogen atoms of one di(*2*-pyridyl)amine as well as by one nitrogen atom of the other amine. The coordination spheres of both tin atoms are completed by a hexamethyldisilazane molecule each. These Sn–N bonds describe four different bonding situations:

i. The Sn–N$_{TMS}$ bond is with 214.4 pm on average by far the shortest of all four Sn–N bonds. It is a Sn–N single bond shortened by electrostatic contributions. It is in good accordance to analogous Sn–N bond reported to the Cambridge Crystallographic Data Center.

ii. The Sn–N$_{bridge}$ bond is 225.7 pm. It is a Sn–N single bond without the additional electrostatic contributions. Therefore, this bond is longer than the one mentioned before.

iii. The Sn–N$_{pyridyl}$ bond coordinating the same tin atom as the bridging nitrogen atom. The average bond length is 247.6 pm. It is a dative bond since the nitrogen atom donates the lone pair to form this bond.

iv. The Sn–N$_{pyridyl}$ bond coordinating the other tin atom as the bridging nitrogen atom. The average bond length is 251.8 pm. This Sn–N bond again is a dative one. The slight elongation compared to the one in iii. is caused by the lack of chelating effects.

These small differences hint to a pronounced charge localization towards the pyridyl ring coordinating the same tin atom in the solid state.
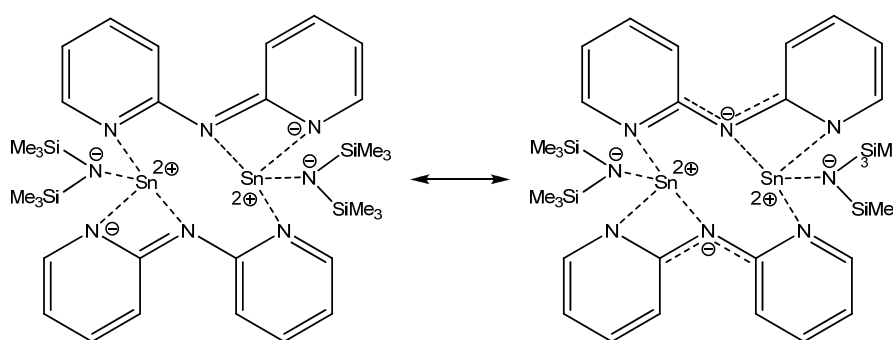
Scheme 9: resonance structures of (**5**).

Scheme 9 shows the two different mesomeric resonance structures of complex 5. In solution all pyridyl rings are equal on the NMR time scale. Hence the slight preference of one pyridyl ring is neutralized.

3.5 Bis(di(*2*-pyridyl)amido)lead (6)

Similar to the group 14 complexes described above an analogous lead species was prepared by addition of lead dichloride to the freshly lithiated ligand in toluene. The reaction of di(*2*-pyridyl)amine and bis(hexamethyldisilzane)lead led to the same product in a lower yield and purity according to NMR experiments. Therefore all further investigations were undertaken from the salt elimination product.
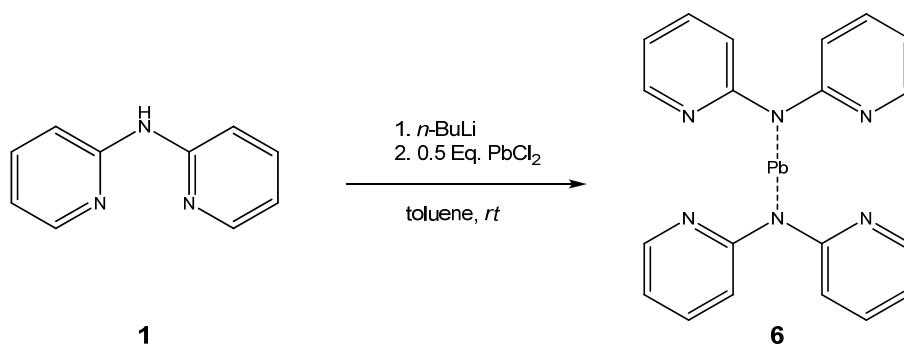
Scheme 10: preparation of bis(di(2-pyridyl)amido)lead (**6**).

NMR-spectroscopic data of the lead compound differ significantly from the germanium- and tin-complexes mentioned above caused by the spin-orbit couppling.[29] By interpretation of the coupling constants in the ^{1}H-NMR spectra and affirmed by an HH-COSY spectrum, a change in the chemical shifts of the hydrogen atoms is to be denoted. The ^{13}C-NMR experiment hints to a change in charge distribution within the pyridyl rings. The ^{15}N-NMR experiment shows a large downfield shift of the pyridyl ring nitrogen atoms by more than ~80 ppm. Furthermore, the bridging nitrogen atom undergoes an upfield shift by ~12 ppm. This indicates the different charge distribution of the lead complex in comparison to those mentioned above.

From these data, a charge transfer from the pyridyl rings towards the bridging nitrogen atom is concluded. An interaction of the pyridyl nitrogen atoms and the lead atom is not detectable in solution. Therefore, the mesomeric formula of the complex goes along with an H-Pb-substitution as shown in Scheme 10.

This is sustained by a Cambridge Crystallographic Data Center search. Only one lead complex is reported with the structural motif shown in Scheme 11**a** while no hits were achieved for the motif shown in Scheme 11**b**. The complex shown in Scheme 11**c** is flat due to the completely sp^2-hybridized backbone and the steric strain thereof.[30] A lead complex of a diphenyl(2-picolyl)iminophosphorane (see Scheme 11**d**) shows a similar evasion of the strained geometry as **6**.[31]

X = any

a   **b**

R= Ph, iPr

c   **d**
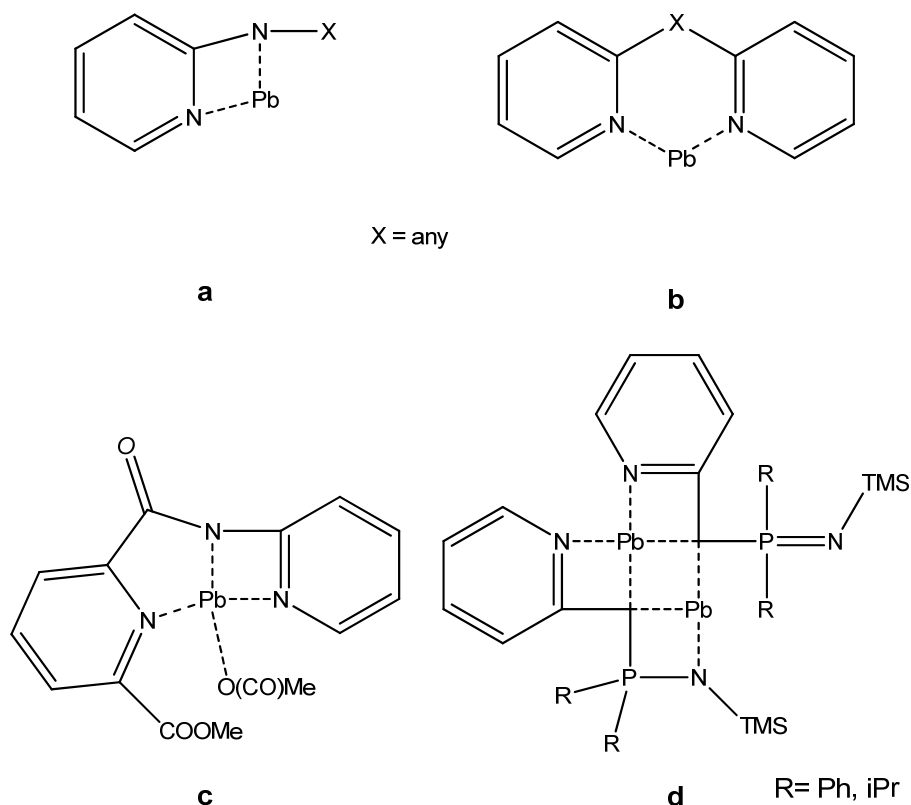
Scheme 11: search on comparable lead complexes with pyridyl side chain donation.

3.6 (Di(*2*-pyridyl)amido)(methyl)zinc (7)

The zincation of di(*2*-pyridyl)amine was performed according to the experiences of the lithiation of di(*2*-pyridyl)amine. Dimethylzinc was added to the dissolved amine dropwise at room temperature. Again, concentrating the filtrate and storage at room temperature yielded crystals suitable for a single crystal X-ray diffraction experiment within a few days. Different di(2-pyridyl)amine:dimethyl zinc rations do not have an influence to the product composition, one methanide always remains at the zinc atom.

1   **7**
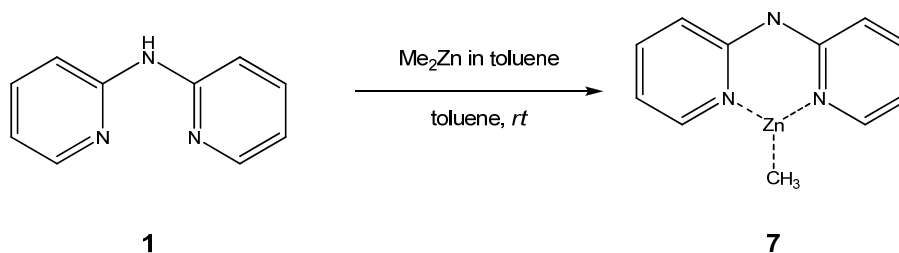
Scheme 12: direct preparation of **7** using Me₂Zn at room temperature.

All analyzed crystals gave highly disordered structures, and it has not been possible to determine a completely anisotropic model yet. Figure 4 illustrates the coordination pattern but the refinement is not yet satisfying to give sufficient geometrical information for a structural comparison.

Complex **7** crystallizes in the triclinic space group $P\bar{1}$ with an asymmetric unit consisting of one trimer as well as two toluene molecules. The single monomers are head-to-tail linked to give trimers. Both possible chiral enatiomers are superposed.
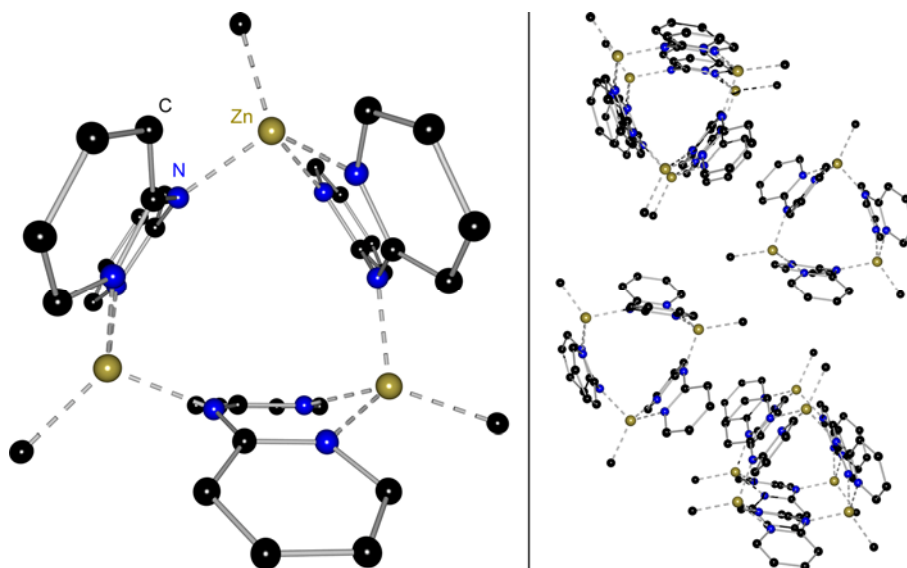
Figure 4: Solid state structure of (di(2-pyridyl)amido)(methyl)zinc (**7**). Hydrogen atoms are omitted for clarity.

The solid state structure shows the deprotonation of one di(*2*-pyridyl)amine per dimethyl zinc. The zinc atom is still bonded to one methanide and is coordinated to one anionic di(*2*-pyridyl)amide ligand by both of its pyridyl nitrogen atoms. The tetrahedral coordination sphere at the zinc atom is completed by the bridging nitrogen atom of a second di(*2*-pyridyl)amide moiety. Three monomers are circularly linked. A preference towards one enantiomer is not recognizable. The pyridyl rings are bended butterfly-like to the outside of the circle.

NMR spectroscopy underlines a charge transfer from the bridging nitrogen atom towards the pyridyl rings. The ^{15}N-NMR experiment shows upfield shift of the pyridyl ring nitrogen atom by ~45 ppm and a downfield shift of ~36 ppm for the bridging nitrogen atom compared to the neutral ligand. These findings are sustained by the ^{1}H- and the ^{13}C-NMR experiments and similar results for aluminum and gallium complexes of di(2-pyridyl)amide.[21]

4 Conclusion

New complexes of di(*2*-pyridyl)amine with group 14 metals as well as a complex of zinc were synthesized and fully charaterized. These compounds exhibit many of the already known coordination modes of di(*2*-pyridyl)amide. Additionally, a *cis-cis* complex only bonded by the bridging nitrogen atom was reported for the first time.

The phenomenon of the different coordination modes can be explained by the small barrier between the different conformers of about 8 kJ/mol.[23] This barrier can easily be overcompensated by metal coordination. Hence, the reported structure of the germanium containing species shows only one of the possible coordination modes. The asymmetric coordination allows a direct comparison of the donating ligands within the same molecule. Nevertheless, in solution a second coordination mode is favored as shown by the NMR spectra.

As a trend downwards group 14 a coordination by the bridging nitrogen atom becomes favorable. This might be explained by a shift of the charge localization from the pyridyl rings towards the bridging nitrogen atom.

Accentuation to one site equalize in solution, as **4** clearly shows. Presumably a similar coordination motif to **4** is available in the case of the germanium containing compound depending on the solvent and applied temperature during the crystallization.

Compounds **5** and **7** show the good accessibility of metalated di(*2*-pyridyl)amides by direct metalation. These allow very pure products in good yields from very well known metal compounds. Therefore, a very high degree of adjustment and reactivity control is possible.

Overall, all reported compounds show the great flexibility of di(*2*-pyridyl)amide as a donor to many metals with individually tailored coordination modes. Furthermore, most complexes are easy to crystallize in ambient conditions. Both features render the presented complexes promising precursors for organometallic synthesis.

5 Experimental

5.1 General

All manipulations were carried out with strict exclusion of air and moiety in nitrogen or argon atmosphere using modified *Schlenk*-techniques or in an argon dry box.[32-35] All solvents were either dried on standard laboratory procedures and were freshly distilled from sodium/potassium alloy prior to use or directly used from a MBraun SPS connected to the glove box. All employed reactants were commercially available or reproduced by literature known procedures.

$$[Sn\{N(SiMe_3)_2\}_2]^{[36]}$$

5.2 Spectroscopic and analytic methods

5.2.1 Nuclear Magnetic Resonance

All probes were prepared and bottled within the argon dry box into Schlenk-NMR-tubes. The NMR-tube was sealed to exclude any impurities. Solvents were dried with potassium. Spectra were recorded at room temperature at a *Bruker Avance 300*, *Bruker Avance 400* or a *Bruker Avance 500* NMR spectrometer.

All chemical shifts δ are given relative to their usual standards and coupling constants *J* are given in Hz. Assignments of the shifts were checked by 2d-correlation spectra. NMR shifts are assigned to the given scheme.

5.2.2 Mass spectrometry

EI-spectra were recorded with a *MAT 95* device (EI-MS: 70 eV). Peaks are given according to the abundance of the main isotope as a mass to charge ratio *m/z*.

5.2.3 Elemental analysis

Elemental analysis was performed as a combustion analysis by the *Analytischen Labor des Institutes für Anorganische Chemie* at the Georg-August Universität Göttingen with an *elementar vario EL III*.

5.3 Bis(di(2-pyridyl)amido)germanium (2) and (3)

1.00 g (5.85 mmol) di(2-pyridyl)amine was dissolved in 50 mL toluene and 4.30 mL (1.4 M in hexane, 6.00 mmol) *n*-buthyllithium were added dropwise at room temperature. After stirring for 15 min. 0.67 g (2.90 mmol) GeCl$_2$*dioxane were added. After stirring 1 h the mixture was filtered and concentrated. Storage at room temperature for 3 days yielded pale yellow crystals suitable for a single crystal X-ray diffraction experiment. NMR experiments show two different sets of coordination modes in a 1:1 ratio.
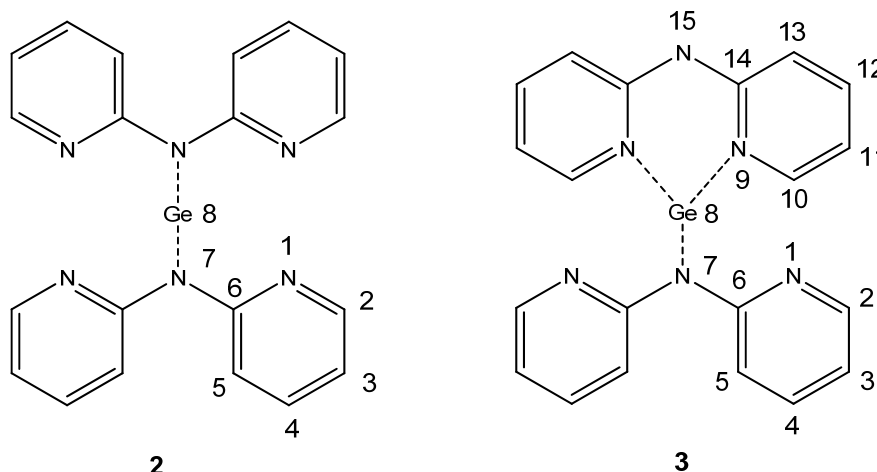
Sum formula: C$_{20}$H$_{18}$GeN$_6$

Molecular weight: 414.06 g/mol

NMR-spectra of 2

^{1}H-NMR (300.13 MHz):   δ: 6.42 (ddd, $^3J_{2,3}$ = 5.0, $^3J_{3,4}$ = 7.2, $^4J_{3,5}$ = 0.9, 4H, *3*); 7.08 (ddd, $^3J_{4,5}$= 8.3, $^4J_{2,4}$ = 1.8, 4H, *4*); 7.35 (d, 4H, *5*); 8.21 (dd, 4H, *2*) ppm.

^{13}C-NMR (75.468 MHz):   δ: 111.96 (s, *5*); 116.17 (s, *3*); 137.31 (s, *4*); 147.95 (s, *2*); 155.08 (s, *6*) ppm.

NMR-spectra of 3

^{1}H-NMR (300.13 MHz):   δ: 6.24 (ddd, $^3J_{2,3}$ = 7.1, $^3J_{3,4}$ = 8.3, $^4J_{3,5}$ = 1.0, 2H, *3*); 6.29 (ddd, $^3J_{10,11}$ = 8.0, $^3J_{11,12}$ = 7.3, $^4J_{11,13}$ = 0.9, 2H, *11*); 6.71 (ddd, $^3J_{12,13}$ = 8.5, $^4J_{10,12}$ = 1.9, 2H, *12*), 6.86 (ddd,

$^3J_{4,5}$ = 8.2, $^4J_{2,4}$ = 1.5, 2H, *4*); 7.23 (d, 2H, *13*); 7.95 (d, 2H, *5*); 8.02 (dd, 2H, *2*); 8,57 (d, 2H, *10*) ppm.

^{13}C-NMR (75.468 MHz): 113.00 (s, *13*); 114.40 (s, *10*); 114.69 (s, *3*); 115.40 (s, *11*); 138.36 (s, *12*); 137.20 (s, *4*); 143.47 (s, *5*); 147.57 (s, 3); 154.75 (s, *14*); 156.17 (s, *6*) ppm.

Due to the low natural abundance of the NMR active nuclei only one signal set was detected for the following nuclei:

^{15}N-NMR (30.424 MHz): δ: -200.65 (1); -105.72(7).

EI-MS: *m/z* (%): 414 (2) [*M*], 244 (14) [*M*-DPA], 170 (100) [DPA].

5.4 Bis(di(*2*-pyridyl)amido)tin (4)

1.00 g (5.85 mmol) di(2-pyridyl)amine was dissolved in 50 mL toluene and 4.30 mL (1.4 M in hexane, 6.00 mmol) *n*-buthyllithium were added dropwise at room temperature. After stirring for 15 min. 0.55 g (2.90 mmol) tindichloride were added. After stirring 1 h the mixture was filtered and concentrated. Storage at room temperature for 3 days yielded colorless crystals suitable for a single crystal X-ray diffraction experiment. NMR experiments show only one set of signals.

Sum formula: $C_{20}H_{18}N_6Sn$

Molecular weight: 460.05 g/mol
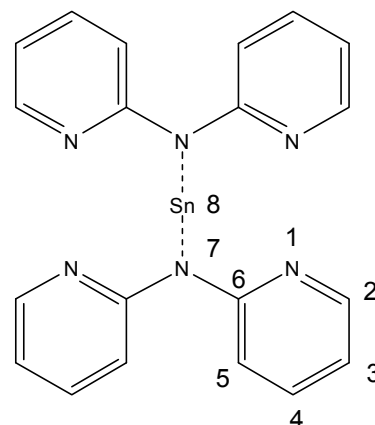
^{1}H-NMR (300.13 MHz): δ: 6.40 (dd, $^3J_{2,3}$ = 4.3, $^3J_{3,4}$ = 7.4, 4H, *3*); 7.02 (dd, $^3J_{4,5}$= 8.4, 4H, *4*); 7.26 (d, 4H, *5*); 8.12 (d, 4H, *2*) ppm.

^{13}C-NMR (75.468MHz): δ: 113.02 (s, *5*); 121.22 (s, *3*); 137.07 (s, *4*); 146.16 (s, *2*); 160.29 (s, *6*) ppm.

^{15}N-NMR (30.424 MHz): δ: -151.83 (1); -80.18 (7).

EI-MS: *m/z* (%):   460 (2) [*M*], 390 (14) [*M*-DPA], 170 (100) [DPA]*.*

5.5 (Di(*2*-pyridyl)amido)tin(hexamethyldisilazane) (5)

1.00 g (5.85 mmol) di(2-pyridyl)amine and 2.83 g (6.00 mmol) bis(hexamethyl-disilzane)tin were mixed in the aron dry box and 50 mL toluene was added. After stirring 12 h all volatile compounds were removed *in vacuo* and re-dissolved in toluene. Storage at room temperature for two weeks yielded pale yellow crystals suitable for a single crystal X-ray diffraction experiment.

Sum formula: $C_{32}H_{52}N_8Si_4Sn_2$

Molecular weight: 900.14 g/mol
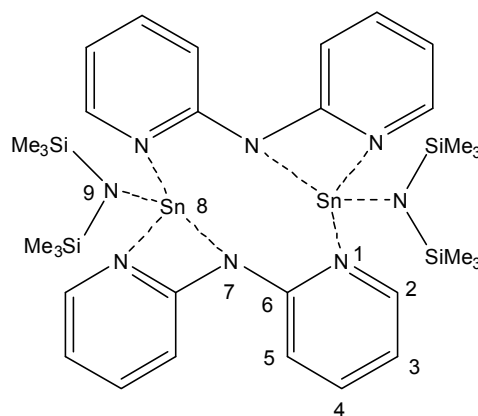
¹H-NMR (300.13 MHz): δ: 0.23 (s, 36H, CH_3); 6.27 (ddd, $^3J_{2,3}$ = 7.0, $^3J_{3,4}$ = 5.2, $^4J_{3,5}$ = 0.9, 4H, *3*); 6.96 (dd, $^3J_{4,5}$ = 8.5, 4H, *4*); 7.09 (d, 4H, *5*); 7.85 (d, 4H, *2*) ppm.

¹³C-NMR (75.468 MHz): δ: 5.90 (s, CH_3); 112.70 (s, *4*); 114.16 (s, *3*); 138.65 (s, *5*); 146.28 (s, *2*); 159.72 (s, *6*) ppm.

²⁹Si-NMR (59.627 MHz): δ: -5.79 (s) ppm.

¹¹⁹Sn-NMR (111.92 MHz): δ: 47.59 (s) ppm.

EI-MS: *m/z* (%):   450 (2) [1/2*M*], 435 (12) [*M*-Me], 289 (36) [*M*-N(SiMe₃)₂], 170 (100) [DPA]*.*

elemental analysis:
CHN, found (calc.):   C: 42.29%(42.77%); H: 5.56%(5.83%); N: 12.45%(12.47%).

5.6 Bis(di(*2*-pyridyl)amido)lead (6)

1.00 g (5.85 mmol) di(2-pyridyl)amine was dissolved in 50 mL toluene and 4.30 mL (1.4 M in hexane, 6.00 mmol) *n*-buthyllithium were added dropwise at room temperature. After stirring for 15 min. 0.81 g (2.90 mmol) leaddichloride was added. After stirring 2 h the mixture was filtered and concentrated.
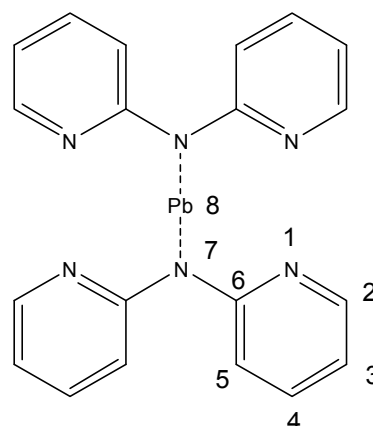
Sum formula: $C_{20}H_{18}N_6Pb$

Molecular weight: 548.12 g/mol

^{1}H-NMR (300.13 MHz):   δ: 6.32 (dd, $^3J_{2,3}$ = 8.3, $^3J_{3,4}$ = 7.1, 4H, *3*); 6.89 (dd, $^3J_{4,5}$= 5.3, 4H, *5*); 7.17 (d, 4H, *4*); 8.16 (d, 4H, *2*) ppm.

^{13}C-NMR (75.468MHz):   δ: 110.73 (s, *3*); 111.67 (s, *5*); 135.11 (s, *4*); 143.83 (s, *2*); 150.23 (s, *6*) ppm.

^{15}N-NMR (30.424 MHz):   δ: -273.59 (1); -31.62 (7).

EI-MS: *m/z* (%):   548 (8) [*M*], 378 (14) [*M*-DPA], 170 (100) [DPA].

5.7 (Di(*2*-pyridyl)amido)(methyl)zinc (7)

1.00 g (5.85 mmol) di(2-pyridyl)amine was dissolved in 50 mL toluene and 4.85 mL (1.2 M in toluene, 5.80 mmol) dimethyl zinc were added dropwise at room temperature over 5 min. After stirring for 30 min. the mixture was filtered and concentrated. Storage at room temperature for 3 days yielded colorless crystals suitable for a single crystal X-ray diffraction experiment.
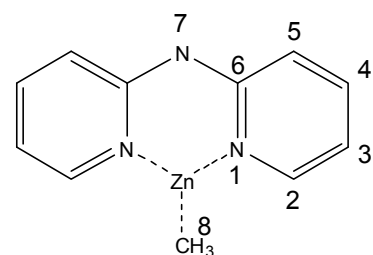
Sum formula: $C_{11}H_{11}N_3Zn$

Molecular weight: 249.02 g/mol

^{1}H-NMR (300.13 MHz):   δ: 0.12 (s, 3H, *8*); 5.99 (dd, $^3J_{2,3}$ = 5.8, $^3J_{3,4}$ = 6.7, 2H, *3*);
6.72 (dd, $^3J_{4,5}$= 8., 2H, *4*); 7.04 (d, 2H, *5*); 7.79 (d, 2H, *2*)
ppm.

^{13}C-NMR (75.468 MHz):   δ:-15.52 (s, *9*); 113.02 (s, *5*); 121.22 (s, *3*); 137.07 (s, *4*);
146.16 (s, *2*); 160.29 (s, *6*) ppm.

^{15}N-NMR (30.424 MHz):   δ: -230.4 (*1*); -151.83 (*7*) ppm.

EI-MS: *m/z* (%):   249 (8) [*M*], 234 (6) [*M*-Me], 170 (100) [DPA].

elemental analysis:

CHN, found(calc.):   C: 54.4%(54.41%); H: 4.56%(4.61%); N: 15.7%(16.03 %).

6 Literature

[1]   M. Afzaal, D. Crouch, M. A. Malik, M. Motevalli, P. O'Brien, J.-H. Park, J. D. Woollins, *Eur. J. Inorg. Chem.* **2004**, *2004*, 171-177.

[2]   V. Passarelli, G. Carta, G. Rossetto, P. Zanella, *J. Chem. Soc., Dalton Trans.* **2003**, 1284-1291.

[3]   M. Veith, *Top. Organomet. Chem.* **2005**, *9*, 81-100.

[4]   M. Pfeiffer, F. Baier, T. Stey, D. Leusser, D. Stalke, B. Engels, D. Moigno, W. Kiefer, *J. Mol. Modeling* **2000**, *6*, 299-311.

[5]   F. Baier, Z. Fei, H. Gornitzka, A. Murso, S. Neufeld, M. Pfeiffer, I. Rüdenauer, A. Steiner, T. Stey, D. Stalke, *J. Organomet. Chem.* **2002**, *661*, 111-127.

[6]   L. Mahalakshmi, D. Stalke, *The R_2M^+ Group 13 Organometallic Fragment Chelated by P-Centered Ligands* in *Structure and Bonding - Group 13 Chemistry I, Vol. 103* (Ed. H. W. R. D. A. Atwood), Springer Verlag, Heidelberg, **2002**, pp. 85-115.

[7]   H. Gornitzka, D. Stalke, *Angew. Chem.* **1994**, *106*, 695-697; *Angew. Chem. Int. Ed. Engl.* **1994**, *33*, 693-695.

[8]   H. Gornitzka, D. Stalke, *Organometallics* **1994**, *13*, 4398-4405.

[9]   A. Steiner, D. Stalke, *J. Chem. Soc., Chem. Commun.* **1993**, 444-446.

[10]   A. Steiner, D. Stalke, *Organometallics* **1995**, *14*, 2422-2429.

[11]   A. Steiner, D. Stalke, *J. Chem. Soc., Chem. Commun.* **1993**, 1702-1704.

[12]   A. Steiner, D. Stalke, *Inorg. Chem.* **1995**, *34*, 4846-4853.

[13]   A. Noor, W. P. Kretschmer, G. Glatz, A. Meetsma, R. Kempe, *Eur. J. Inorg. Chem.* **2008**, *2008*, 5088-5098.

[14]   S. Qayyum, G. G. Skvortsov, G. K. Fukin, A. A. Trifonov, W. P. Kretschmer, C. Döring, R. Kempe, *Eur. J. Inorg. Chem.* **2010**, *2010*, 248-257.

[15]   H. Noss, M. Oberthür, C. Fischer, W. P. Kretschmer, R. Kempe, *Eur. J. Inorg. Chem.* **1999**, *1999*, 2283-2288.

[16]   C. Döring, W. P. Kretschmer, T. Bauer, R. Kempe, *Eur. J. Inorg. Chem.* **2009**, *2009*, 4255-4264.

[17]   C. Döring, W. P. Kretschmer, R. Kempe, *Eur. J. Inorg. Chem.* **2010**, *2010*, 2853-2860.

[18]   F. A. Cotton, L. M. Daniels, G. T. Jordan IV, C. A. Murillo, *J. Am. Chem. Soc.* **1997**, *119*, 10377-10381.

[19]   R. Fandos, C. Hernandes, A. Otero, A. Rodrigues, M. J. Ruiz, *J. Organomet. Chem.* **2005**, *690*, 4828-4834.

[20]   R. Clerac, F. A. Cotton, L. M. Daniels, K. R. Dunbar, C. A. Murillo, X. Wang, *Inorg. Chem.* **2001**, *40*, 1256-1264.

[21]   H. Gornitzka, D. Stalke, *Eur. J. Inorg. Chem.* **1998**, 311-317.

[22]   J. Ashenhurst, L. Brancaleon, S. Gao, W. Liu, H. Schmider, S. Wang, G. Wu, Q. G. Wu, *Organometallics* **1998**, *17*, 5334-5341.

[23]   M. Pfeiffer, A. Murso, L. Mahalakshmi, D. Moigno, W. Kiefer, D. Stalke, *Eur. J. Inorg. Chem.* **2002**, *2002*, 3222-3234.

[24]   A. F. Gushwa, A. F. Richards, *Journal of Chemical Crystallography* **2006**, *36*, 851-856.

[25]   J. A. Joule, K. Mills, *Heterocyclic Chemistry*, Blackwell Publishing, Chichester, **2000**.

[26]   G. J. Pyrka, A. A. Pinkerton, *Acta Crystallogr., Sect. C.* **1992**, *C48*, 91-94.

[27]   J. E. Johnson, R. A. Jacobson, *Acta Crystallogr., Sect. B.* **1973**, *B29*, 1669-1674.

[28]   L. M. Engelhardt, M. G. Gardiner, C. Jones, P. C. Junk, C. L. Raston, A. H. White, *J. Chem. Soc., Dalton Trans.* **1996**, 3053-3057.

[29]   A. Murso, M. Straka, M. Kaupp, R. Bertermann, D. Stalke, *Organometallics* **2005**, *24*, 3576-3578.

[30]   H. Xu, Z. Chao, Y. Sang, H. Hou, Y. Fan, *Inorg. Chem. Commun.* **2008**, *11*, 1436.

[31]   W.-P. Leung, K.-W. Wong, Z.-X. Wang, T. C. W. Mak, *Organometallics* **2006**, *25*, 2037-2044.

[32]   T. T. Tidwell, *Angew. Chem.* **2001**, *113*, 343-349; *Angew. Chem. Int. Ed.* **2001**, *40*, 331-337.

[33]   W. Schlenk, *Die Methoden der Organischen Chemie* in *Die Methoden der Organischen Chemie* (Ed. J. Houben), G. Thieme, Leipzig, **1924**, p. 720.

[34]   W. Schlenk, J. Holtz, *Ber. Dtsch. Chem. Ges.* **1917**, *50*, 262-274.

[35]   W. Schlenk, A. Thal, *Ber. Dtsch. Chem. Ges.* **1913**, *46*, 2840-2854.

[36]   M. J. S. Gynane, D. H. Harris, M. F. Lappert, P. P. Power, P. Rivière, M. Rivière-Baudet, *J. Chem. Soc., Dalton Trans.* **1977**, 2004-2009.

1 Introduction

Aiming on new metal coordination of *Janus-head* ligands, this work focuses on di(*2*-benzothiazolyl)phosphane. This ligand was developed and first isolated by *Stey* and *Stalke*.[1-3] It is based on a phosphorous centered double heteroaromatic substituted ligand continuing the ongoing research in the *Stalke* group.

This chapter gives insights into the preparation of the ligand as well as possible manipulations thereof. Additionally, it is the basis to understand the approach to the presented complexes in the following chapters.

2 Synthesis and structure

2.1 Di(*2*-benzothiazolyl)phosphane

The synthesis of the di(*2*-benzothiazolyl)phosphane leans on the preparation of di(*2*-pyridyl)phosphane. This is synthesized by a reaction of the tertiary phosphane with elemental lithium undergoing a carbon–phosphorus bond cleavage yielding the divalent phosphane. Different from the classical synthesis pathways to tertiary phosphane by direct coupling of lithiated organyls and phosphorous trichloride tri(*2*-bezothiazolyl)phosphane cannot be prepared directly. Direct reaction of (*2*-benzothiazolyl)lithium and phosphorous trichloride yields mainly the coupling product *2,2'*-dibenzothiazole as shown in scheme 1.[4]
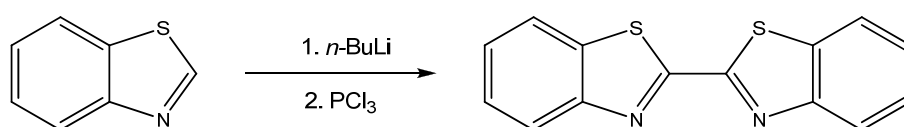
Scheme 1: formation of the coupling product.

To avoid the coupling reaction *Whitesides* and *Moore* synthesized the desired tertiary phosphane indirectly by a lithiation of benzothiazole with *n*-butyllithium at -78°C and quenching with trimethyl chlorosilane.[5] This intermediate can be purified by distillation, followed by addition of phosphorous trichloride at room temperature.[6] This slight detour avoids in addition the often complicating removal of lithium chloride from the phosphane in a very elegant way.

As mentioned above, a carbon–phosphorous bond is cleaved with elemental lithium followed by hydrolysis. Within this step a major problem occurs. On the one hand, the lithiation is carried out in tetrahydrofuran in order to achieve a good turnover, but the

desired product is not stable in that solvent. Hence, a solvent change after the lithiation is obligatory before one can precede the reaction by adding degassed water. Old lithium wire turned out to have the best reactivity for the cleavage. Pure and fresh powder leads mainly to a hardly controllable mixture, since a slow addition is problematic under the very necessary *Schlenk*-techniques and the exothermic reaction starts abruptly after a while. Turnings and fresh wire work much nicer than powder, and the reaction stays controllable.[7-9] Still older samples of lithium wire worked best. This might be reasoned by the higher impurities, mainly sodium.

According to *Stey*, di(2-benzothiazolyl)phosphane is only stable in diethyl ether, therefore it is the first choice as solvent. After hydrolyzing the reaction mixture, the product is purified using the "*Duchnick-Stey-Phospanapperille*" as Figure 1 shows.[1-3] This apparatus was developed due to failure of classical purification methods. Their failure is mainly caused by the low stability of the phosphane and its incompatibility towards many solvents. Additionally, its use provides a small thermal impact during the extraction, due to the low boiling point of diethyl ether.
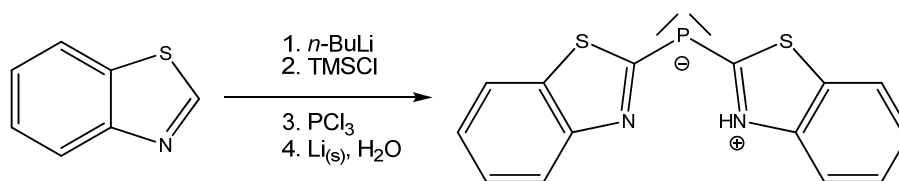
Scheme 2: preparation of di(2-benzothiazolyl)phosphane from benzothiazole.

The "*Duchnick-Stey-Phospanapperille*" combines extraction and drying directly from the reaction mixture in one step, and significantly increases the amount of pure product.

Dry diethyl ether is refluxed in the template flask (1) and passes gaseously through the riser (2). After condensing in the *Dimroth* cooling unit (3) it drops into the extractor (4) with a porous basis. This forces the solvent to get in contact with the reaction mixture in the extraction flask (5) and to enrich with the desired product. The solvent rises up to an overflow and runs back towards the template flask after being dried with magnesium sulfate (6). The diethyl ether starts off the cycle again while the phosphane stays in the template flask. Clean product precipitates in the template flask while the concentration rises. After 6-8 h of extraction time per 80 mmol pure product, the precipitate is filtered and dried *in vacuo*. The product is storable in an argon atmosphere at –40°C for about 2 months.
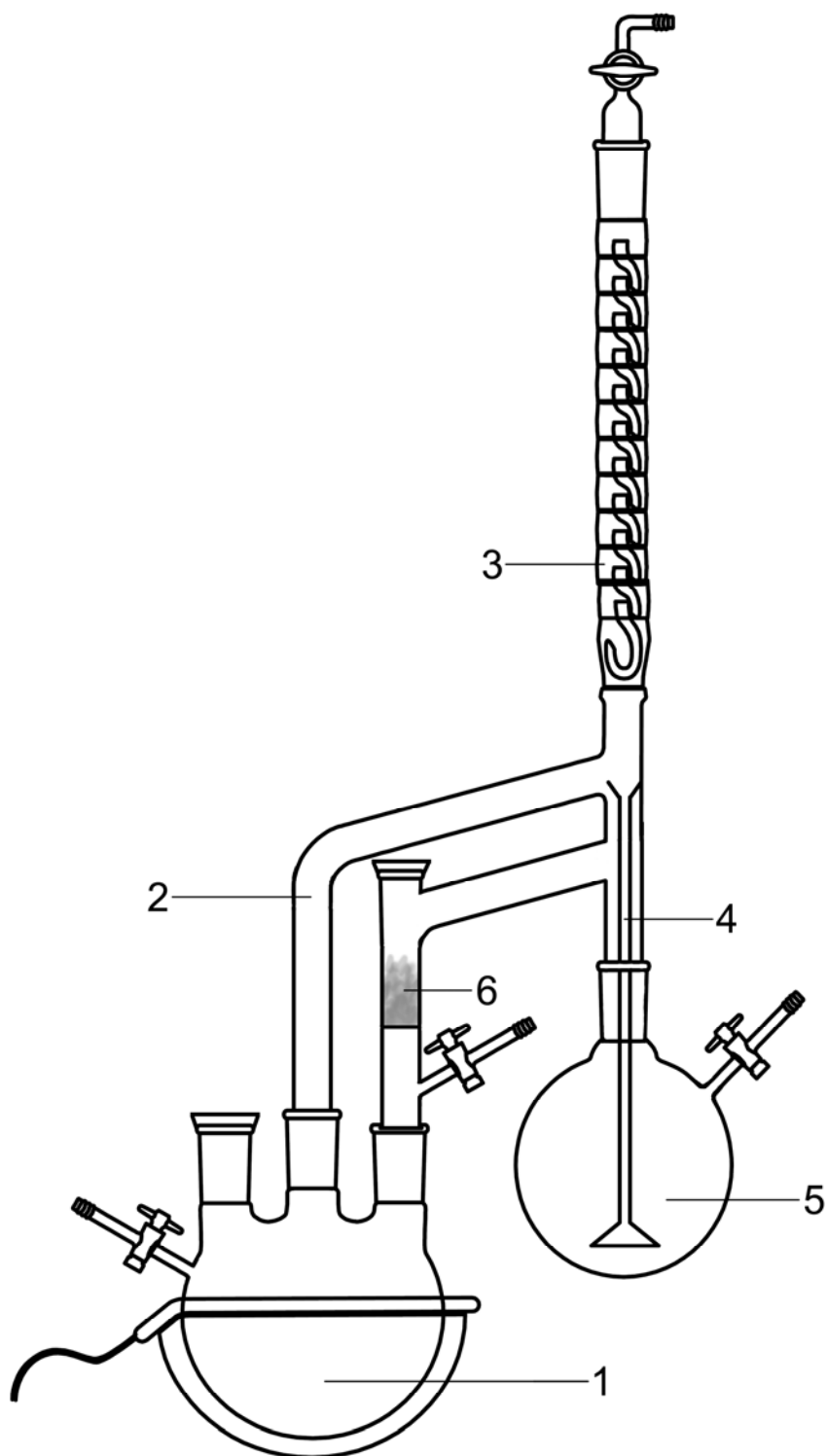
Figure 1: The new developed "*Duchnik-Stey-Phosphanapparille*" with a template flask (1), a riser (2), a Dimroth cooling unit (3), an extractor (4), an extraction flask (5), and a stock of $MgSO_4$(6).
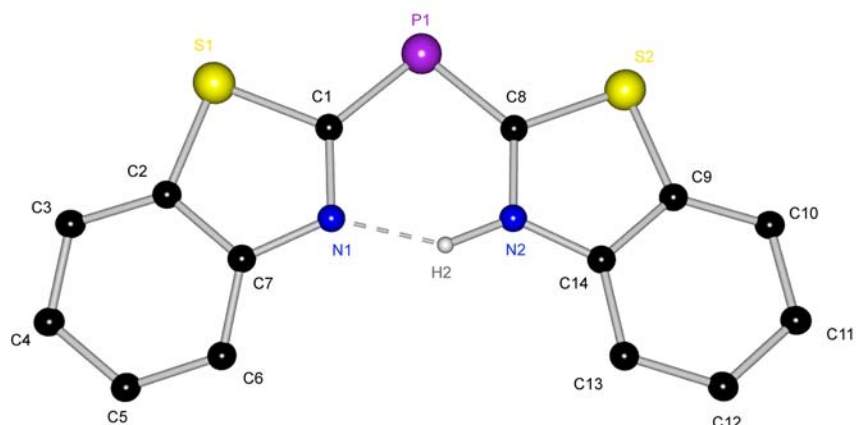
Figure 2: solid state structure of di(2-benzothiazolyl)phosphane (**1**). Hydrogen atoms omitted for clarity.

Table 1: Selected bond lengths [pm] and angles [°] of di(2-benzothiazolyl)phosphane (**1**).

P1–C1	178.4(5)	C1–P1–C8	98.7(2)
P1–C8	177.8(4)	P1–C1–N1	128.6(3)
C1–N1	133.1(6)	P1–C8–N2	129.0(4)
C8–N2	133.4(5)	C1–N1···H2	103.5(14)
N1···H2	192(5)	C8–N2–H2	119(3)
N2–H2	85(5)	bth–bth'	10.4

Di(2-benzothiazolyl)phosphane crystallizes in the orthorhombic space group *Pbca* with the whole molecule in the asymmetric unit. The secondary phosphane contains a divalent phosphorous atom. Interestingly, it is only bonded to both benzothiazole molecules. A third bond to a hydrogen atom is not found. Both, the N–C_{ipso} and the P–C bond distances are equal within their standard deviation and located between a double and single bond. The best planes of the benzothiazole units are twisted by only 10.4°.

As previously predicted, the hydrogen atom is located at the N2 and interacts with N1 by a hydrogen bridge. This hydrogen bridge has a rather short bond distance of only 192 pm.[10] It includes an angle of 140°. Comparing both nitrogen atoms shows a few differences. N1 is bonded to its nearby carbon atoms slightly shorter than N2, but within their estimated standard deviations the bonds are equal. Both are within the best planes standard deviation of their associated benzothiazole and their angle sum adds up to 359.3° at N1 and 358.1° at N2 respectively. The C–N–H angles differ because of the different N–H bond lengths. All these facts hint to a sp²-hybridisation.

The benzene rings do not show significant differences in bond length and angles to those of the comparable tri(2-benzothiazolyl)phosphane.[3]

NMR studies on the ligand do not show a $^1J_{P-H}$ coupling underlining the absence of a P–H bond even in solution.

The reported results are in contrast to the earlier reported di(2-pyridyl)phosphane. Divalent phosphanes were reported earlier by *Becker* and *Westerhausen* but are still much unexpected products due to the uncommon electronic situation within the molecule.[11-13] Therefore it is difficult to find a Lewis structure displaying all features in an adequate way.

On the one hand one could think of a phosphanide-like structure as shown in Scheme 3**a** or a phosphane like character as shown in **b**. The phosphanide-like structure is a four electron donor at the phosphorous atom therefore a bridging coordination behavior is anticipated. In contrast the phosphane-like structure is a two electron donor with a divined terminal coordination behavior.
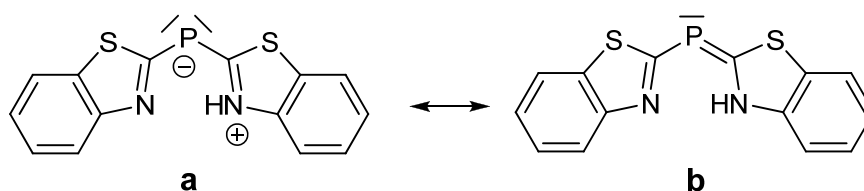
Scheme 3: resonace formula of HP(bth)$_2$ as a phosphanide-like structure
(**a**) und as a phosphane-like structure (**b**).

During this work it was possible to determine the structure at 15 K at high resolution. Preliminary results of a charge density study by *Jakob Hey* from the *Stalke* workgroup showed two lone-pairs at the phosphorous atom. Additionally, he showed contrary to the before postulated aromatic character of the benzothiazole two lone pairs at each sulfur atom.[14] Figure 3 shows the Laplacian plots at the phosphorous atom and at each sulfur atom illustrating the lone pairs at the heteroatoms.

The preliminary results from the experimental charge density study emphasize the earlier reported phosphanide-like structure of HP(bth)$_2$. In addition it clearly shows the sp^3-hybridisation of the phosphorous atom and the sulfur atoms accompanied with the non-aromatic character of the five-membered rings. Counting electrons on the basis of these results ends up with P(bth)$_2^-$ as potentially 4 electron donor – four electrons from the two sulfur atoms, four electrons from the phosphorous atom and two electrons from the non-protonated nitrogen atom.
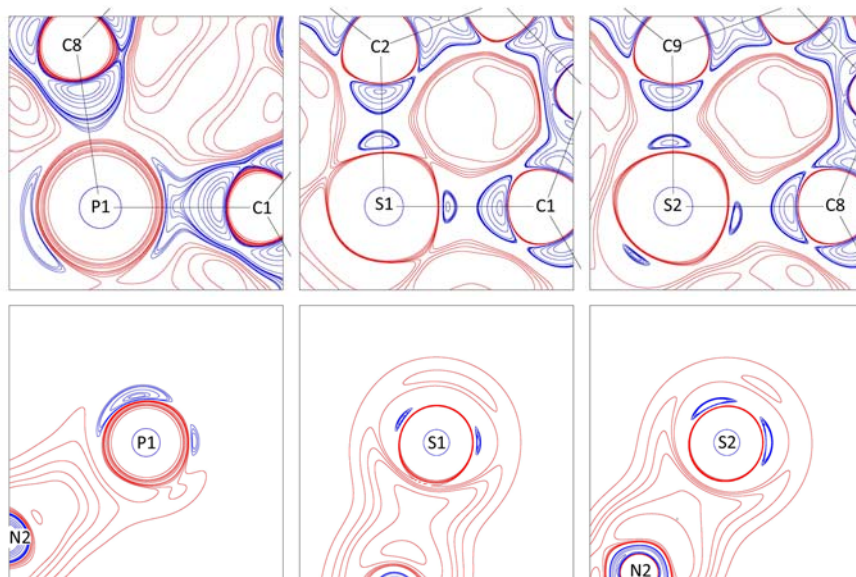
Figure 3: VSCC-plots from the experimental charge density study by
Jakob Hey on HP(bth)$_2$.

As mentioned above, HP(bth)$_2$ was described to be unstable in any other solvent than diethyl ether while its metalated products tolerate most solvents. A crystallization attempt yielded only the pure ligand with co-crystallized toluene as shown in Figure 4. This surprising result provided the basis for the heterobimetallic complexes reported in chapter 6 even if its solubility in toluene is rather poor.
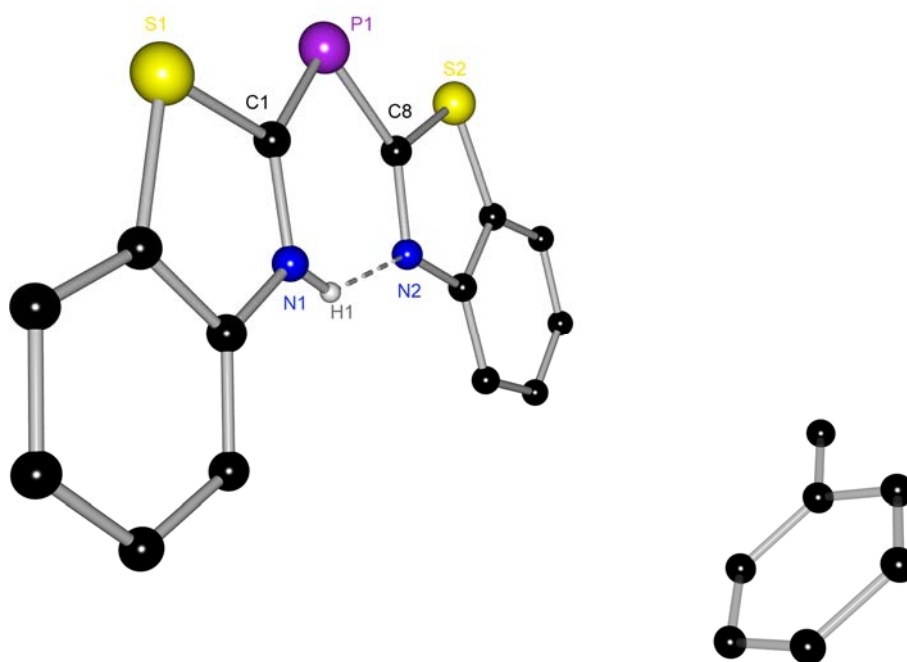
Figure 4: solid state structure of di(*2*-benzothiazolyl)phosphane with toluene
(**2**). Hydrogen atoms omitted for clarity.

Table 2: Selected bond lengths [pm] and angles [°] of di(*2*-benzothiazolyl)phosphane with toluene (**2**)

P1–C1	175.4(2)	C1–P1–C8	98.90(10)
P1–C8	180.5(2)	P1–C1–N1	129.28(15)
C1–N1	133.6(3)	P1–C8–N2	130.08(16)
C8–N2	131.2(2)	C1–N1–H2	118.9
N1–H2	81.4	C8–N2–H2	101.1
N2-H2	197.8	bth–bth'	4.4

As expected, the HP(bth)$_2$ does not show particular differences in bond lengths and angles within apart from the toluene.

2.2 Modification at the benzothiazole

Modifications at the benzothiazole are interesting for many reasons. On the one hand it influences the donation ability of the ligand. On the other hand it can provide steric bulk to protect and stabilize interactions at the coordinated metal atom. Last but not least it can provide chiral information transferred into a catalytic cycle.

Focusing on the given ligand, modifications at the benzothiazole should be accomplished in an early state of the preparation due to its low stability. Hence, we decided to modify the benzothiazole in a first step and build up the ligand in similar way as mentioned above. Taking the bend structure of the ligand into account, the 4 position of the benzothiazole seemed favorable. By our requirements the prospective modification had to be free of heteroatoms as potential donors, flexible and small enough to keep the ligands planar backbone. Hence, we decided on an isopropyl-group.
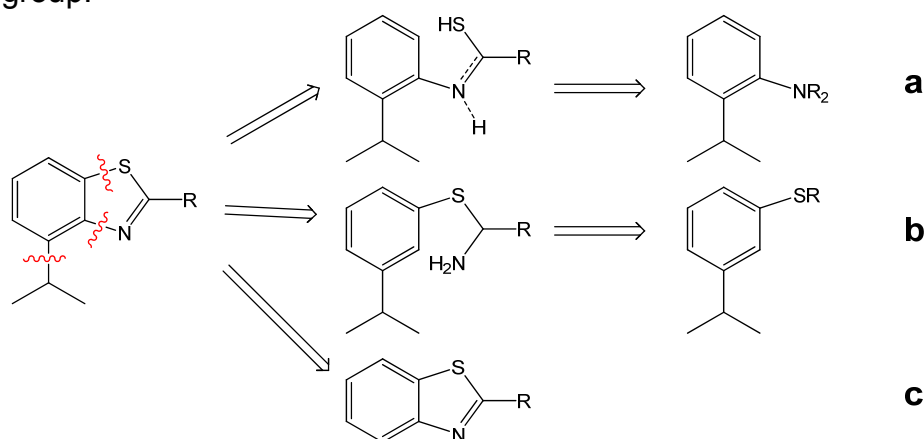
Scheme 4: retro-synthesis of 4-substituted benzothiazole.

Scheme 4 shows the retro-synthesis of the *4*-substituted benzothiazole. Route **a** leads to substituted aniline. Aniline and its derivatives are widely spread, easy to handle and commercially available at low cost. In addition a lot of amine chemistry as well as reactions of the aniline are reported in the literature. Similar is route **b** starting from (*3*-isopropyl)benzenethiol. Again, the compound is commercially available but far more expensive than aniline. Furthermore, there are two potential regionisomers for the ring closing reaction. Route **c** starts from the benzothiazole. Therefore a selective substitution directly at the benzene is necessary. Some examples of are reported to the literature, either in *6*- or *7*-position or introducing mainly oxygen at the *4*-position. In 2009 *Wunderlich* and *Knochel* showed a highly chemoselective preparation of a *4*-substituted benzothiazole.[15] The reaction cascade starts with the lithiation of an imine with *tert*-butyllithium, followed by a transmetallation with aluminum trichloride. In the presence of zinc dichloride and accrued lithium chloride this base deprotonates the benzothiazole chemoselectively in *4*-position. In a palladium(0) catalysed coupling a new group is inserted. In order to achieve acceptable yields these new groups are limited to (substituted) benzene iodides. Within this work it was possible to reproduce the substitution, but an upscale to more than 1 g product was not possible.

For economic reasons and need of high yields we decided to start from (*2*-isopropyl)aniline.
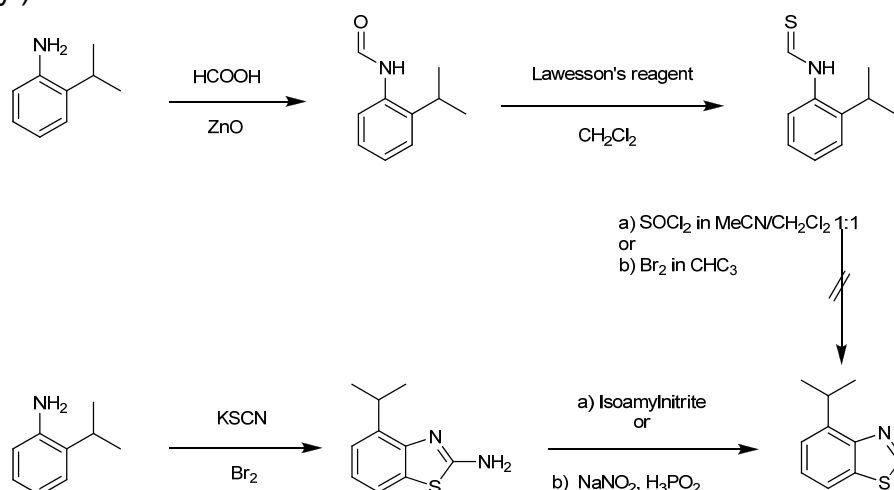
Scheme 5: reaction pathways from (*2*-isopropyl)aniline to the

(*4*-isopropyl)benzothiazole.

Scheme 5 shows the different tested reaction pathways from (*2*-isopropyl)aniline to the (*4*-isopropyl)benzothiazole. In the upper pathway the first step is formylation of aniline followed by oxygen sulfur exchange.[16-18] Both reactions are straight forward

organic reactions followed by convenient purification effort. It was not possible to find a suitable ring closing reaction since the yield was poor and the product hard to purify.[19,20] The second reaction is also really easy to perform.[21] A mixture of (2-isopropyl)aniline, KSCN and bromine in acetic acid is stirred for 2 days. After neutralization the (2-isopropyl)benzothialzolylamin is extracted with dichloromethane. Removal of the amine is a common reaction one can easily find in many textbooks on organic chemistry. It is possible to upscale this approach on (4-isopropyl)-benzothiazole to any laboratory-scale.

As mentioned above, a similar procedure to convert the substituted benzothiazole to a divalent phosphane as for the non-substituted was expected. Indeed, a different behavior towards the lithiation was found.
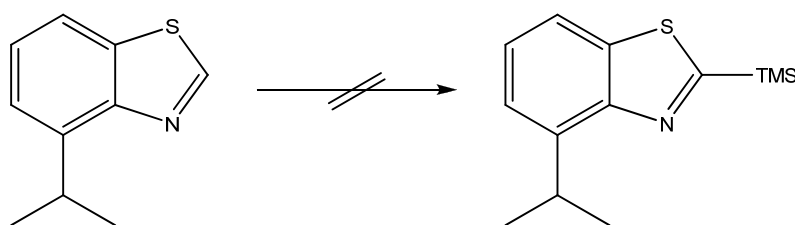
Scheme 6: a direct reaction pathway analog to the non-substituted benzothiazole is not possible.

While the non-substituted benzothiazole is only deprotonated at the 2-position, the new (4-isopropyl)benzothiazole is deprotonated at the isopropyl-residue as well. Thus a product mixture was found after quenching with trimethylchlorosilane. Separation and purification of the mixture is not possible by destillation or liquid chromatography. Unfortunately this happens in all experiments with different lithium organics even at – 78°C. Hence, another pathway to introduce the silyl group was necessary.
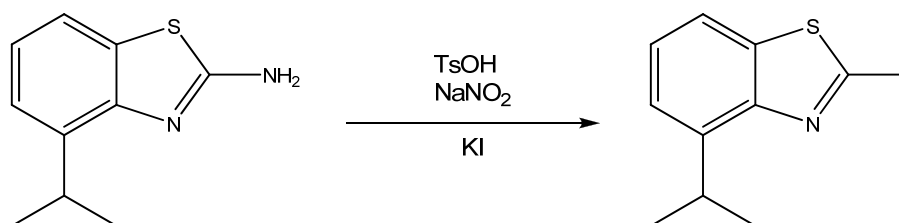
Scheme 7: preparation of (2-iodo)(4-isopropyl)benzothiazole analog to *Knochel* and coworkers.

For synthesis of (4-isopropyl)benzothiazolylamine exist different pathways. In a *Sandmeyer* reaction amines quickly react with nitrite to form a diazonium salt.[22,23] This decomposes with a given nucleophile. *Knochel* and co-workers designed in

2007 conditions especially for (2-amino)benzothiazole.[24] Their recipe can be transferred to the substituted benzothiazole with minor changes as Scheme 7 shows. The (2-iodo)(4-isopropyl)benzothiazole allows two different reaction pathways: on the one hand a reaction with lithium organics might be possible due to the pronounced lithium-halogen exchange compared to a deprotonation at low temperatures followed by an addition of trimethylchlorosilane. On the other hand it is the basis for *Grignard* reactions. Both possibilities should allow a carbon–phosphorous coupling as a next step leading towards tri-substituted phosphane.

To cut a long story short none of these possibilities worked. Lithium organics again were not regioselective, and the Grignard organic of benzothiazole could not be generated neither by reaction with activated magnesium nor by reaction with other Grignard organics.

2.3 Di(*2*-benzothiazolyl)phosphanide lithium

Lithium complexes are commonly used as a basis for transmetallation reactions. To keep the equivalents right it is very important to know the exact constitution. Additionally, the structure allows a prognosis on the reactivity and the hints to coordination modes of further metals. *Stey* presented a monomeric lithium structure already.[2,25] In the monomer lithium is *N,N*-coordinated and two molecules of diethyl ether fill up its coordination sphere. During this work it was possible to crystallize another lithium complex. As before, it was prepared by the addition on *n*-butyl lithium to the ligand in diethyl ether at –78°C.
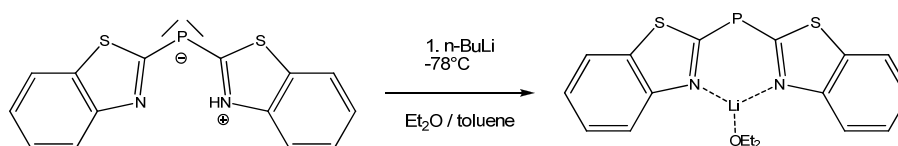
Scheme 8: preparation of [(Et$_2$O)$_2$Li(bth)$_2$P]$_2$.

In contrast to the earlier reported structure it was crystallized from the non-donating solvent toluene. Figure 5 shows the dimeric structure. Other then assumed the phosphorous atom can obviously coordinate hard metals as well if the coordination sphere is not filled up with a second donor molecule. This structural motif is also known from the softer metals zinc and cadmium.[1-3] [(Et$_2$O)Li(bth)$_2$P]$_2$ crystallizes in the monoclinic spacegroup *P*2$_1$/*n*. Both ligands do not differ due to their symmetrical equality. The lithium atom is coordinated equally by the nitrogen atoms, hence the

inequivalency of both heteroaromatic rings like in the di(2-benzothiazolyl)phosphane is not longer pronounced. Additionally one diethyl ether molecule is coordinated to the lithium. The coordination sphere is completed by the phosphorus atom of another ligand to form the dimer. The P–Li–P'–Li' four membered ring forms a rhomb with an inner angle of 78° at the phosphorous atoms and 102° at the lithium atoms. Both benzothiazoles best planes are twisted by 10.3°. The lithium atom is 45.4 pm beneath the N–P–N plane. P'–Li bond length is 284.0 pm.
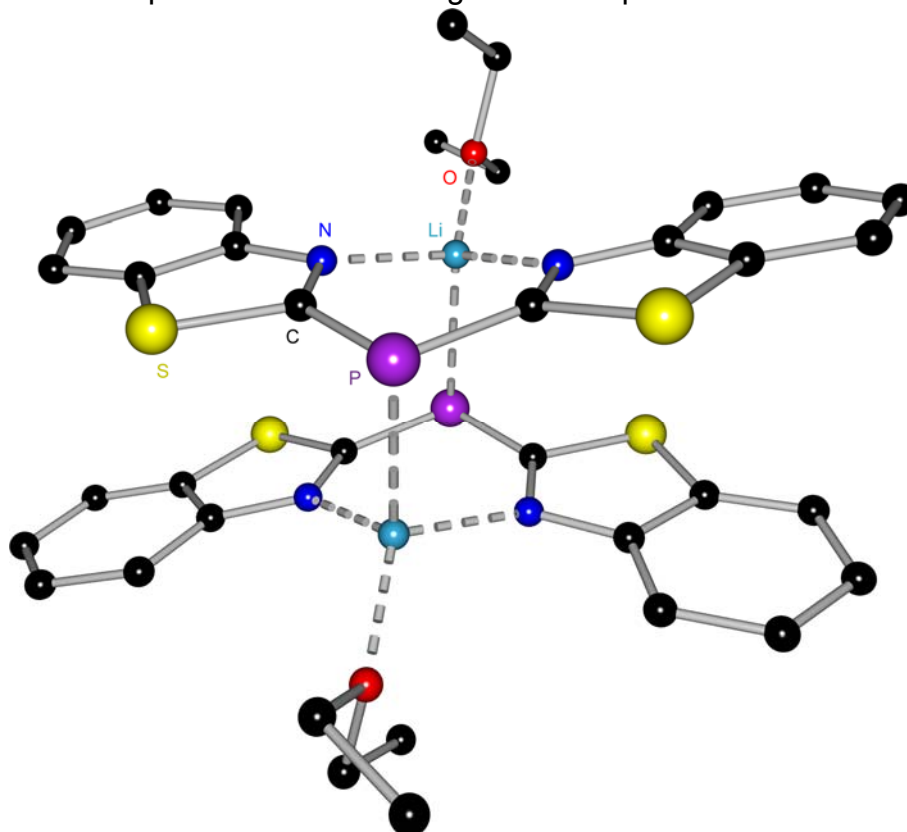
Figure 5: solid state structure of $[(Et_2O)Li(bth)_2P]_2$, hydrogen atoms omitted for clarity.

Table 3: Selected bond lengths [pm] and angles [°] of di(2-benzothiazolyl)phosphanid lithium.

P1–C1	179.3(3)	C1–P1–C8	104.13(12)
P1–C8	178.7(3)	P1–C1–N1	133.3(2)
C1–N1	131.8(3)	P1–C8–N2	132.8(2)
C8–N2	132.0(3)	C1–N1–Li1	121.5(2)
N1–Li1	201.2(4)	C8–N2–Li1	122.2(2)
N2-Li1	1.992(4)	P1–Li1–P1'	117.1(2)
P1–Li1'	284.0(11)	C1–P1–Li1'	96.50(12)
Li1–O1	194.6(4)	bth–bth'	10.3

The bond lengths and angles are similar to their analogous reported by *Stey*.[1-3] The structural motif underlines again the posphanide nature of the ligand.

Even in a solution of deutero toluene the complex is stable as e.g. the downfield shift in the ^{31}P-NMR shows. Only the donating diethyl ether was removed while drying the crystals.

3 Conclusion

There were two major difficulties to yield the desired di(*2*-benzothiazolyl)phosphane. On the one hand the preparation of the tertiary phosphane, solved by *Whitesides* and *Moore*,[5] on the other hand the purification of the di(2-benzothiazolyl)phosphane after the carbon–phosphorous bond cleavage. For the latter *Stey* and his technician developed the "*Duchnick-Stey-Phospanapperille*".[25] With the help of this apparatus di(2-benzothiazolyl)phosphane is available in moderate yields at a good purity.

Still unsolved is the storage due to the low stability. Temperatures beneath –40° might be useful but are hardly possible in an argon glove box. The latter is very important for the handling in an inert gas atmosphere.

The new determined structure with co-crystallized toluene hints to a sufficient stability in other solvents. Using this quality chapter VI presents new approaches to heterobimetallic complexes of the ligand presented within this chapter.

Furthermore, a very easy and versatile method to approach 4-substituded benzothiazole was demonstrated. This new route is very tolerant towards many substitutions of the starting aniline.

Unfortunately, it was not possible to convert the chosen (*4*-isopropyl)benzothiazole to an analogous divalent phosphane. The occurred problems should be avoided by another substituent.

Finally, a coordination motif so far only known including soft metals was transferred to the hard metal lithium. This underlines the immense versatility of the presented Janus head ligand.

4 Experimental

4.1 General

All manipulations were carried out with strict exclusion of air and moiety in nitrogen or argon atmosphere using modified *Schlenk*-techniques or in an argon dry box.[7-9] All solvents were either dried on standard laboratory procedures and were freshly distilled from sodium/potassium alloy prior to use or directly used from a MBraun SPS connected to the glove box. All employed reactants were commercially available or reproduced by literature known procedures.

4.2 Spectroscopic and analytic methods

4.2.1 Nuclear Magnetic Resonance

All probes were prepared and bottled within the argon dry box into Schlenk-NMR-tubes. The NMR-tube was sealed to exclude any impurities. Solvents were dried with potassium. Spectra were recorded at room temperature at a *Bruker Avance 300* or a *Bruker Avance 500* NMR spectrometer.

All chemical shifts δ are given relative to their usual standards and coupling constants *J* are given in Hz. Assignments of the shifts were checked by 2d-correlation spectra. NMR shifts are assigned to the given scheme.

4.2.2 Mass spectrometry

EI-spectra were recorded with a *MAT 95* device (EI-MS: 70 eV). Peaks are given according to the abundance of the main isotope as a mass to charge ratio *m/z*.

4.3 (*2*-amino)(*4*-isopropyl)benzothiazole

7.0 mL (6.8 g, 50 mmol) (*2*-isopropyl)aniline were dissolved in 60 mL acetic acid and 20 g (206 mmol) KSCN and stirred at room temperature. Afterwards 2.5 mL (60 mmol) bromine in 30 mL acetic acid were added within 15 min. and the mixture was stirred at room temperature for 20 h.

After the mixture was poured over ice water it was neutralized by NaOH (2N) and extracted with dichloromethane (4 x 150 mL). The combined organic phases were dried with $MgSO_4$ and all volatile material was removed *in vacuo*. The product was isolated as a yellow oil.

Sum formula:	$C_{10}H_{12}N_2S$

Molecular weight:	192.3 g/mol

^{1}H-NMR (200 MHz):   δ: 1.26 (d, ^3J = 6.8, 6 H, 2'-H$_3$, 2''-H$_3$), 2.87 (h, ^3J = 6.8, 1 H, 1'-H), 6.75 (d, ^3J = 8.2, 1 H, 5-H), 7.23 (dd, ^3J = 8.2, ^4J = 2.2, 1 H, 6-H), 7.30 (s$_{br}$, 2 H, NH$_2$), 7.32 (d, ^4J = 2.2, 1 H, 7-H) ppm.

EI-MS: *m/z* (%):   192 (60) [M], 177 (100) [M-NH$_2$], 150 (20) [M-*i*Pr], 135 (8) [M-NH$_2$-*i*Pr].

4.4 (*2*-iodo)(*4*-isopropyl)benzothiazole

9.6 g (50 mmol) (*2*-amino)(*4*-isopropyl)benzothiazole and 29 g (150 mmol) *p*-toluenesulfonic acid were dissolved in 180 mL MeCN and 6.7 g (97 mmol) NaNO$_2$ in 20 mL water were added slowly at 0°C. Afterwards 20 g (120 mmol) KI in 20 mL water were added drop wise. After stirring 3 h at room temperature the mixture was diluted with 750 mL water and the pH = 9–10 adjusted with solid NaHCO$_3$. After washing with a aqueous thiosulfate solution the mixture was extracted with dichloromethane (4 x 250 mL). The combined organic phases were dried over MgSO$_4$ and all volatile material was removed in vacuo. The product was isolated as an orange oil.

Sum formula:	$C_{10}H_{10}INS$

Molecular weight:	303.2 g/mol

^{1}H-NMR (300.13 MHz):   δ: 1.26 (d, ^3J = 6.8, 6 H, 2'-H$_3$, 2''-H$_3$), 3.20 (h, ^3J = 6.8, 1 H, 1'-H), 7.06 (dd, ^3J = 8.2, ^4J = 2.2, 1 H, 6-H), 7.34 (d, ^4J = 2.2 Hz, 1 H, 7-H), 7.86 (d, ^3J = 8.2, 1 H, 5-H) ppm.

EI-MS: *m/z* (%):   303(100) [M], 288 (83) [M-CH$_3$], 177 (3) [M-I], 161 (32)[M-I-CH$_3$].

4.5 di(*2*-benzothiazolyl)phosphanide lithium

1.0 g (3.33 mmol) di(*2*-benzothiazolyl)phosphane was dissolved in 50 mL diethyl ether and 2.50 mL n-butyl lithium(1.4 M in hexane, 3.5 mmol) were added drop wise at –78°C. After stirring 1 h all volatile were removed in vacuum. Crystallization from a saturated solution in toluene yielded suitable single crystals for an X-ray diffraction experiment at 4°C within one month.

Sum formula: $C_{36}H_{36}Li_2N_4O_2P_2S_4$

Molecular weight: 760.16 g/mol

^{1}H-NMR (300.13MHz):   δ: 7.10–7.19 (m, 8H, *5, 6*); 7.57–7.68 (m, 8H, *4, 7*) ppm.

^{7}Li-NMR (116.642 MHz): δ: 1.24 (s) ppm.

^{13}C-NMR (75.468MHz):   δ: 121.80 (s, *4*); 124.09 (s, *7*); 126.11 (s, *6*); 128.35 (s, *5*); 135.72 (s, *7a*); 136.32 (s, *3a*); 153.39 (d, *2*) ppm.

^{15}N-NMR (30.423 MHz):   δ: –63.47 (s) ppm.
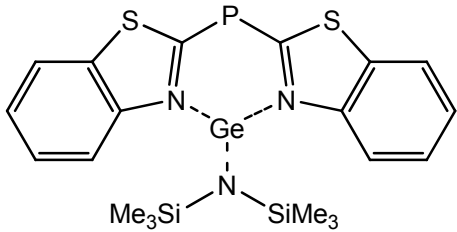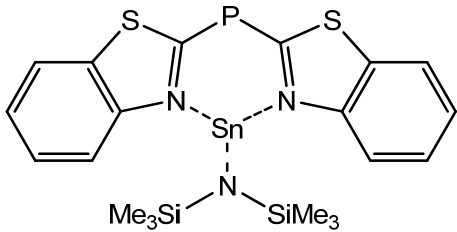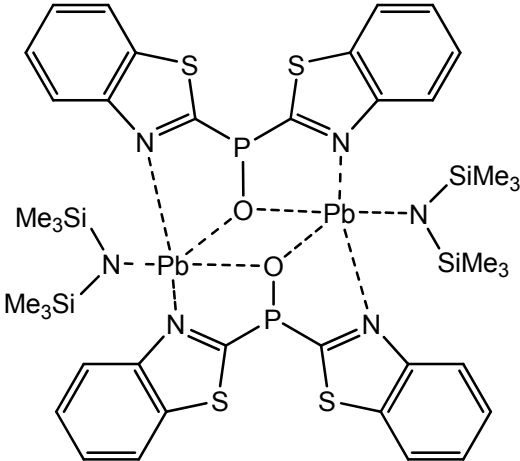
^{31}P-NMR (121.495 MHz): δ: 0.91 (s) ppm.

5 Literature

[1]   T. Stey, D. Stalke, *Z. Anorg. Allg. Chem.* **2005**, *651*, 2931-2936.

[2]   T. Stey, J. Henn, D. Stalke, *Chem. Commun.* **2007**, 413-415.

[3]   T. Stey, M. Pfeiffer, J. Henn, S. K. Pandey, D. Stalke, *Chem. Eur. J.* **2007**, *13*, 3636-3642.

[4]   A. Steiner, D. Stalke, *J. Chem. Soc., Chem. Commun.* **1993**, 444-446.

[5]   S. S. Moore, G. M. Whitesides, *J. Org. Chem.* **1982**, *47*, 1489-1493.

[6]   F. H. Pinkerton, S. F. Thames, *Organosilicon Compounds* **1971**, 257.

[7]   W. Schlenk, A. Thal, *Ber. Dtsch. Chem. Ges.* **1913**, *46*, 2840-2854.

[8]   W. Schlenk, J. Holtz, *Ber. Dtsch. Chem. Ges.* **1917**, *50*, 262-274.

[9]   T. T. Tidwell, *Angew. Chem.* **2001**, *113*, 343-349; *Angew. Chem. Int. Ed.* **2001**, *40*, 331-337.

[10]   G. R. Desiraju, T. Steiner, *The Weak Hydrogen Bond* in *IUCr Monographs on Crystallography 9*, Oxford University Press, Oxford, **1999**.

[11]   G. Becker, H. P. Beck, *Z. Anorg. Allg. Chem.* **1977**, *430*, 77-90.

[12]   G. Becker, W. Becker, M. Schmidt, M. Westerhausen, *Z. Anorg. Allg. Chem.* **1991**, *605*, 7-23.

[13]   G. Becker, M. Schmidt, M. Westerhausen, *Z. Anorg. Allg. Chem.* **1992**, *608*, 33-42.

[14]   J. Hey, *Private Communication* **2010**.

[15]   S. H. Wunderlich, M. Kienle, P. Knochel, *Angew. Chem.* **2009**, *121*, 7392-7396; *Angew. Chem. Int. Ed.* **2009**, *48*, 7256-7260.

[16]   R. I. C. Hurd, G. de la Mater, *Chem. Rev.* **1961**, *61*, 41-86.

[17]   M. Hosseini-Sarvari, H. Sharghi, *J. Org. Chem.* **2006**, *21*, 6652-6654.

[18]   M. P. Wentland, X. Sun, Y. Bu, R. Lou, D. J. Cohen, J. M. Bidlack, *Bioorg. Med. Chem. Lett.* **2005**, *15*, 2547-2551.

[19]   M. Chakrabarty, N. Ghosha, Y. Harigaya, *Tetrahedron Lett.* **2004**, *45*, 4955-4957.

[20]   T. Papenfuhs, *Angew. Chem.* **1982**, *94*, 544; *Angew. Chem. Int. Ed. Engl.* **1982**, *21*, 1155-1166.

[21]   P. Jimonet, F. Audiau, M. Barreau, J.-C. Blanchard, A. Boireau, Y. Bour, M.-A. Cole´no, A. Doble, G. Doerflinger, C. Do Huu, M.-H. Donat, J. M. Duchesne, P. Ganil, C. Gueremy, E. Honore, B. Just, R. Kerphirique, S. Gontier, P. Hubert, P. M. Laduron, J. Le Blevec, M. Meunier, J.-M. Miquet, C. Nemecek,

M. Pasquet, O. Piot, J. Pratt, J. M. Rataud, Reibaud, J.-M. Stutzmann, S. Mignani, *J. Med. Chem.* **1999**, *42*, 2828-2843.

[22]   T. Sandmeyer, *Ber. Dtsch. Chem. Ges.* **1884**, *17*, 2650-2653.

[23]   T. Sandmeyer, *Ber. Dtsch. Chem. Ges.* **1884**, *17*, 1633-1635.

[24]   E. A. Krasnokutskaya, N. I. Semenischeva, V. D. Filimonov, P. Knochel, *Synthesis* **2007**, *1*, 81-84.

[25]   T. Stey, Ph.D. thesis, Universität Würzburg (Germany), **2004**.

1 List of compounds

Name	number	Lewis formula
Di(2-benzothiazolyl)phosphanid bis-(trimethylsilyl)amide germanium(II)	**1**	
Di(2-benzothiazolyl)phosphanid bis-(trimethylsilyl)amide tin(II)	**2**	
Di(2-benzothiazolyl)phosphanid-bis(trimethylsilyl)amidelead(II)oxid	**3**	

2 Introduction

One of the greatest milestones in human evolution has been the discovery of hardening the easily melted and rather soft copper with tin. This marks the beginning of bronce.

Modern tin chemistry dates back to 1605 to the experiments of *Libavius* preparing tin(IV) chloride. The first organotin compound, namely diethyl tin diiodide, was already prepared in 1849 by *Frankland*.[1]

Nowadays, group 14 complexes are in the focus of research because of their multiple bonding behavior as higher carbon homologues, their use as carbenes in catalysis and different pharmaceutical applications.[2-9]

Hexamethyldisilyl amide metal complexes were the main research subjects in the past. By now many synthetic routes towards main group and transition metals in different oxidation states are available. The amides are mostly available by transmetalation from their alkali metal amides and very efficient purification methods are reported in literature.[10-15] Due to their amidic character, these metal compounds are good starting material for direct metalation by deprotonation. The main advantage of this reaction pathway is the low purification efforts at the end of the reaction since the residual products are volatile. Therefore, metal complexes of hexamethyldisilyl amides are efficient starting materials for metallization reactions. By now, *Stey* showed the suitability of hexamethyldisilyl metal amides in various cases. A tin complex that was characterized by X-ray and ^{1}H-NMR analysis has to be mentioned in this context.

This motivated us to take a closer look onto the analogous group 14 elements and to complete the spectroscopic data. For this purpose, the reported procedure was repeated and improved. Afterwards it was extended to germanium and lead whereas the resulting products have been fully characterized.

3 Synthesis and structure

3.1 Di(*2*-benzothiazolyl)phosphanide-bis(trimethylsilyl)amide-germanium(II)

Inspired by a reported tin complex of di(*2*-benzothiazolyl)phosphane by *Stey*, other complexes of group 14 homologous are predictable.[16] Hence, freshly prepared [Ge{N(SiMe$_3$)$_2$}$_2$] was added to a diethyl ether solution of the ligand at –78°C.[2] While warming up, a reaction became slowly observable by the color changing from yellow to red. While rerunning this reaction, the conditions were optimized. A convenient reaction pathway is to mix all reactants in a dry box, where they are well storable, and add diethyl ether outside the dry box at –10°C using *Schlenk* techniques. This allows an easy handling while achieving a good yield and high purity.
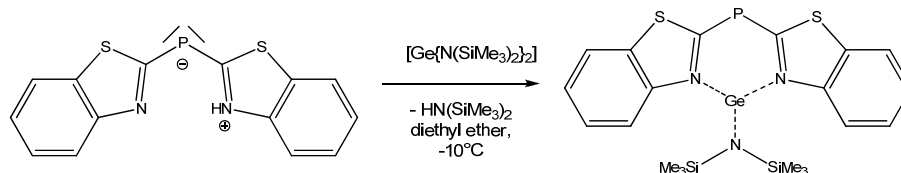
Scheme 1: preparation of di(2-benzothiazolyl)phosphanide-bis(trimethylsilyl)amide-germanium(II).

The reaction mixture was allowed to reach room temperature, while stirring over night. After removal of all volatile material *in vacuo*, the residual solid was dissolved in diethyl ether again. From the saturated solution single crystals suitable for an X-ray experiment were obtained over night. Repetition of the experiment in order to achieve a double coordination of the metal atom yielded always the mono coordinated species.
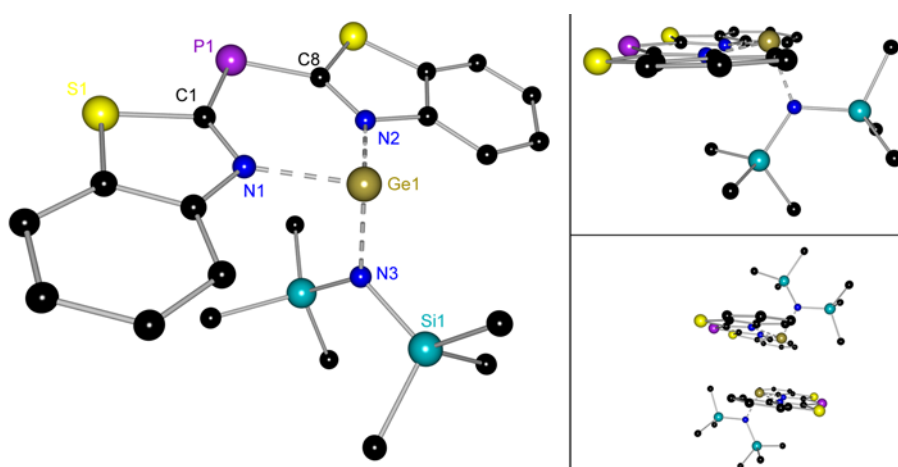
Figure 1: solid state structure of di(*2*-benzothiazolyl)phosphanide-bis(trimethylsilyl)-amide-germanium(II). Hydrogen atoms omitted for clarity.

Table 1: Selected bond lengths [pm] and angles [°] of di(2-benzothiazolyl)phosphanide-bis(trimethylsilyl)amide-germanium(II).

P1–C1	176.83(15)	C1–P1–C8	101.31(7)
P1–C8	176.74(16)	C1–N1–Ge1	130.31(10)
C1–N1	133.54(18)	C8–N2–Ge1	130.62(10)
C8–N2	133.27(18)	N1–Ge1–N2	89.93(5)
N1–Ge1	204.72(12)	N1–Ge1–N3	97.90(5)
N2-Ge1	205.41(12)	N2–Ge1–N3	98.74(5)
N3–Ge1	190.50(11)	bth–bth'	7.9

Di(2-benzothiazolyl)phosphanide-bis(trimethylsilyl)amide germanium(II) crystallizes in the triclinic space group $P\bar{1}$. The asymmetric unit contains two formula units. The cationic germanium atom is coordinated by the nitrogen atoms of both benzothiazole units and the nitrogen atom of the bis(trimethylsilyl)amide unit. The P–C$_{ipso}$ bond distances are 176.4 pm in average. These distances are between those expected for a single (185 pm) and a double bond (167 pm). The N–C$_{ipso}$ bonds are slightly shorter than in the undeprotonated ligand. The C–P–C angle is 101.4°, therefore close to the earlier reported complexes. The best planes of the benzothiazole units are twisted by only 7.9°. The phosphorous atom is in the C$_{ipso}$–C'$_{ipso}$–N–N' plane. All bond lengths and angles of the benzothiazole units do not show significant differences. A Ge–P contact to another molecules in the crystal seems possible on the first sight, but a distance of ~460 pm contradicts a bond. These results hint to a charge-localization at the phosphorous atom to form a phosphanide. Hence, the phosphorous atom is sp^3-hybridized carrying two lone pairs. These lone pairs couple in the benzothiazole rings and as a consequence the P–C$_{ipso}$ bonds are shorter.

Formally, the germanium has a double positive charge. The Ge–N$_{bth}$ bond distances are average 205.5 pm and the Ge–N$_{amide}$ average to 197.3 pm. These are comparable to the other Ge–N bond length reported to the *Cambridge Crystallographers Data Centre* (mean 196.5 pm). The N$_{bth}$–Ge–N$_{bth}$ angle averages to 90.0°, while the N$_{bth}$–Ge–N$_{amide}$ angles are 98.6° in average. Therefore, the sum of angles averages to 287.2°. The germanium atom is seen as non-hybridized and is appears as a pyramid. The germanium atom is out of the ligands best plane by 28 pm. A possible explanation to this displacement is the non-hybridized character of the germanium atom, as well as the steric demand of the amide residue. If the metal atom was in-plane with the ligand to achieve a better overlap of the metals p-orbitals

with the sp^2-orbitals of the nitrogen atoms, one trimethylsilyl group would compulsory come close to the ligand. Additionally, the P–C bonds were elongated and/or the C–P–C angle widened.

Due to the good and easy availability this complex is a good basis for further research. Therefore reactions at the residual amide are favorable. On the one hand, an exchange to a halogen atom opens routes to metal–metal bonds *via* reduction as well as further coupling reactions. On the other hand, the residual amide with its basic character might deprotonate acidic protons to form further coupling reactions.

The transformation of the amide residue to a halogen atom was reported in the literature using either tri(organyl)(halogeno)silanes or tri(organyl)(halogeno)tin compounds.[17-22] Until now it was not possible to isolate pure product in analogous reaction with di(2-benzothiazolyl)phosphanide-bis(trimethylsilyl)amide germanium(II). The product was identified by mass spectrometry; detection *via* NMR studies was impossible due to the large number of side products.

3.2 Di(*2*-benzothiazolyl)phosphanide-bis(trimethylsilyl)amide-tin(II)

The structure of the tin-amide complex was already reported by *Stey*.[16] Apart from the structure only ^{1}H-NMR data was obtained. To complete the analytic data to the same level as the analogue germanium complex the complex was prepared again.

Different to *Stey* and analogous to the germanium complex, the reactants were mixed within an argon dry box and outside the dry box diethyl ether was added at –10°C using *Schlenk* techniques. Removal of all volatile material and re-suspending in diethyl ether let to single crystals. Redetermination of the unit-cell parameters affirmed the same product as reported earlier quadrupling the yield. These single crystals were isolated und used for the further analytics. The purity of the isolated product is underlined by the elemental analysis and the NMR data.
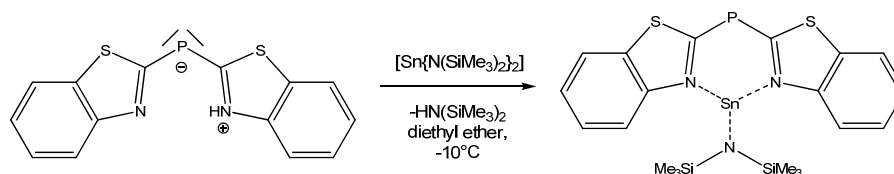
Scheme 2: preparation of di(*2*-benzothiazolyl)phosphanide-bis(trimethylsilyl)amide-tin(II).

As the germanium complexes, the tin analogue is stable if air and moisture are excluded. Therefore, further reactions and modifications at the tin atom were

attempted. Unfortunately, the products could only be found by mass spectrometry and not been isolated purely. Again, reactions of two equivalents of di(2-benzothiazolyl)phosphane with one equivalent [Sn{N(SiMe$_3$)$_2$}$_2$] only yielded the same product as above independently of the reaction time or the reaction temperature.

3.3 Di(2-benzothiazolyl)phosphanide-bis(trimethylsilyl)amidelead(II)oxid

To complete the row of metal complexes down group 14, the lead complex moved into focus of interest. Therefore the ligand was mixed with freshly prepared [Pb{N(SiMe$_3$)$_2$}$_2$]in an argon dry box.[2] Based on the experience with the germanium and tin complexes diethyl ether was added at –10°C outside the dry box. Analysis of the resulting product showed a very different layout. The phosphorus atom was shielded as the upfield shift in the ^{31}P-NMR hints. This fact is validated by X-ray structure by an additional oxygen substituent.
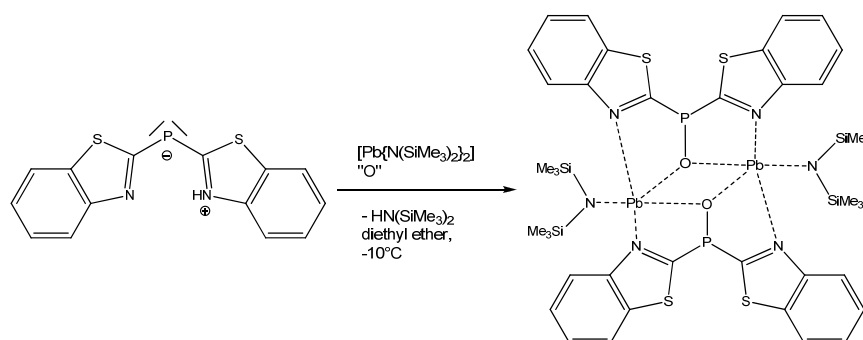
Scheme 3: preparation of di(2-benzothiazolyl)phosphanide-bis(trimethylsilyl)amidelead(II)oxid.

This reaction (Scheme 3) leads always to the oxo-complex above which is not the intended product. In the beginning an inadequate *Schlenk*-technique or impurities in the reactants were assumed. Neither analysis of the reactants nor several repetitions of the reaction to ensure proper *Schlenk* technique headed to different results. At any time the same product was achieved in good yields and very pure. Thus the oxygen atom is originated from the reaction. Another possibility is an ether cleavage reaction.[23-27]

 The ability to perform an ether cleavage reaction with metal complexes of di(2-benzothiazolyl)phosphane is shown in chapter VI. The ether cleavage reaction could be proven by using ^{18}O-labeled solvent. A proof thereof was dismissed for economical reasons.
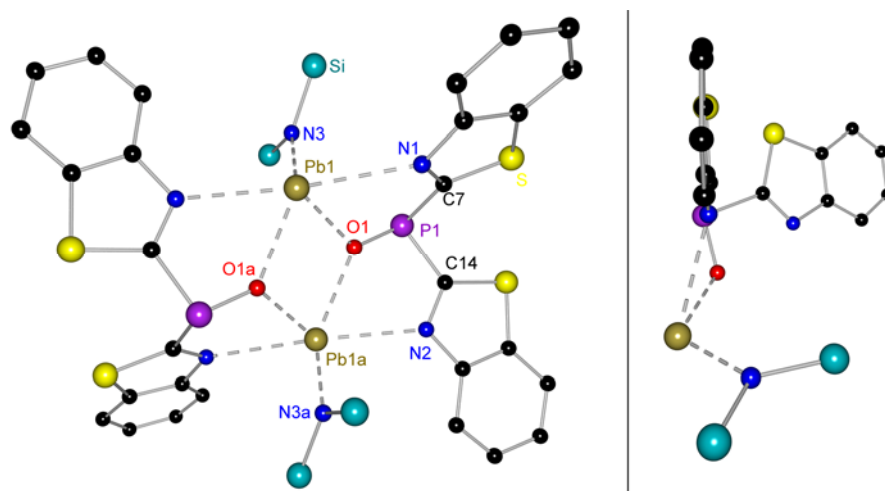
Figure 2: Solid state structure of di(2-benzothiazolyl)phosphanide-bis(trimethylsilyl)amidelead(II)oxid. Hydrogen atoms and carbon atoms at the silyl-residues omitted for clearity.

Table 2: Selected bond lengths [pm] and angles [°] of di(2-benzothiazolyl)phosphanide-bis(trimethylsilyl)amidelead(II)oxid.

P1–C7	185.1(5)	C7–P1–C1	96.6(2)
P1–C14	185.0(5)	C7–P1–O1	100.03(19)
C7–N1	130.3(6)	C14–P1–O1	101.7(2)
C14–N2	130.1(6)	O1–Pb1–O1a	65.96(12)
N1–Pb1	278.4(4)	Pb1–O1–Pb1a	114.04(12)
N3–Pb1	225.6(4)	O1–Pb1–N1	122.81(11)
O1–Pb1	233.9(3)	O1–Pb1–N3	117.7912
O1–Pb1a	256.7(3)	bth–bth'	62.9

Di(2-benzothiazolyl)phosphanid-bis(trimethylsilyl)amidelead(II)oxid crystallizes as a dimer in the monoclinc space group $P2_1/c$ with half a molecule of diethyl ether per asymmetric unit. The ligand lost its planarity as clearly seen at the C7–P1–C14 angle of a 96.5°. Additionally, the P–C_{ipso} bonds are elongated to 185 pm. This characterizes the P–C_{ipso} bonds as single bonds. The P–O bond is 157.0 pm, the exact mean of a *Cambridge Crystallographers Data Centre* research of all reported P–O single bonds, as Figure 3 shows. The bonds of the phosphorous atom span a trigonal pyramid. This hints to a sp³-hybidization of the phosphorous atom. The tetrahedral coordination is completed by a lone pair. The oxygen atom linked to the phosphorous atom did not oxidize it since the oxidation state did not change. Due to

addition of the oxygen atom the phosphanidic character of the phosphorous atom is lost.
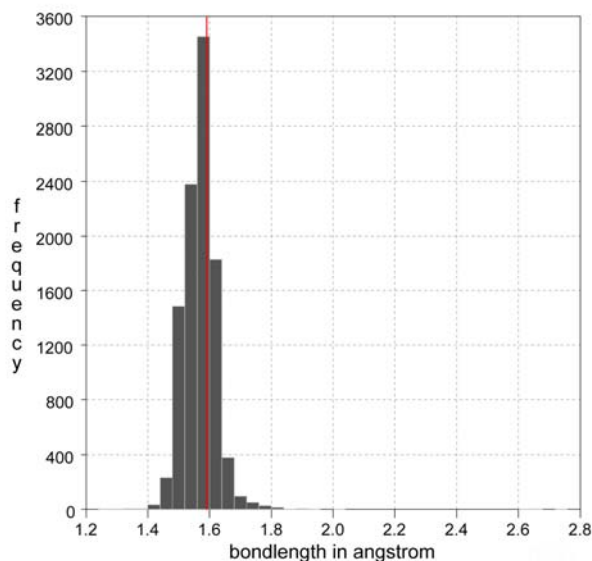
Figure 3: frequency of P–O bond lengths reported to the CCDC.

The best planes of the benzothiazole residues span an angle of 62.9°. The phosphorous atom is 16.83 pm, respectively 13.82 pm, out of the best planes of the benzothiazole residues, while the coordinated lead atom is 70.86 pm, respectively 71.36 pm, out of these planes.

The lead atom is coordinated by the oxygen atom, one nitrogen atom of the benzothiazole substituents and an amide residue. The coordination sphere at the lead atom is completed by another oxygen and nitrogen atom of a symmetrically generated further molecule. The inner angle of the central $(Pb-O)_2$ ring includes an 66° angle at the lead atom and 114.0° at the oxygen atom. The symmetric bonding and the angle sum of 359.5° hint to a sp^2-hybridization at the oxygen atom. The ligands are contrariwise arranged with the phosphorous atoms on the one side of the plain while the benzothiazole substituents are located on the other side.

The Pb1–O1 distance of 256.9 pm is slightly shorter than the mean bond length of the PB–O distances reported to the *Cambridge Crystallographers Data Centre* (260.3 pm). The Pb–O1A bond is 233.8 pm and thus a rather short Pb-O bond.

The Pb–N1 bond is 278.9 pm and within the range of the longer bond lengths reported to the *Cambridge Crystallographers Data Centre*. The Pb1a–N2 bond is 288.7 pm and therefore among the longest Pb–N contacts reported to the *Cambridge Crystallographers Data Centre*.
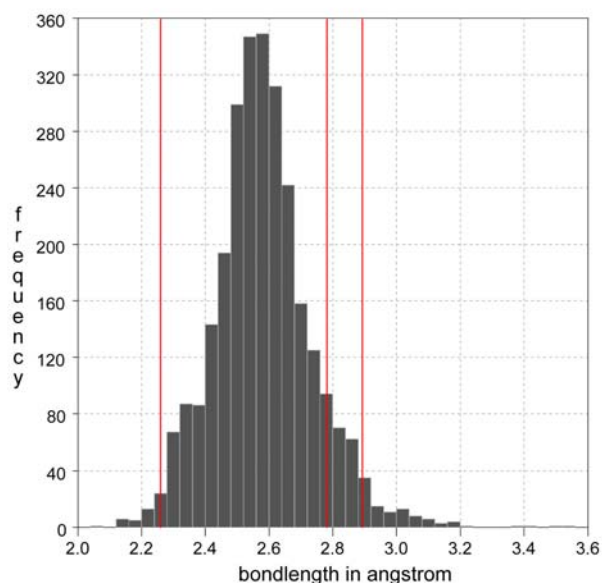
Figure 4: frequency of P–N bond lengths reported to the CCDC.

Since it is comparably short a far stronger Pb–N interaction is expected and justifies the conclusion of two different bond types. On the one hand the Pb–N3 bond has a strong ionic character due to the charges of the metal and the amide. On the other hand the Pb–N1/2 bonds are dative bonds as the nitrogen atoms donate their lone pair. The interaction of the ring nitrogen atoms is accompanied by significant shortening of the benzene and the N–C_{ipso} bonds.

Over the entire bonding situation in the complex is strained. This explains the atypical out of plane distances with regard to the benzothiazole residuals. In solution the slight difference within the benzothiazole rings disappears as in the NMR studies appear symmetric.

4 Conclusion

Within this chapter two new group 14 metal complexes were presented and fully characterized. Additionally, missing NMR studies on the tin containing complex **2** were determined. All three complexes are available directly from the pure ligand reacting with appropriate metal-hexamethyldisilazane.

The oxidation states of the phosphorous atoms in the achieved complexes is +III. The nitrogen atoms of the benzothiazole substituents coordinate the metal atoms. Additionally, one amide ligand stays at the metal atom. A substitution of a second ligand instead of the amide was neither achieved independently of the applied ligand to metal amide ratio, nor by variation of the reaction time or temperature. This can be explained on the one hand by steric demand of a second ligand. On the other hand the basicity of the hexamethyldisilane might be decreased, so that a further deprotonation is impossible.

 In the germanium and the tin complex the divalent character of the phosphorous atom persists. Therefore, the ligand remains nearly planar. The nitrogen atoms coordinate the same metal atom and form a monomer in both cases. The metal atoms are triple coordinated slightly above the ligands best plane while the amide residue is underneath the plane.

The lead complex always includes an oxygen atom. Most probably it derives from a ether cleavage reaction. This explanation is substantiated in chapter VI where products of the cleavage reaction are shown within the structure and the NMR experiments. Due to the addition of oxygen the coordination motif in the lead structure changed completely. The metal atom is coordinated by the oxygen atom and one of both nitrogen atoms while the other coordinates a second metal to form a dimer. Due to the third substituent at the phosphorous atom the oxidation state stays unchanged but the divalent character is lost. The benzothiazole rings are no more planar and therefore allow the formation of a dimer.

The reported new complexes provide many opportunities for further research. The practicability of an exchange of the residual amide was shown; even if it was not possible to find a quantitative route yet. This will open up routes to metal–metal bonding or linkage *via* e.g. oxygen.

The preparation of the oxygen free complex was not successful yet. Due to the proclaimed instability in other solvents than diethyl ether, the experiment was not

repeated yet. As chapter II showed the ligand is stable in toluene as well. An oxygen free preparation seems feasible.

The introduction of the silicon atom was attempted by salt elimination reaction and hydrochloride elimination with acid interceptor. The former reaction pathway leads to a non-separable product mixture. The latter always resulted in a ligand degeneration to tri(2-benzothiazolyl)-phosphane.

5 Experimental

5.1 General

All manipulations were carried out with strict exclusion of air and moiety in nitrogen or argon atmosphere using modified *Schlenk*-techniques or in an argon dry box.[28-31] All solvents were either dried on standard laboratory procedures and were freshly distilled from sodium/potassium alloy prior to use. All employed reactants were commercially available or reproduced by literature known procedures.

$[Ge\{N(SiMe_3)_2\}_2]$[2] $[Sn\{N(SiMe_3)_2\}_2]$[2]

$[Pb\{N(SiMe_3)_2\}_2]$[2]

5.2 Spectroscopic and analytic methods

5.2.1 Nuclear Magnetic Resonance

All probes were prepared and bottled within the argon dry box into Schlenk-NMR-tubes. The NMR-tube was sealed to exclude any impurities. C_6D_6 was dried with potassium. Spectra were recorded at room temperature at a *Bruker Avance 500* NMR spectrometer.

All chemical shifts δ are given relative to their usual standards and coupling constants *J* are given in Hz. Assignments of the shifts were checked by 2d-correlation spectra.

5.2.2 Mass spectrometry

EI-spectra were recorded with a *MAT 95* device (EI-MS: 70 eV). Peaks are given according to the abundance of the main isotope as a mass to charge ratio *m/z*.

5.2.3 Elemental analysis

Elemental analysis was performed as a combustion analysis by the *Analytischen Labor des Institutes für Anorganische Chemie* at the Georg-August Universität Göttingen with an *elementar vario EL III*.

5.3 Di(*2*-benzothiazolyl)phosphanide-bis(trimethylsilyl)amide-germanium(II)

1.0 g (3.33 mmol) di(2-benzothiazolyl)phosphane and 1.31 g (3.33 mmol) [Ge{N(SiMe$_3$)$_2$}$_2$] were mixed in a argon dry box. Outside the dry box 50 mL diethyl ether were added at –10°C and stirred over night. Afterwards all volatile material was removed *in vacuo*. Storage of a saturated solution in diethyl ether at 4°C yielded orange-red crystals suitable for a single crystal X-ray diffraction experiment over night.

.
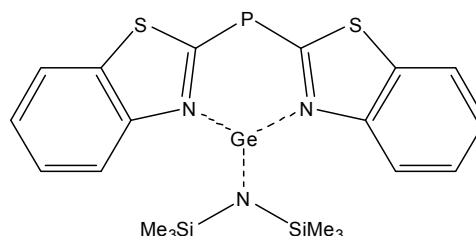
Sum formula: C$_{20}$H$_{26}$GeN$_3$PS$_2$Si$_2$

Molecular weight: 532.36 g/mol

^{1}H-NMR (500.13 MHz):   δ: 0.22 (s, 18H, SiMe$_3$); 6.76 (ddd, $^3J_{4,5}$ = 8.19, $^3J_{5,6}$ =7.30, $^4J_{5,7}$ = 1.01, 2H, *H-5*); 6.90 (dd, $^4J_{4,6}$ = 1.28, 2H, *H-4*), 7.05 (dd, $^3J_{6,7}$= 8.39, 2H, *H-6*); 8.07 (d, 2H, *H-7*) ppm.

^{13}C-NMR (125.77 MHz):   δ: 4.85 (s, SiMe$_3$); 116.63 (s, *C-7*); 121.40 (s, *C-4*); 124.36 (s, *C-5*); 125.53 (s, *C-6*); 132.15 (s, *C-7a*); 149.55 (s, *C-3a*); 187.35 (d, $^2J_{C,P}$ = 81.73, *C-2*) ppm.

^{15}N-NMR (50.68 MHz):   δ: –303.9 (s, N(SiMe$_3$)$_2$); –158.5 (s, N(bth)) ppm.

^{29}Si-NMR (99.36 MHz):   δ: 2.81 (s) ppm.

^{31}P-NMR (81.01 MHz):   δ: –3.03 (s) ppm.

Elemental analysis:

CHN, found (calc.):   C: 43.8% (45.12%); H: 4.35% (4.92%); N: 8.53% (7.89%); S: 12.9% (12.05%).

5.4 Di(*2*-benzothiazolyl)phosphanide-bis(trimethylsilyl)amide-tin(II)

1.0 g (3.33 mmol)   di(2-benzothiazolyl)phosphane   and   1.58 g   (3.33 mmol) [Sn{N(SiMe$_3$)$_2$}$_2$] were mixed in a argon dry box. Outside the dry box 50 mL diethyl ether were added at –10°C and stirred over night. Afterwards all volatile material was removed *in vacuo*. Storage of a saturated solution at 4°C in diethyl ether yielded orange crystals suitable for a single crystal X-ray diffraction experiment within two days.

.
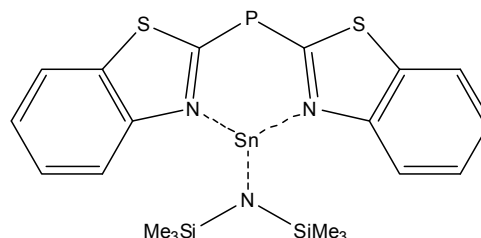
Sum formula: C$_{24}$H$_{36}$N$_3$OPS$_2$Si$_2$Sn

Molecular weight: 652.55 g/mol

^{1}H-NMR (500.13 MHz):   δ: 0.24 (s, 18H, SiMe$_3$); 6.73 (ddd, $^3J_{4,5}$ = 8.03, $^3J_{5,6}$ =8.30, $^4J_{5,7}$ = 1.11, 2H, *H-5*); 6.93 (dd, $^4J_{4,6}$ = 1.09, 2H, *H-4*), 7.05 (ddd, $^3J_{6,7}$= 8.25, 2H, *H-6*); 8.08 (d, 2H, *H-7*) ppm.

^{13}C-NMR (125.77 MHz):   δ: 5.69 (s, SiMe$_3$); 116.67 (s, *C-7*); 121.56 (s, *C-4*); 124.33 (s, *C-5*); 125.73 (s, *C-6*); 132.94 (s, *C-7a*); 150.55 (s, *C-3a*); 188.76 (d, $^2J_{C,P}$ = 87.19, *C-2*) ppm.

^{15}N-NMR (50.68 MHz):   δ: –295.2 (s, N(SiMe$_3$)$_2$); –150.8 (s, N(bth)) ppm.

^{29}Si-NMR (99.36 MHz):   δ: 2.75 (s) ppm.

^{31}P-NMR (81.01 MHz):   δ: –3.37 (s) ppm.

^{119}Sn-NMR (186.48 MHz): δ: 126.88 (s) ppm.

Elemental analysis:

CHN, found (calc.):   C: 41.5% (41.53%); H: 4.49% (4.53%); N: 7.31% (7.26%); S: 10.96% (11.09%).

5.5 Di(*2*-benzothiazolyl)phosphanide-bis(trimethylsilyl)amide-lead(II)oxid

1.0 g (3.33 mmol)   di(*2*-benzothiazolyl)phosphane   and   1.76 g   (3.33 mmol) [Pb{N(SiMe$_3$)$_2$}$_2$] were mixed in a argon dry box. Outside the dry box 50 mL diethyl ether were added at −10°C and stirred over night. Afterwards all volatile material was removed *in vacuo*. Storage of a saturated solution at 4°C in diethyl ether yielded orange crystals suitable for a single crystal X-ray diffraction experiment within 30 days.
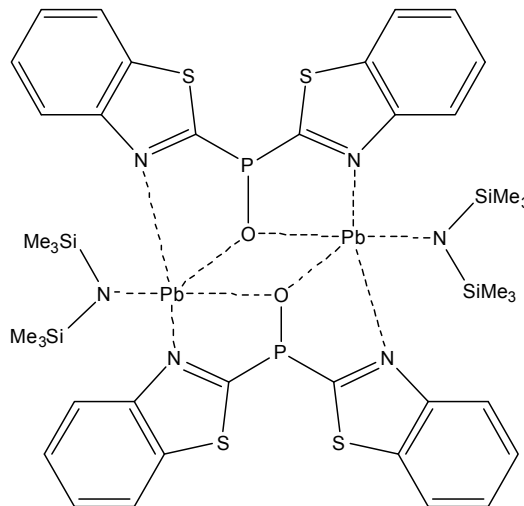
Sum formula: C$_{20}$H$_{26}$N$_3$OPPbS$_2$Si$_2$

Molecular weight: 682.91 g/mol

^{1}H-NMR (500.13 MHz):   δ: 0.29 (s, 18H, SiMe$_3$); 6.92–6.96 (m, 2H, *H-5*); 7.07 (ddd, $^3J_{5,6}$ = 7.2, $^3J_{6,7}$ = 8.3, $^4J_{4,6}$ = 1.2, 2H, *H-6*), 7.31–7.33 (m, 2H, *H-4*); 8.10 (dd, $^4J_{5,7}$ = 1.2, 2H, *H-7*) ppm.

^{13}C-NMR (125.77 MHz):   δ: 2.59 (s, SiMe$_3$); 121.65 (s, *C-7*); 124.30 (s, *C-4*); 126.08 (s, *C-5*); 126.47 (s, *C-6*); 137.85 (s, *C-7a*); 155.52 (s, *C-3a*); 167.33 (s, *C-2*) ppm.

^{29}Si-NMR (99.36 MHz):   δ: −21.43 (s) ppm.
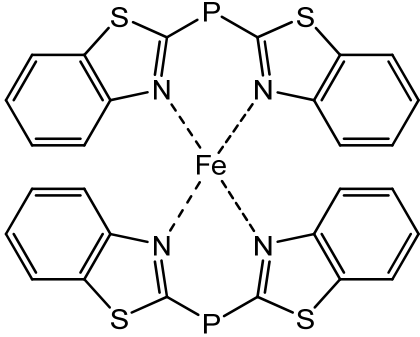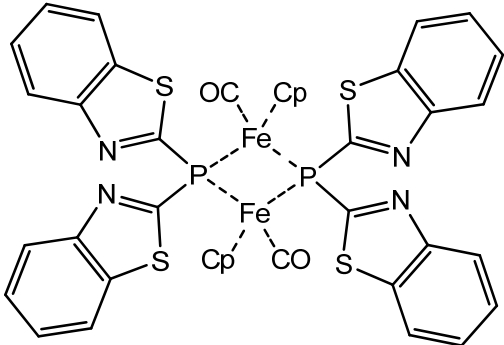
^{31}P-NMR (81.01 MHz):   δ: −21.58 (s) ppm.

6 Literature

[1]   E. Frankland, *Justus Liebigs Ann. Chem.* **1849**, *71*, 177-213.

[2]   M. J. S. Gynane, D. H. Harris, M. F. Lappert, P. P. Power, P. Rivière, M. Rivière-Baudet, *J. Chem. Soc., Dalton Trans.* **1977**, 2004-2009.

[3]   Y. Peng, B. D. Ellis, X. Wang, J. C. Fettinger, P. P. Power, *Science* **2009**, *325*, 1668-1671.

[4]   L. Pu, B. Twamley, P. P. Power, *J. Am. Chem. Soc.* **2000**, *122*, 3524-3525.

[5]   G. H. Spikes, J. C. Fettinger, P. P. Power, *J. Am. Chem. Soc.* **2005**, *127*, 12232-12233.

[6]   Y. Peng, B. D. Ellis, X. Wang, P. P. Power, *J. Am. Chem. Soc.* **2008**, *130*, 12268-12269.

[7]   A. D. Philips, R. J. Wright, M. M. Olmstead, P. P. Power, *J. Am. Chem. Soc.* **2002**, *124*, 5930-5931.

[8]   P. P. Power, *Nature* **2010**, *463*, 171-177.

[9]   M. Stender, A. D. Philips, R. J. Wright, P. P. Power, *Angew. Chem.* **2002**, *114*, 1863-1865; *Angewandte Chemie International Edition* **2002**, *41*, 1785-1787.

[10]   M. Westerhausen, *Inorg. Chem.* **1991**, *30*, 96-101.

[11]   B. A. Vaartstra, J. C. Huffman, W. E. Streib, K. G. Caulton, *Inorg. Chem.* **1991**, *30*, 121-125.

[12]   M. Westerhausen, H.-D. Hausen, W. Schwarz, *Z. Anorg. Allg. Chem.* **1992**, *618*, 121-130.

[13]   M. Westerhausen, W. Schwarz, *Z. Naturforsch., B: Chem. Sci.* **1992**, *47*, 453-459.

[14]   M. P. Bernstein, D. B. Collum, *J. Am. Chem. Soc.* **1993**, *115*, 8008-8018.

[15]   E. W. Olson, J. M. Standard, *J. Mol. Struct. (Theochem)* **2005**, *719*, 17-30.

[16]   T. Stey, Ph.D. thesis, Universität Würzburg (Germany), **2004**.

[17]   S. Nembenna, H. W. Roesky, S. Nagendran, A. Hofmeister, J. Magull, P.-J. Wilbrandt, M. Hahn, *Angew. Chem.* **2007**, *119*, 2564-2566; *Angew. Chem. Int. Ed.* **2007**, *46*, 2512-2514.

[18]   C. Wang, H.-K. Luo, M. van Meurs, L. P. Stubbs, P.-K. Wong, *Organometallics* **2008**, *27*, 2908-2910.

[19]   Y. Yang, T. Schulz, M. John, A. Ringe, H. W. Roesky, D. Stalke, J. Magull, H. Ye, *Inorg. Chem.* **2008**, *47*, 2585-2592.

[20]   A. Jana, H. W. Roesky, C. Schulzke, A. Döhring, T. Beck, A. Pal, R. Herbst-Irmer, *Inorg. Chem.* **2009**, *48*, 193-198.

[21]   P. L. Arnold, S. T. Liddle, *Chem. Commun.* **2005**, *45*, 5638-5640.

[22]   S. P. Sarish, H. W. Roesky, M. John, A. Ringe, J. Magull, *Chem. Commun.* **2009**, 2390-2932.

[23]   A. Maercker, *Angew. Chem.* **1987**, *99*, 1002-1019; *Angew. Chem. Int. Ed. Engl.* **1987**, *26*, 972-989.

[24]   A. Maercker, W. Demuth, *Angew. Chem.* **1973**, *85*, 90-92; *Angew. Chem. Int. Ed. Engl.* **1973**, *12*, 75-76.

[25]   A. Maercker, W. Demuth, *Justus Liebigs Ann. Chem.* **1977**, *11*, 1909-1937.

[26]   A. R. Kennedy, J. Klett, R. E. Mulvey, D. S. Wright, *Science* **2009**, *326*, 706-708.

[27]   R. E. Mulvey, V. L. Blair, W. Clegg, A. R. Kennedy, L. Russo, *Nature Chemistry* **2010**, *2*, 588-591.

[28]   W. Schlenk, A. Thal, *Ber. Dtsch. Chem. Ges.* **1913**, *46*, 2840-2854.

[29]   W. Schlenk, J. Holtz, *Ber. Dtsch. Chem. Ges.* **1917**, *50*, 262-274.

[30]   T. T. Tidwell, *Angew. Chem.* **2001**, *113*, 343-349; *Angew. Chem. Int. Ed.* **2001**, *40*, 331-337.

[31]   W. Schlenk, *Die Methoden der Organischen Chemie* in *Die Methoden der Organischen Chemie* (Ed. J. Houben), G. Thieme, Leipzig, **1924**, p. 720.

1 List of compounds

Name	number	Lewis formula
N,N-bis[di(*2*-benzothiazolyl)phosphanide]iron	**1**	
[*P*-{di(*2*-benzothiazolyl)phosphanide}(cyclopentadienyl)(carbonyl) iron]₂	**2**	

2 Introduction

Iron is a very versatile element. Since it was discovered, the mankind used iron for arms and instruments. Until today a life without iron is vitually impossible due to the fact that most of our life is still dominated by iron and products thereof.

Additionally, iron is an essential trace element to many creatures. It has influence on the photosynthesis in plants and the formation of chlorophyll. In humans and animals iron is mainly found in the oxidation states +II and +III. On the one hand, iron as the central atom in heme enzymes, such as P450, peroxidase, heme oxygenase and nitric acid synthase, catalyzes many different and important transformations, all including oxygen. The exact pathway and chemistry of the reaction at the active sites is not fully understood yet. For example in the case of cyptochrome P450 a ferric hydroperoxo-intermediate is anticipated.[1]

On the other hand iron plays an important role in iron sulfur clusters in many enzymes. In the past decades, many insights in their chemistry and biological application and assembly were studied.[2]

Within the field of material science and physics, iron-based superconductors were a major breakthrough and still provide avenues for understanding the high transition temperature phenomenon.[3]

At chemical reactions iron and its compounds are known as activators and catalysts, e.g. *Friedel-Crafts* alkylation and acylation reactions.[4] Recently, especially direct C–H activation and the functionalizing hydrocarbons became a very hot area in chemical research.[5,6] The economically most important process catalyzed by iron is the *Haber-Bosch* process using iron and its oxides.[7,8]

As there are many applications of iron it would go beyond the scope of this thesis to name and describe all. In all of its uses the ability of iron depends on its oxidation state and its surrounding. These facts make iron so versatile and an interesting target for research. Within this chapter iron complexes of the *Janus-head* ligand di(2-benzothiazolyl)phosphane are presented. The ability to introduce a metal atom selectively to designated coordination sites is remarkable. The two different complexes underline the versatility of this ligand towards the same metal in the same oxidation state.

3 Synthesis and structure

3.1 *N,N*-bis[di(*2*-benzothiazolyl)phosphanide]iron (1)

Chapter II and Chapter IV demonstrate the advantages of the use of metal bis[di(trimethylsilyl)]amides. This concept was extended to iron(II) bis[di(trimethylsilyl)]amide.

This compound was synthesized and characterized previously by *Stey*.[9] In line with the earlier reported metal complexes, he reacted the di(*2*-benzothiazolyl)phosphane with iron(II)bis[di(trimethylsilyl)]amide. The ligand reacts in a ligand to amide ratio of 2:1. This is in contrast to all other reactions of di(*2*-benzothiazolyl)phosphane with metal bis[di(trimethylsilyl)]amides known at that time to react in a 1:1 ratio .
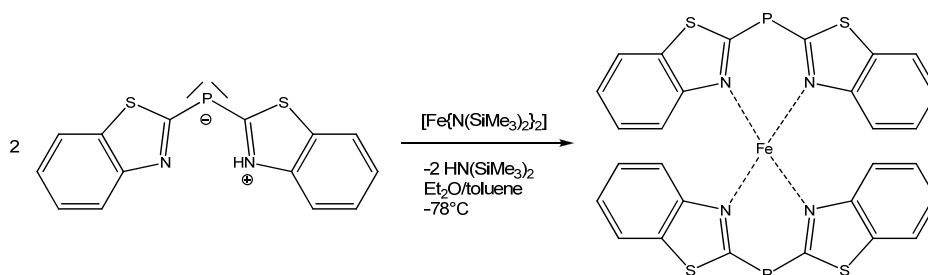
Scheme 1: preparation of *N,N*-bis[di(*2*-benzothiazolyl)phosphanide]iron (**1**).

N,N-bis[di(*2*-benzothiazolyl)phosphane]iron (**1**) crystallizes in the triclinic space group $P\bar{1}$. The asymmetric unit contains two complete formula units as well as a toluene molecule. Both formula units differ only slightly. All values given below are averaged.

The iron atom is fourfold coordinated by the nitrogen atoms of two ligands. Due to the steric demand of the benzene rings a planar coordination as in porphyrin is impossible. Therefore, the coordination motif at the iron atom is tetrahedral. Both ligands are twisted by 82° against each other while the ligands themselves are nearly planar (twisted by 4.3° to 12.3°). The Fe–N bonds are similar to those reported in the *Cambridge Crystallographic Data Center* and best described between an amidic and a dative bond. The P–C$_{ipso}$ bond lengths are in average 177.5 pm and therefore between a single and a double bond.

Due to the changes in bond lengths in the benzothiazole substituents, a charge transfer from the phosphorous centre to the heteroaromatic rings is anticipated. Besides the double coordination of the metal atom by two ligands, the phosphanidic character of the ligand is similar to the other reported metal complexes.
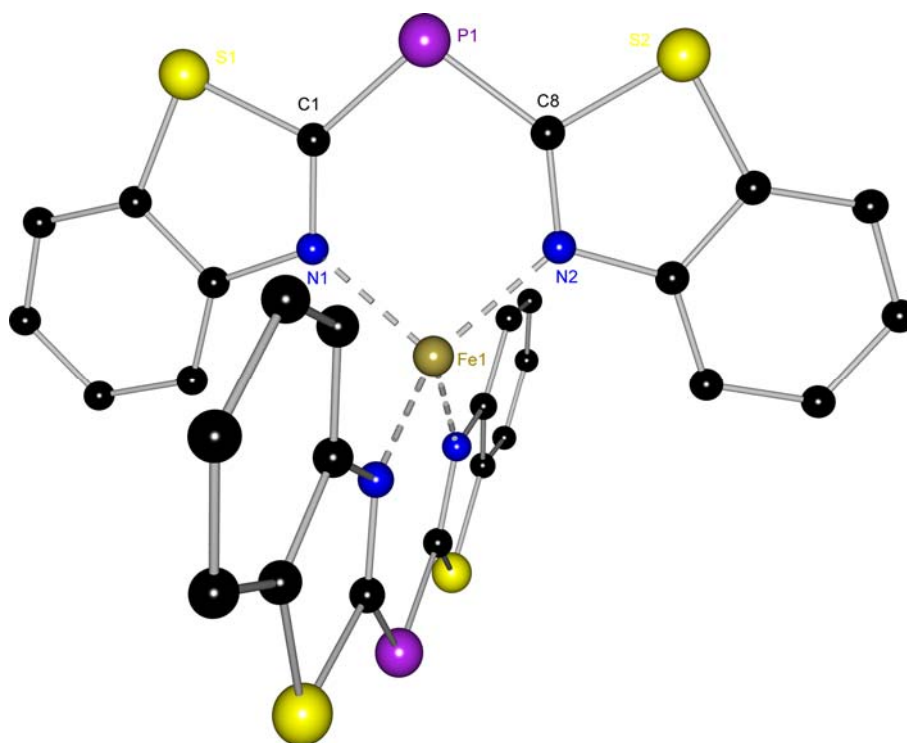
Figure 1: solid state structure of *N,N*-bis[di(2-benzothiazolyl)phosphanide]iron (**1**).

Hydrogen atoms omitted for clarity.

Table 1: Selected bond lengths [pm] and angles [°] of *N,N*-bis[di(2-benzothiazolyl)phosphanide]iron (**1**).

P1–C1	176.83(15)	C1–P1–C8	101.31(7)
P1–C8	176.74(16)	C1–N1–Ge1	130.31(10)
C1–N1	133.54(18)	C8–N2–Ge1	130.62(10)
C8–N2	133.27(18)	N1–Ge1–N2	89.93(5)
N1–Ge1	204.72(12)	N1–Ge1–N3	97.90(5)
N2-Ge1	205.41(12)	N2–Ge1–N3	98.74(5)
N3–Ge1	190.50(11)	bth–bth'	7.9

Interestingly the reported complex is a 14-valence electron complex. Hence, it is coordinatively unsaturated. To date, only a couple of 14 valence electron complexes of iron are reported and they are assumed to be very promising to catalyze ethylene polymerization.

3.2 [*P*-{di(*2*-benzothiazolyl)phosphanide}(cyclopentadienyl) (carbonyl)iron] dimer (2)

Due to the versatility of iron and the proven ability of the ligand to complex iron, further iron complexes are an interesting research targets. Aiming a monomeric iron complex of di(2-benzothiazolyl)phosphane for further investigations, a trans-metalation was performed. [Zinc(methyl){di(2-benzothiazolyl)phosphanide}]was reacted with (η^5-cyclopentadienyl)dicarbonyliironiodid in toluene and stirred for 24 hours. After filtration the solution was concentrated and stored at room temperature for crystallization. After more than 3 month red single crystals suitable for an X-ray experiment were yielded.
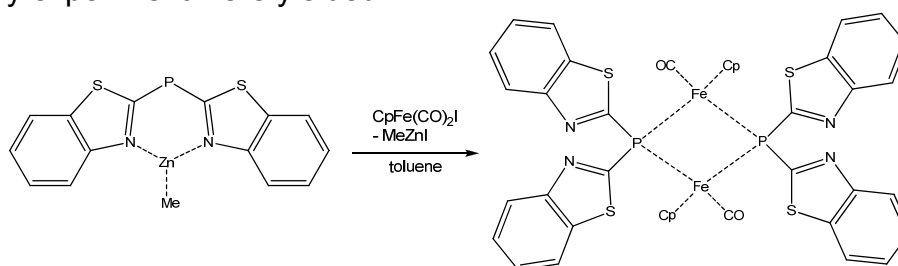
Figure 2: preparation of [*P*-{di(*2*-benzothiazolyl)phosphanide}(cyclopentadienyl) (carbonyl)iron] dimer (**2**).

The iron complex **2** is an 18 valence electron complex. Differently to compound **1**, this complex coordinates the iron atom with its phosphorous atoms. Interestingly, it is not a direct metal exchange, as the donor atom changed. A possible explanation is iodide elimination in a first step and the accompanied loss of methyl zinc iodide. Since there is only one vacant coordination position and due to the steric demand of the cyclopentadienyl residue, the phosphorus atom is taken as donor site. In a second step, the dimerisation takes place by eliminating carbon monoxide to form the (Fe–P)$_2$ four membered ring. This last step might be promoted by heat and/or exposure to sunlight during the long time of crystallization or by entropic reasons since a gas is evolved.

The [*P*-{di(2-benzothiazolyl)phosphanide}(cyclopentadienyl)(carbonyl)iron]dimer (**2**) crystallizes in the triclinic space group *P*$\overline{1}$. The asymmetric unit contains half of the dimer. The iron(II) atom is fourfold coordinated by carbon monoxide, a cyclopentedienyl ring and twice by the phosphorous atoms of the di(2-benzothiazolyl)phosphane. The average Fe–P bond distance is 223.7 pm and therefore in the range of a standard Fe–P bond length reported to the *Cambridge Crystallographic Data Center* (224.8 pm). Also the Fe–C$_{carbonyl}$ distance with

175.2 pm is similar to the reported (177.9 pm) while the distance to best plane of the cyclopentedienyl ring is 172.0 pm. The ligands include an angle of 76.8° at the iron atom. Hence, the iron has a tetrahedral coordination motif as in **1**.

In contrast to **1**, the ligand is no more planar. The benzothiazole substituents include an angle of 94.2° and their twisted best planes intercept an angle of 93°. The phosphorous atom is out of their best planes by 13.9 pm and 14.7 pm, respectively. The phosphorous atom is fourfold coordinated in a tetrahedral environment. The C_{ipso}–P–Fe angle is 106.6° on average. The P–C_{ipso} bonds are elongated to 184.5 pm in average and therefore in the range of a classical P–C single bond. All these facts hint to a sp^3-hybridized phosphorous atom.

Both benzothiazole substituents do not show many differences and can therefore be regarded being equally.
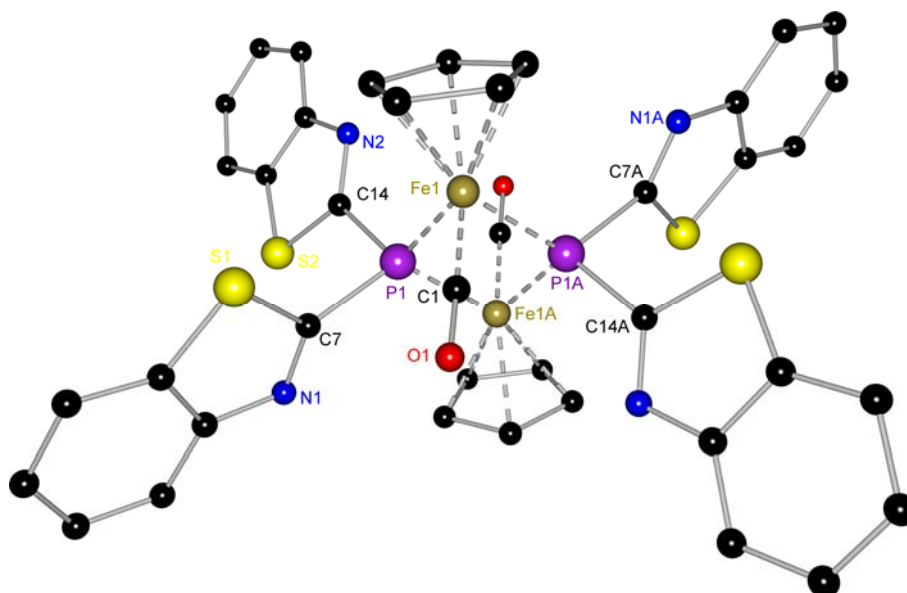
Figure 3: solid state structure of [*P*-{di(2-benzothiazolyl)phosphanide}-(cyclopentadienyl)(carbonyl)iron] dimer (**2**). Hydrogen atoms omitted for clarity.

Table 2: Selected bond lengths [pm] and angles [°] of [*P*-{di(2-benzothiazolyl)phosphanide}-(cyclopentadienyl)(carbonyl)iron] dimer (**2**).

P1–C7	184.2(2)	C7–P1–C14	94.21(10)
P1–C14	184.7(2)	P1–Fe1–P1'	76.81(2)
P1–Fe1	222.95(6)	Fe1–P1–Fe1'	103.19(2)
Fe1–C1	175.2(2)	P1–Fe1–C1	89.78(7)
Fe1–Cp	172.04(12)	bth–bth'	93.00

In solution, the equivalency of both benzothiazole substituents is underlined even if the NMR studies are hampered due to the paramagnetic feature of the iron atom. The observed downfield shift in the ^{31}P-NMR hints to a lower charge concentration at the phosphorous atom compared to the uncoordinated ligand.[10]

Taking all these findings in account, a enhanced phosphanidic character of complex **2** becomes apparent. All results point onto a negatively charged phosphorous atom.

It should be noted that this is the first and only reported complex of the di(2-benzothiazolyl)phosphane as a *Janus-head* ligand that only coordinates with its phosphorous atom. A similar structural motif was earlier only reported for di(2-pyridyl)phosphanides.[11] All other related complexes including a P–metal contact do always show a second coordination at their *N,N*-site. Thus this example also affirms all early predictions of the phosphanidic character of the ligand.[12]

4 Conclusion

Within this chapter two different coordination motifs of the same ligand with the same metal in the same oxidation state were presented. On the one hand, a double *N,N*-coordinated iron complex with only 14 valence electron is accessible by the addition of iron bis[di(trimethylsilyl)]amide to the pure ligand. On the other hand, an 18 valence electron complex with a strong phosphanidic character is applicable by transmetalation.

This demonstrates the flexibility of the employed di(*2*-benzothiazolyl)phosphane. As iron is a catalytically very active and economically very interesting element, these different abilities of the ligand become even more interesting. Due to the capability to stabilize iron as a 14 valence electron complex up to an 18 valence electron complex the high potential is demonstrated. These features are especially useful to the implementation in a catalytic process. Thanks to the differently used coordination sites the choice of second catalytic active elements is not hindered and still all different utilizations are possible.

Noticeably **2** is the first and only example of the phosphorous donation of this *Janus-head* ligand. It consequently verifies all prior forecasts.

In consideration of the fact, that both presented complexes still have vacant donor sites they provide a good basis for further research towards heterobimetallic complexes and thereof application in catalytic processes.

5 Experimental

5.1 General

All manipulations were carried out with strict exclusion of air and moiety in nitrogen or argon atmosphere using modified *Schlenk*-techniques or in an argon dry box.[13-15] All solvents were either dried on standard laboratory procedures and were freshly distilled from sodium/potassium alloy prior to use or directly used from a *MBraun SPS* connected to the glove box. All employed reactants were commercially available or reproduced by literature known procedures.

5.2 Spectroscopic and analytic methods

5.2.1 Nuclear Magnetic Resonance

All probes were prepared and bottled within the argon dry box into Schlenk-NMR-tubes. The NMR-tube was sealed to exclude any impurities. Solvents were dried with potassium. Spectra were recorded at room temperature at a *Bruker Avance 300*, or a *Bruker Avance 500* NMR spectrometer.

All chemical shifts δ are given relative to their usual standards and coupling constants *J* are given in Hz. Assignments of the shifts were checked by 2d-correlation spectra. NMR shifts are assigned to the given scheme.

5.2.2 IR-spectroscopy

All IR-spectra were recorded at the department of chemistry at the Georg-August University on a *Varian FTS 1000*.

5.2.3 Mass spectrometry

ESI-spectra were recorded with a *Bruker HTCultra*. Peaks are give according to the abundance of the main isotope as a mass to charge ratio *m/z*.

5.2.4 Elemental analysis

Elemental analysis was performed as a combustion analysis by the *Analytischen Labor des Institutes für Anorganische Chemie* at the Georg-August Universität Göttingen with an *elementar vario EL III.*

5.3 [*P*-{di(*2*-benzothiazolyl)phosphanide}(cyclopentadienyl) (carbonyl)iron]dimer (2)

1.0 g (2.65 mmol) [zinc(methyl){di(*2*-benzothiazolyl)phosphanide}] was dissolved in 50 mL toluene and 1.82 g (6.00 mmol) $CpFe(CO)_2I$ in 30 mL toluene was added dropwise at 0°C. After stirring 24 h at room temperature the mixture was filtered and concentrated. Storage at room temperature for 3 month yielded red crystals suitable for a single crystal X-ray diffraction experiment.
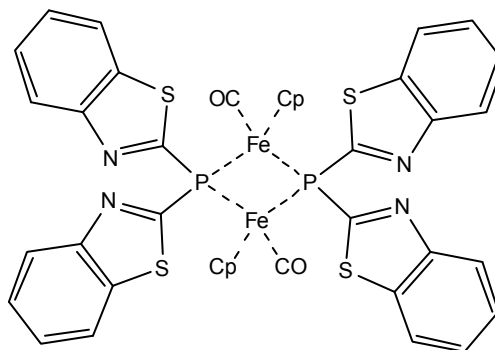
Sum formula: $C_{40}H_{26}Fe_2N_4O_2P_2S_4$

Molecular weight: 893.91 g/mol

¹H-NMR (300.13 MHz):   δ: 3.90 (s, 10H, H_{Cp}); 6.44–6.55 (m, 4H, *6*); 6.61–6.79 (m, 4H, *5*); 7.25–7.31(m, 4H, *4*); 7.34–7.42 (m, 4H, *7*) ppm.

¹³C-NMR (75.368 MHz):   δ: 80.89 (s, C_{Cp}); 125.63 (s, *7*); 127.86 (s, *4*); 128.51 (s, *5*); 129.27 (s, *6*); 137.84 (s, *7a*); 152.23 (s, *3a*); 171.96 (s, *2*); 199.12 (s, *C*O) ppm.

¹⁵N-NMR (30.423 MHz):   δ: –31.24 (s) ppm.

³¹P-NMR (121.495 MHz): δ: 30.85 (s) ppm.

IR (nujol, cm⁻¹):   1942, 1880.

ESI-MS: *m/z* (%):   799 (5) [*M*-Cp-CO], 679 (100) [*M*-bth-Cp-CO], 579 (30) [*M*-Pbth-Cp-CO], 549 (8) [*M*-Pbth₂-Cp-CO], 519 (8) [*M*-Pbth₂-Cp-2CO], 300 (90) [Pbth₂].

Elemetal analysis:
CHNS, found (calc.):   C: 43.3% (43.17%); H: 2.39% (2.28%); N: 3.82% (3.37%); S: 7.82% (8.54%).

6 Literature

[1] S. P. de Visser, J. S. Valentine, W. Nam, *Angew. Chem.* **2010**, *112*, 2143-2146; *Angew. Chem. Int. Ed.* **2010**, *49*, 2099-2101.

[2] R. Lill, *Nature* **2009**, *460*, 831-839.

[3] I. I. Mazin, *Nature* **2009**, *464*, 183-186.

[4] M. Rueping, B. J. Nachtsheim, *Beilstein J. Org. Chem.* **2010**, *6*.

[5] L. Ackermann, R. Vicente, A. R. Kapdi, *Angew. Chem.* **2009**, *121*, 9976-10011; *Angew. Chem. Int. Ed.* **2009**, *48*, 9792-9826.

[6] S. Shaik, *Nature Chemistry* **2010**, *2*, 347-349.

[7] G. Ertl, *Angew. Chem.* **1990**, *102*, 1258-1266; *Angw. Chem. Int. Ed. Engl.* **1990**, *29*, 1219-1227.

[8] R. Schlögl, *Angew. Chem.* **2003**, *115*, 2050-2055; *Angew. Chem. Int. Ed.* **2003**, *42*, 2004-2008.

[9] T. Stey, Ph.D. thesis, Universität Würzburg (Germany), **2004**.

[10] H. Schmidbaur, W. Buchner, D. Scheutzow, *Chem. Ber.* **1973**, *106*, 1251-1255.

[11] M. Pfeiffer, T. Stey, H. Jehle, B. Klüpfel, W. Malisch, D. Stalke, V. Chandrasekhar, *Chem. Commun.* **2001**, *4*, 337-338.

[12] J. Henn, K. Meindl, A. Oechsner, G. Schwab, T. Koritsanszky, D. Stalke, *Angew. Chem.* **2010**, *122*, 2472-2476; *Angew. Chem. Int. Ed.* **2010**, *49*, 2422.

[13] W. Schlenk, A. Thal, *Ber. Dtsch. Chem. Ges.* **1913**, *46*, 2840-2854.

[14] T. T. Tidwell, *Angew. Chem.* **2001**, *113*, 343-349; *Angew. Chem. Int. Ed.* **2001**, *40*, 331-337.

[15] W. Schlenk, *Die Methoden der Organischen Chemie* in *Die Methoden der Organischen Chemie* (Ed. J. Houben), G. Thieme, Leipzig, **1924**, p. 720.

1 List of compounds

name	number	Lewis formula
(Di(2-benzothiazolyl)phosphanyl)-(methyl)zinc	**1**	
Bis(di(2-benzothiazolyl)phosphanyl)zinc	**2**	
[{(MeCp)(OC)$_2$Mn}{P(bth)$_2$Zn(bth)$_2$P}{Mn(CpMe)(CO)$_2$}]$_2$	**3**	
[Di(2-benzothiazolyl)phosphanyl](tricarbonyl)nickel	**4**	
Bis[di(2-benzothiazolyl)phosphanyl](dicarbonyl)nickel	**5**	
[{(OC)$_2$NiP(bth)$_2$ZnMe)(P(bth)$_2$ZnOEt)}$_2$]	**6**	

2 Introduction

One of the major goals in catalysis research is the synthesis of heterobimetallic complexes. As lots of enzymes posses two or more metal atoms in their active site, this field of research is often bio-inspired.[1]

In order to transfer these models to smaller systems, very versatile ligands with given geometry and therefore a certain pre-organization are necessary. The transfer from native living systems to modern catalysis research also allows insights into natures basic functions, like magnetism or electron transfer, beside the economical value creation. Understanding and controlling reaction pathways is of great importance in the design and development of new materials.[2-12]

The first step in synthesis towards heterobimetallic complexes always is the sequentially introduction of various metals. Consequently efficient and convenient purification methods as well as high yields of the resulting metal complexes are required. Additionally, the obtained metal complex has to be tolerant towards the insertion of a second metal ion. Therefore, the order of metal introduction is vital.

Zinc organyls and their mixed metal complexes moved in the research focus during the last decade due to their high potential in selective deprotonation and polydeprotonation of arenes, (hetero-)aromatics and metalocenes.[13] In addition, the bio appearance and compatibility of zinc makes it an interesting metal in applied catalysis.[14]

By now, [*P*-{di(*2*-benzothiazolyl) phosphanide}(cyclopentadienyl)(carbonyl)iron]$_2$ is the only known phosphanide complex of di(*2*-benzothiazolyl)phosphane (see chapter V) with a vacant hard donor site. This iron complex had been prepared by a transmetalation reaction; therefore coordination at the hard donor site seems the best choice as a first step. *Stey* used an analogous way aiming towards heterobimetallic complexes.[15] He used lithiated or aluminated di(*2*-benzothiazolyl)phosphanide and reacted it with activated metal carbonyls. Differently activated carbonyl complexes had been prepared, purified and their turnover constants were determined in different solvents by IR-spectroscopy.[16,17]

Due to the modest yields of only 70% and the sophisticated purification of lithiated di(*2*-benzothiazolyl)phosphanide – which is also the starting material towards the aluminum complex – another approach was prospected by using zinc.

3 Synthesis and structure

Di(*2*-benzothiazolyl)phosphane was dissolved in diethyl ether and dimethyl zinc was added dropwise. Performing the reaction at –78°C and not allowing the reaction to warm to room temperature gave only low yields. Repeating the reaction at 0°C resulted in an inseparable product mixture. Two different compounds were identified and fully characterized using ^{1}H-, ^{31}P-, HH–COSY- and DOESY–NMR techniques. A ligand to metal ratio of 1:1 was found beside one a 2:1 product. In the first case, the one of the di(*2*-benzothiazolyl)phosphane molecules is deprotonated by dimethyl zinc which is chelated by both nitrogen atoms while the second methanide ligand stays bonded to the zinc atom. This second methyl group can deprotonate a second di(*2*-benzothiazolyl)phosphane molecule to form a product a with ligand to metal ratio of 2:1. These products underline the versatile character of the applied ligand.
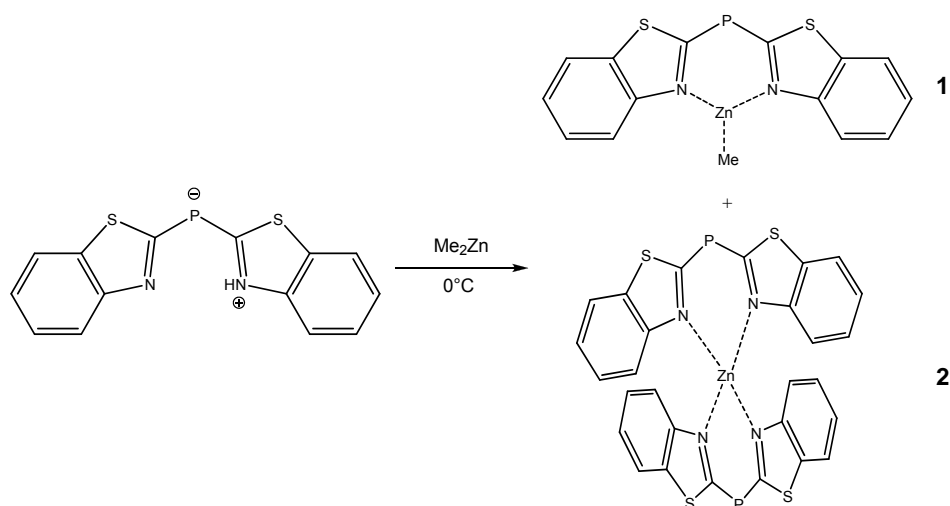
Scheme 1: zincation of di(*2*-benzothiazolyl)phosphane.

Both products would have been a good basis for further investigations if the reaction had not yielded an inseparable mixture of both complexes. Thus, further optimization of the reaction conditions was undertaken.

3.1 (Di(*2*-benzothiazolyl)phosphanyl)(methyl)zinc (1)

As shown in chapter 3 the ligand is stable in toluene, which is in contrast to earlier reports. Repeating the reaction in toluene at the same conditions lead to the same result as in diethyl ether. Hence, this is not a possible pathway to complex **1**. This is only possible by a slow addition of the ligand to an excess of dimethyl zinc. Pure product was only achieved if this reaction was performed in toluene. If the reaction

was performed in diethyl ether, small amounts of methane and **2** were always detected by NMR methods.
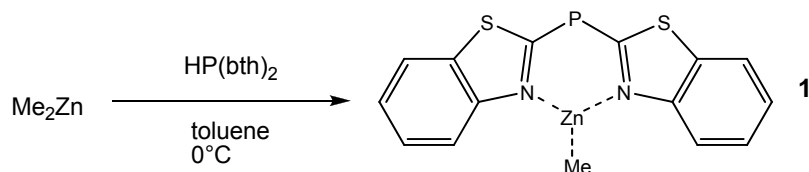
Scheme 2: preparation of (di(2-benzothiazolyl)phosphanyl)(methyl)zinc (**1**).

The reaction shown in Scheme 2 is the basis for further studies on heterobimetallic complexes. Further coordination is possible either via the phosphorus atom in the ligands backbone or by e.g. oxo-bridging via hydrolysis. Further chemistry of this is shown in section 3.5.

To date, it had not been possible to obtain single crystals for structure determination. NMR studies approve this compound and agree with the earlier one determined from the mixture.

3.2 Bis[di(2-benzothiazolyl)phosphanyl]zinc (2)

In order to isolate pure bis(di(2-benzothiazolyl)phosphanyl)zinc (**2**), the reaction of di(2-benzothiazolyl)phosphane with slightly less than half an equivalent of dimethyl zinc was conducted in toluene. NMR tracking indicated the necessity of reflux to complete the reaction as shown in Scheme 3. Pure product can be obtained without any further purification by precipitation. Tiny single crystals suitable for an X-ray diffraction experiment were obtained from a saturated solution in toluene at room temperature after 3 months.
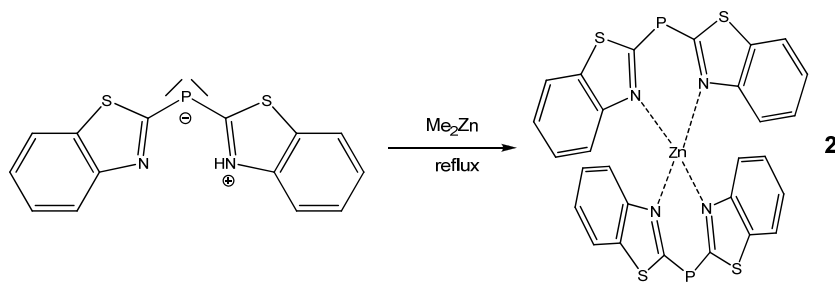
Scheme 3: preparation of bis(di(2-benzothiazolyl)phosphanyl)zinc (**2**).

In contrast to the zinc complex obtained from bis[bis(trimethylsilyl)amid] zinc, this complex is coordinated by two ligands. Zinc is coordinated twice by di(2-benzothiazolyl)phosphane ligands. This underlines the assumption of a lowered basicity of the amide residue if one di(2-benzothiazolyl)phosphanide ligand is already coordinated to the metal center.

Bis(di(2-benzothiazolyl)phosphanyl)zinc (**2**) crystallizes in the triclinic space group $P\bar{1}$ with two molecules and one toluene molecule in the asymmetric unit. Both molecules are equivalent within their estimated standard deviations. Therefore, all values in the following text are given as an average.

The center of this 18 valence electron complex is a zinc atom. It is tetrahedrally coordinated by two di(2-benzothiazolyl)phosphanide ligands via their nitrogen atoms. The N–Zn distance is 197.7 pm on average, and thus slightly shorter compared to other [di(2-benzothiazolyl)phosphanyl]zinc complexes, but still in good accordance to analogous complexes reported to the *Cambridge Crystallographic Data Center*.[18] Angles at the zinc atom are tetrahedral; the angle between two nitrogen atoms of the same ligand is slightly smaller (101°).
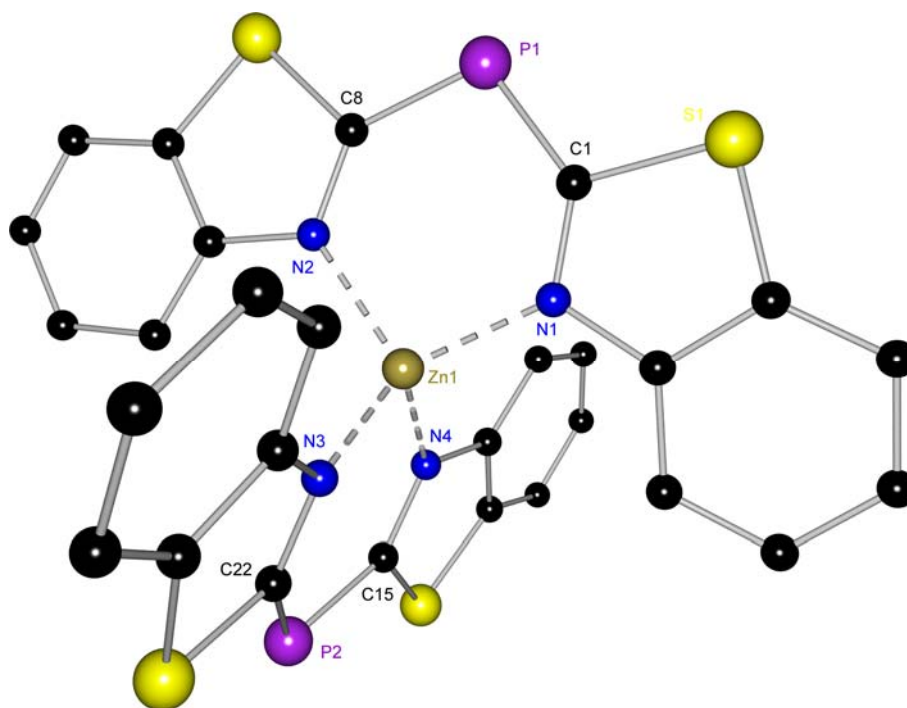
Figure 1: solid state structure of bis(di(2-benzothiazolyl)phosphanyl)zinc (**2**).

Hydrogen atoms omitted for clarity.

Table 1: Selected bond lengths [pm] and angles [°] for bis(di(*2*-benzothiazolyl)phosphanyl)zinc (**2**).

Zn1–N1	196.8 (3)	N1–Zn1–N2	100.97 (13)
Zn1–N2	197.9 (3)	N3–Zn1–N4	101.01 (14)
Zn1–N3	198.0 (3)	C1–P1–C8	103.88 (18)
Zn1–N4	198.2 (3)	C15–P2–C22	103.54 (18)
P1–C1	177.2 (4)	lig(P1)–lig(P2)	84.6
P1–C6	177.9 (4)	bth(N1)–bth(N2)	6.9
P2–C15	177.4 (4)	bth(N3)–bth(N4)	13.0
P2–C22	177.7 (4)		

Both ligands include an angle of 84.6°. The two ligands differ in the solid state. In the ligand containing P1 both benzothiazoles include an angle of only 6.9° while in the other ligand containing P2 this angle is 13.0°. The zinc atom is nearly in plane with the ligand containing P1 – only 2.8 pm out of plane – while it is 32.6 pm out of plane of the ligand containing P2. These differences are detectable for both molecules in the solid state structure. In solution, there are no differences between the ligands on the NMR time scale.

Both ligands show an average P–C$_{ipso}$ bond length of 175.5 pm and a C$_{ipso}$–P–C'$_{ipso}$ angle of 103.7°. The bond length range between a single and a double bond. The angle hints to a sp^3-hybridized phosphorous atom. The N–C$_{ipso}$ bond length is 133.2 pm and is in good accordance to the earlier reported metal complexes of di(*2*-benzothiazolyl)phosphanide.

In the benzothiazole backbone of all di(*2*-benzothiazolyl)phosphane ligands no unusual bond and angles appear. The geometry is very similar to those of earlier reported structures.

3.3 Activation of carbonyls

The advantage of d-block elements in catalysis is well established.[19-23] Carbonyl complexes are a promising due to their good availability and application. An activation of the carbonyls is possible by an exchange of a carbonyl group to a more labile ligand like a solvent molecule e.g. tetrahydrofuran or acetonitrile. The replacement can either be achieved in a photolysis reaction and in some cases also thermally. A photolysis is the more versatile method and due to the availability of an

intense UV light source thermal activation was neglected. Scheme 4 shows the general activation of a metal carbonyl complex.

$$M(CO)_n \xrightarrow[\text{MeCN}]{UV} M(CO)_{n-1}(MeCN)$$
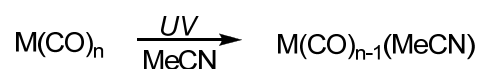
Scheme 4: general activation of carbonyl complexes in a photolysis reaction.

In the experiments for this thesis, all photolysis reactions were performed in an apparatus as shown in Figure 2. The procedure was always conducted in the following manner: A defined amount of carbonyl complex was dissolved in acetonitrile and introduced into the reaction chamber **B** applying *Schlenk* techniques. An UV light source **A** was installed protected by glass housing. As UV light source a mercury vapor lamp was used. This lamp has its main emission bands at 185 nm and 254 nm, this is at 39370 cm^{-1} and 54054 cm^{-1}, respectively. Because of the great amount of heat produced by the lamp, the reaction mixture was cooled by a continuous flow of alcohol at –35°C in the cooling chamber **C**. Thus evaporation of the solvent was excluded. For a better yield and shorter reaction time, the arising carbon monoxide was expelled by bubbling argon through the mixture.
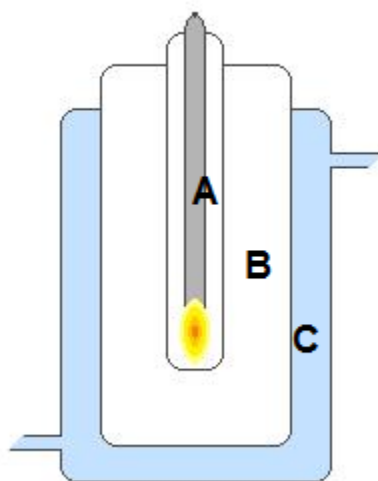
Figure 2: photolysis reaction chamber.

The photolysis reaction was monitored by IR-spectroscopy. For this purpose every 30 min. a probe was taken and turnover determined by integration of the vibration shifts of the reactants. The intensity of the shifts is according to the Beer-Lambert law direct proportional to the concentration.
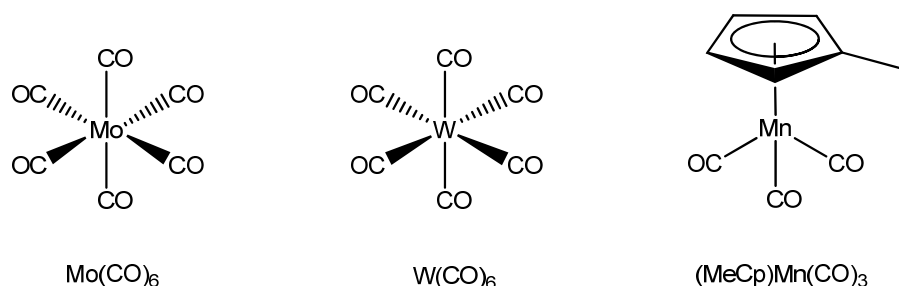
Scheme 5: examples of analyzed carbonyl complexes.

Several metal carbonyls were analyzed. Scheme 5 shows a few chosen examples. All reactions were performed in a solution either of tetrahydrofurane or acetonitrile. The turnover was more than 95% after only 30 min. irradiation in the case of $W(CO)_6$ and $(MeCp)Mn(CO)_3$ while it took more than 2 h for $Mo(CO)_6$ to achieve the same turnover. An increased turnover and a higher yield were achieved in acetonitrile. Therefore, all further photolysis reactions were performed in acetonitrile.

3.4 [{(MeCp)(OC)₂Mn}{P(bth)₂Zn(bth)₂P} {Mn(CpMe)(CO)₂}]₂ (3)

Due to the availability of the above reported zinc compound **2**, a robust and storable starting material towards heterobimetallic complexes is provided. Till now only three complexes of di(*2*-benzothiazolyl)phosphanide with a metal–phosphorous bond are known. On the one hand there is the reported iron complex [*P*-{di(*2*-benzothiazolyl) phosphanide}(cyclopentadienyl)(carbonyl) iron]₂ in chapter V, on the other hand the bimetallic complexes of [Li(bth)₂P{Mn(CO)₂}₂]ₙ and [(OC)₄W(bth)₂PW(CO)₅] by *Stey*.[15] All of these are d-block elements. As a phosphorous–manganese complex of the di(*2*-benzothiazolyl)phosphanide was reported earlier and activated (MeCp)Mn(CO)₂(MeCN) is available, the reaction was performed with bis(di(*2*-benzothiazolyl)phosphanyl)zinc (**2**).[16]

Both reactants were mixed at –10°C in toluene. The temperature was allowed to reach room temperature and the mixture stirred for 24 h. After removal of all volatiles compounds in vacuum, a saturated solution in toluene was stored at room temperature for crystallization. After about 3 months suitable single crystals for an X-ray experiment were obtained.
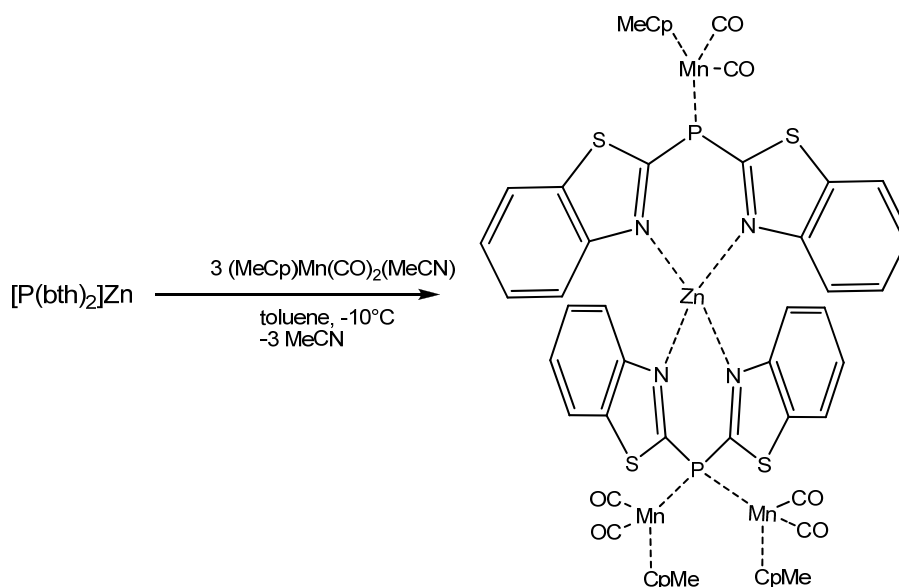
Scheme 6: preparation of [{(MeCp)(OC)$_2$Mn}{P(bth)$_2$Zn(bth)$_2$P}{Mn(CpMe)(CO)$_2$}]$_2$ (**3**).

[{(MeCp)(OC)$_2$Mn}{P(bth)$_2$Zn(bth)$_2$P}{Mn(CpMe)(CO)$_2$}]$_2$ crystallizes in the triclinic space group *P*$\bar{1}$ with one molecule and a disordered toluene molecule in the asymmetric unit. The central bis(di(*2*-benzothiazolyl)phosphanyl)zinc is similar to **2** and stays chemically intact with major changes in the shape. Both phosphorous atoms are bonded to Mn-residues asymmetrically. P1 coordinates only one while P2 bonds to two Mn-residues. These different bonding situations are also reflected in the geometry of the di(*2*-benzothiazolyl)phosphanide residues.
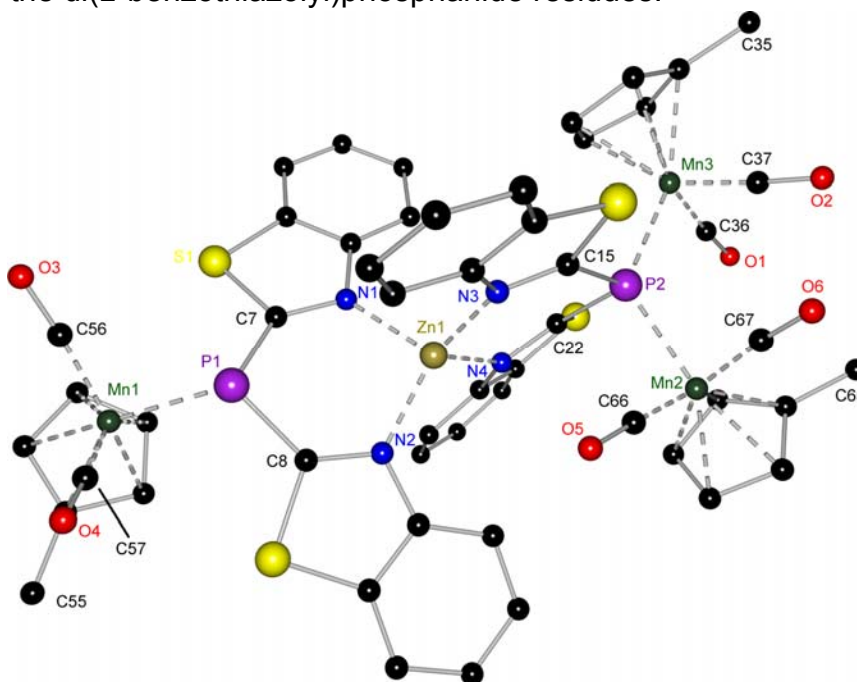
Figure 3: solid state structure of [{(MeCp)(OC)$_2$Mn}{P(bth)$_2$Zn(bth)$_2$P}{Mn(CpMe)(CO)$_2$}]$_2$

(**3**). Hydrogen atoms omitted for clarity.

Table 2: Selected bond lengths [pm] and angles [°] for [{(MeCp)(OC)$_2$Mn}{P(bth)$_2$Zn(bth)$_2$P}
{Mn(CpMe)(CO)$_2$}]$_2$ (**3**).

		P2–Mn2	231.00(15)
Zn1–N1	201.2(4)	P2–Mn3	226.60(14)
Zn1–N2	198.2(3)	N1–Zn1–N2	98.76(14)
Zn1–N3	198.9(3)	N3–Zn1–N4	100.10(14)
Zn1–N4	200.0(3)	C7–P1–C8	100.4(2)
P1–C7	179.7(3)	C15–P2–C22	100.49(19)
P1–C8	180.7(3)	Mn2–P2–Mn3	126.45(6)
P1–Mn1	225.17(13)	lig(P1)–lig(P2)	85.5
P2–C15	184.5(5)	bth(N1)–bth(N2)	148.1
P2–C22	185.8(4)	bth(N3)–bth(N4)	16.2

The zinc atom is in the center of the complex. The N–Zn bonds are slightly elongated to 199.6 pm compared to the starting complex. Additionally, the average angles between two nitrogen atoms of the same ligand are slightly smaller (99.4° compared to 101.0°). The coordination sphere at the zinc atom is still tetrahedral. Both di(*2*-benzothiazolyl)phosphanide ligands are twisted by 85.5° against each other. At their phosphorous atoms the ligands are asymmetrically coordinated by [(methyl)cyclopentadienyl](dicarbonyl)manganese moieties.
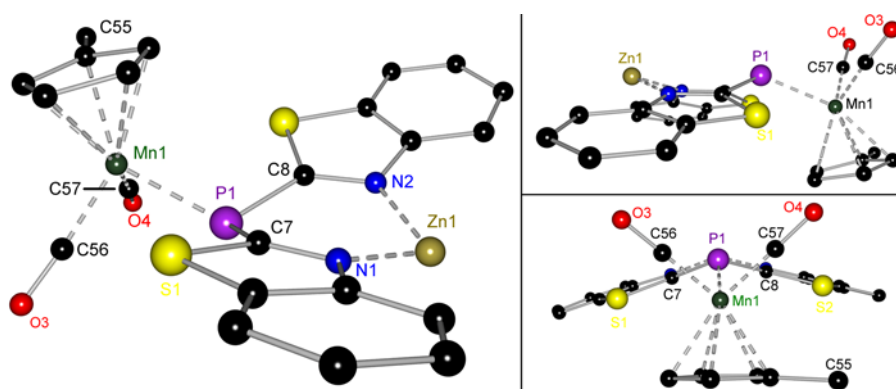
Figure 4: details of [{(MeCp)(OC)$_2$Mn}{P(bth)$_2$Zn(bth)$_2$P}{Mn(CpMe)(CO)$_2$}]$_2$
(**3**). Hydrogen atoms omitted for clarity.

The geometry at P1 should be discussed first. The ligand shows a butterfly-like arrangement; the best planes of the benzothiazole moieties intersect at an angle of 148.1°. The phosphorous atom P1 is not in plane with a benzothiazole, it is 50.1 pm out of the C7–C8–N1–N2 plane. The zinc atom Zn1 is 42.4 pm out of that plane. The

P–C$_{ipso}$ bonds are 180.2 pm on average and thus elongated in comparison to the free ligand. The C7–P1–C8 angle is 100.4° and the C$_{ipso}$–P1–Mn1 angles are 114.9° and 116.1°. The Mn1–P1 bond is 225.2 pm. The coordination sphere at P1 resembles that of a sp³-hybridized phosphorous atom. The bond lengths and angles within the benzothiazole itself are very similar to the free ligand. Only the C$_{ipso}$–N bond is slightly shorter.

The phosphorous atom P1 coordinates one manganese fragment. This manganese atom Mn1 is additionally coordinated by two carbon monoxide moiety as well as an η⁵-(methyl)cyclopentadienide.

The two carbon monoxide molecules span an angle of 89.9° and point to the convex side of the bent ligand. The average P1–Mn1– C$_{carbonyl}$ angle is 90.3°. The ligands of the manganese atom as well as those of the phosphorous atom show a staggered conformation.

As anticipated, the methyl substituted cyclopentadienyl ring is planar. The average Mn1–C$_{ring}$ distance is 214.7 pm. Its methyl group shows an ecliptic conformation with respect to the carbonyl group consisting of C57 and O4.
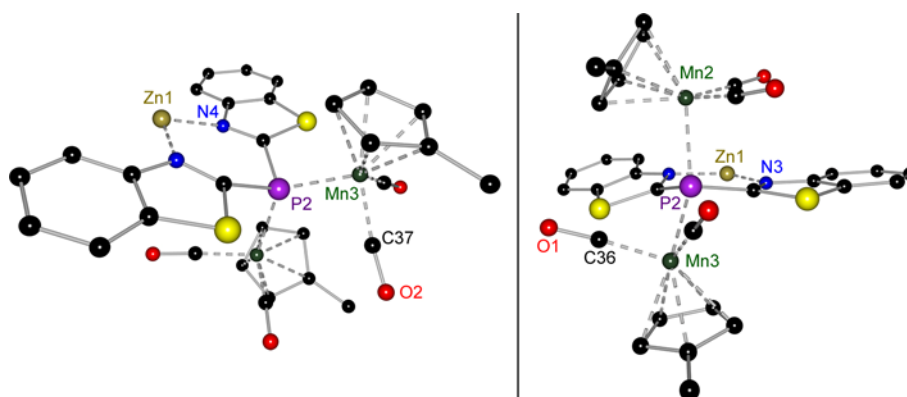
Figure 5: details of [{(MeCp)(OC)$_2$Mn}{P(bth)$_2$Zn(bth)$_2$P}{Mn(CpMe)(CO)$_2$}]$_2$
(**3**). Hydrogen atoms omitted for clarity.

The second di(2-benzothiazolyl)phosphanide containing P2 is twisted. The best planes intersects at an angle of 16.2°. The central phosphorous atom P2 is out of these best planes by 46.1 pm and 64.9 pm, respectively. In analogy, the zinc atom also is out of these planes by 25.1 pm and 58.5 pm, respectively. The P2–C$_{ipso}$ bonds are 185.2 pm in average and thus in the typical range of a P–C single bond. These bonds include an angle of 100.5°. The phosphorous atom P2 coordinates two manganese fragments with its lone pairs. Thus the phosphorous atom P2 seems to be sp³-hybridized and the coordination sphere is tetrahedral.[24]

The N–C$_{ipso}$ bonds are shortened to 132.7 pm on average and therefore the double bond character is more distinguished.

The manganese fragments each consist of two carbon monoxides and an η^5-coordinated (methyl)cyclopentadienide molecules. The carbon monoxide molecules are again arranged almost perpendicular to the P–Mn bond.

The fragment containing the manganese atom Mn3 is similarly orientated as the Mn1 to the analogous phosphorous atom P1. Again, the planar (methyl)cyclopentadienide molecule points away from the ligand while the carbon monoxide molecules towards the opposite site of the ligand. The ligands of the manganese atom as well as the phosphorous atom exhibit a staggered conformation. The methyl group (C35) of the (methyl)cyclopentadienide shows a nearly ecliptic conformation to the carbon monoxide containing C37 and O2.

In contrast to the very similar manganese fragments – Mn1 and Mn3 – the last manganese fragment containing Mn2 sticks nearly rectangular onto the ligand.

The ligands at the manganese atom Mn2 are staggered arranged towards the ligands at the phosphorous atom P2. The carbon monoxides include an angle of 89.2° and are nearly coplanar to the benzothiazole plane. One carbon monoxide containing C66 and O5 points in the same direction as the P2–N3 vector. The corresponding (methyl)cyclopentadienide points away from the ligand avoiding steric demand.

3.5 Reactions of di(*2*-benzothiazolyl)phosphane with tetracarbonyl nickel (4 and 5)

In order to move to other catalytically prominent metals and allow comparison studies, a heterobimetallic complex with nickel was an interesting research target. Nickel as pure metal finds large application as a hydrogenation catalyst in the hardening of fats. In industry, the economically most interesting use is the *Shell higher olefin process* in the production of linear alpha olefins. Within this process, a nickel phosphane complex produces a mixture of even-numbered α-olefins via ethene oligomerization and olefin metathesis.[25,26]

In 1890 *Ludwig Mond* discovered tetracarbonyl nickel.[27] In 1926 he was the co-founder of the *Imperial Chemical Industries* ICI. From his discovery, the *Mond* process to extract and purify nickel was established.[28] In this process, nickel is converted in an exothermic reaction into tetracarbonyl nickel gas at 50 – 60°C. After

transferring the gas, tetracarbonyl nickel decomposes upon heating to 220 – 250°C to give pure nickel.

A main obstacle in using tetracarbonyl nickel is its high toxicity, which is much higher than that of the carbon monoxide since additionally nickel is released in the body.

Its smell provides no reliable warning against a fatal exposure. The LC_{50} is only 3 ppm compared to 135 ppm of HCN.[29]

A relatively save way to handle pure tetracarbonyl nickel is the use of a solution in diethyl ether. Additionally, the solution alleviates the measurements of the needed reaction equivalents. Tetracarbonyl nickel is susceptible to attacks of nucleophiles. Well known are reactions with triphenylphosphane to give $Ni(CO)_3(PPh_3)$ and $Ni(CO)_2(PPh_3)_2$.[30,31]

Thus a reaction with the ligands phosphorous atom is conjecturable. An ethereal solution of tetracarbonyl nickel was added dropwise to a solution of di(2-benzothiazolyl)phosphane in diethyl ether at –78°C.
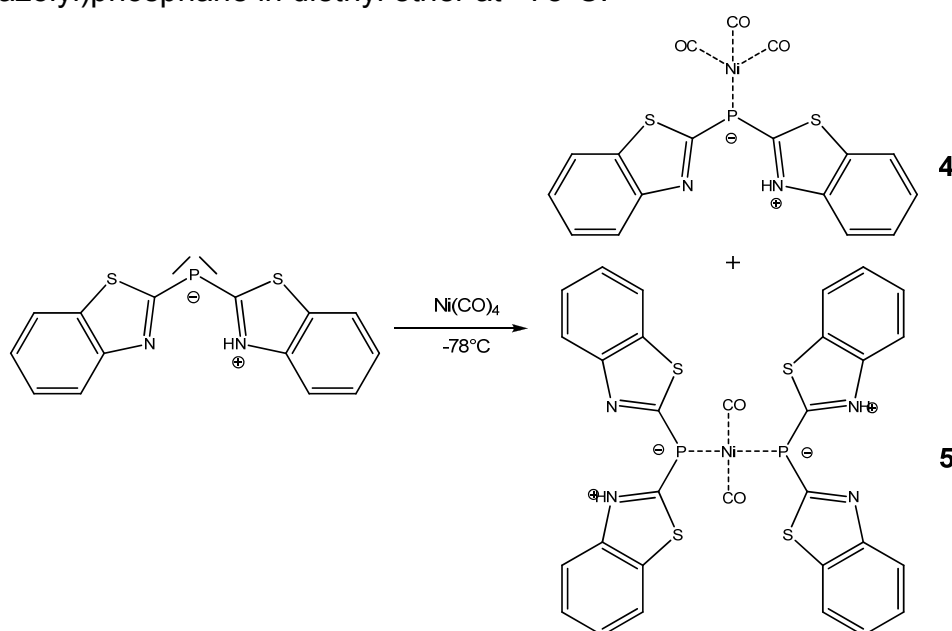
Scheme 7: preparation of di(2-benzothiazolyl)phosphane with tetracarbonyl nickel to give **4** and **5**.

The temperature was allowed to rise to room temperature and the mixture was stirred for 24 h. Removal of the solvent after filtration yielded the product as a non-separable yellow powder in a 1:1 ratio according to the NMR. Within the argon dry box the product is stable at room temperature.

It has neither been possible to separate the products nor to crystallize them within eight months. For crystallization, saturated solutions of diethyl ether, tetrahydrofuran, hexane and toluene, respectively were stored at room temperature, 4°C, -32°C, -

45°C and -86°C successivly. In every case, only decomposed product was recoverd as a black powder. Thus, instability in solution for a longer period gas to be assumed. Identification of the products was possible by NMR studies and mass spectrometry. In none of the cases any evidence of ether cleavage was found.

3.6 [{(OC)₂NiP(bth)₂ZnMe)(P(bth)₂ZnOEt)}₂] (6)

As it was not possible to isolate a monometalated nickel carbonyl complex a reaction of zincated phosphanide **1** in toluene with tetracarbonyl nickel was performed.
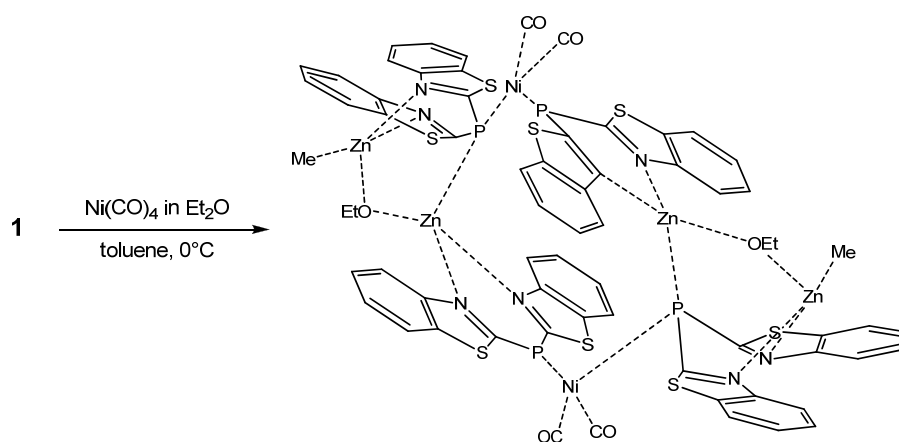
Scheme 8: preparation of [{(OC)₂NiP(bth)₂ZnMe)(P(bth)₂ZnOEt)}₂] (**6**).

To a solution of **1** in toluene, tetracarbonyl nickel in diethyl ether was added dropwise at 0°C. The reaction temperature was allowed to rise to room temperature and after the evolution of carbon monoxide stopped, all volatile material was removed *in vacuo*. Storage of a saturated solution in toluene at room temperature led to suitable single crystals for an X-ray structure determination after 3 months.
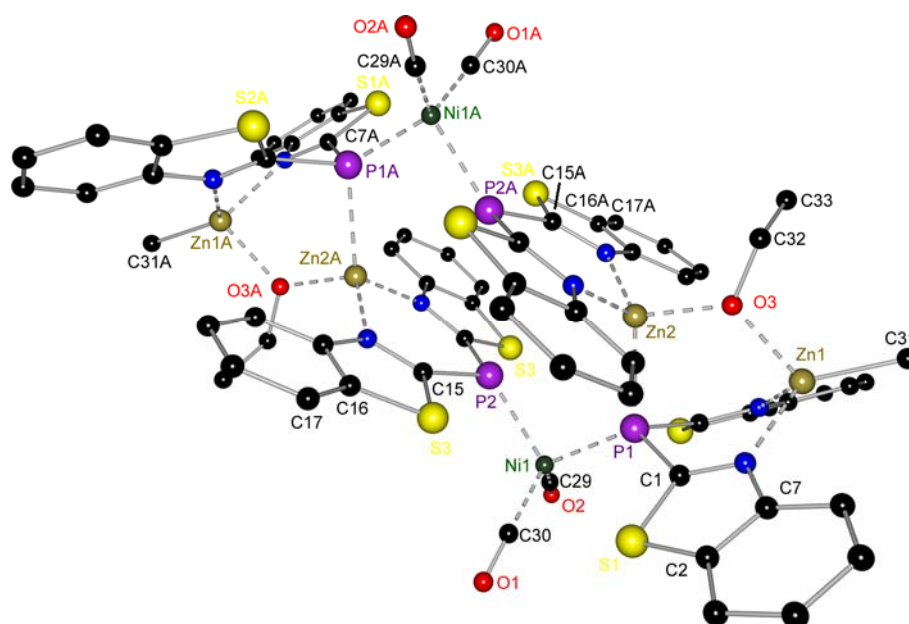
Figure 6: solid state structure of [{(OC)$_2$NiP(bth)$_2$ZnMe)(P(bth)$_2$ZnOEt)}$_2$] (**6**). Hydrogen atoms omitted for clarity.

Table 3: Selected bond lengths [pm] and angles [°] for [Ni(CO)$_2$][P(bth)$_2$ZnMe][P(bth)$_2$ZnOEt] (**6**).

Zn1–N1	211.57(6)	P2–Ni1	224.76(3)
Zn1–N2	210.57(6)	Zn1–O3	200.35(6)
Zn2–N3'	202.47(6)	Zn2–O3	193.90(6)
Zn2–N4'	202.22(6)	N1–Zn1–N2	91.06(2)
P1–C1	182.82(7)	N3–Zn1'–N4	99.55(2)
P1–C8	182.62(6)	C1–P1–C8	99.02(3)
P1–Ni1	222.86(3)	C15–P2–C22	105.43(3)
P1–Zn2	242.94(4)	P1–Ni1–P2	94.509(15)
P2–C15	177.53(6)	bth(N1)–bth(N2)	34.2
P2–C22	177.89(7)	bth(N3)–bth(N4)	7.4

[Ni(CO)$_2$][P(bth)$_2$ZnMe][P(bth)$_2$ZnOEt] (**6**) crystallizes as a dimer in the monoclinic space group P2$_1$/c with two molecules of toluene per asymmetric unit. Each monomer consists of two di(*2*-benzothiazolyl)phosphanide subunits. Each coordinated to a zinc atom *via* the nitrogen atoms. The subunits are linked by a P–Zn bond and by the bridging oxygen atom O3 of an ethanolate moiety connecting Zn1 and Zn2. The dimers are bridged by the nickel atom Ni1. It is an 18 valence electron complex concerning the zinc atoms and a 18 valence electron complex with the focus on the nickel atoms.
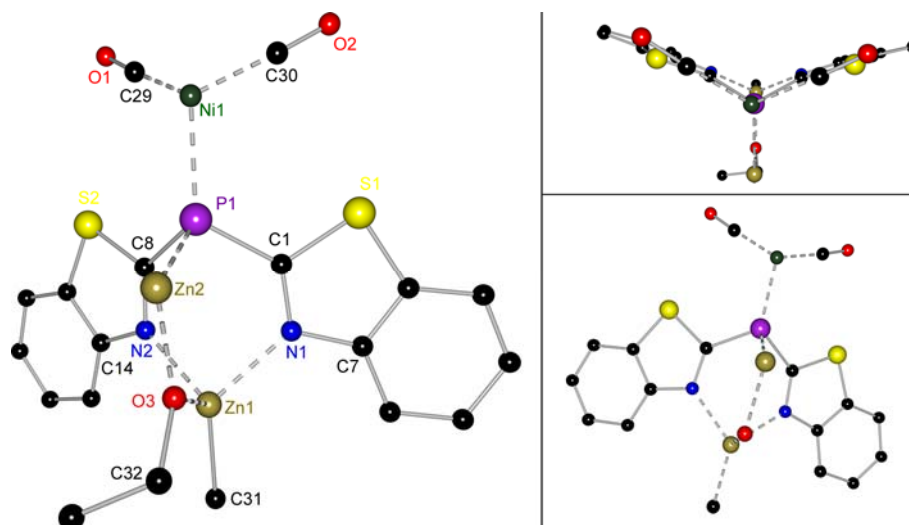
Figure 7: details of [{(OC)$_2$NiP(bth)$_2$ZnMe)(P(bth)$_2$ZnOEt)}$_2$] (**6**). Hydrogen atoms omitted for clarity.

The di(*2*-benzothiazolyl)phosphanide ligand containing P1 is bent to a butterfly-like arrangement. The best planes of the benzothiazole heterocyclic rings intersect at an angle of 145.8°. The zinc atom Zn1 is coordinated by the nitrogen atoms of the benzothiazole. Zn1 is above the best planes of both benzothiazole residues. It additionally bonds to the carbon atom C31 in a distance of 198.1 pm. The coordination sphere of Zn1 is completed by a bond towards O3. The Zn1–O3 bond length is 200.4 pm. At the other side of the ligand, coordinates the nickel atom Ni1 at the phosphorous atom P1. Furthermore, P1 shows a bond to Zn2 with a length of 242.9 pm. This bond length is slightly shorter than the reported P–Zn bond in [(Me$_3$Si)$_2$NZn(bth)$_2$P] with 248.7 pm.[18] The P1–C$_{ipso}$ bond lengths are 182.8 pm (C1) and 182.6 pm (C8), respectively. Due to this more pronounced single bond character, the N–C$_{ipso}$ bonds are slightly shortened compared to the other ligand in the molecule and feature more double bond character. The C1–P1–C8 angle is 99.02°. This clearly hints to a sp^3-hybridized phosphorous atom. The tetra-coordinated nickel atom is located at a distance of 222.9 pm from P1 and 224.8 pm from P2A. The coordination sphere at the nickel atom is completed by two carbon monoxide molecules. They include an angle of 108.8° and point to the concave side of the bend ligand. The substituents at Ni1 and P1 and Ni1 and P2A, respectively, show an ecliptic conformation.
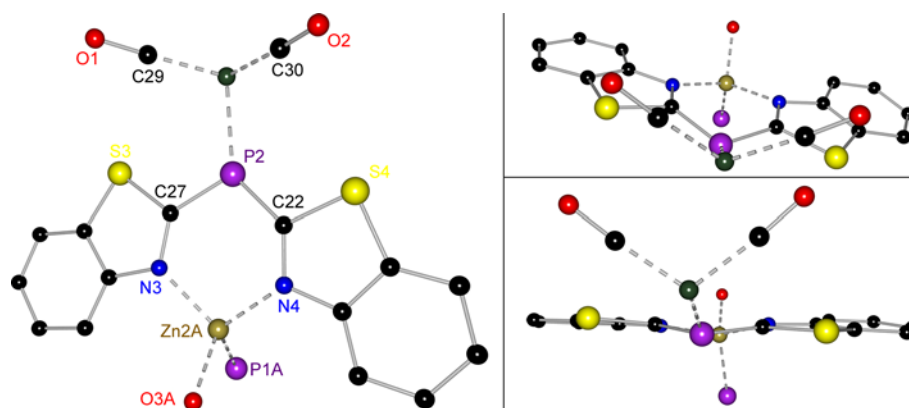
Figure 8: details of [{(OC)$_2$NiP(bth)$_2$ZnMe)(P(bth)$_2$ZnOEt)}$_2$] (**6**). Hydrogen atoms omitted for clarity.

The second benzothiazole residues of the di(*2*-benzothiazolyl)phosphanide ligand containing P2 are slightly twisted by 7.4° in respect to their best planes. The zinc atom Zn2 – coordinated by its nitrogen atoms N3 and N4 – is just slightly out of plane. Beside the above-mentioned P1 it coordinates also an ethanolate residue at O3. At phosphorus atom P2 coordinates Ni1 to form the dimer and bonds to the *ipso*-carbon atoms C15 and C22. These bond lengthss are 177.5 pm (C15) and 177.9 pm (C22) and thus shorter than the comparable P–C$_{ipso}$ bonds in the other ligand. This more pronounced double bond character in accordance to the slight extension of the N–C$_{ipso}$ bonds. A possible P2–Zn2A or P2A–Zn2 bond has to be neglected due to the distance of more than 350 pm and the necessary quintuple coordination at the corresponding zinc atom.

Within the benzothiazole moieties no noticeable changes were found except the above mentioned.

The solid state structure shows an ethoxy group at one of the to one of the zinc atoms. Its origin is not proven yet. Two different aproachs to such a residue are possible.

On the one hand, is a simple insertion of carbon monoxide generated for the reaction of the phosphanide and the tetracarbonyl nickel is possible. Due to the high resolution X-ray diffraction data this can be neglected. It is an ethoxy group with two hydrogen atoms. Its origin cannot be explained by an insertion.

On the other hand, the residue could be originated by an ether cleavage reaction. Since tetracarbonyl nickel is handled as a solution in diethyl ether for safety reasons, ether exclusion was not possible. An *ipso* cleavage of the diethyl ether consigns an ethoxy residue stabilizing the charge at the zinc atom while the residual C$_2$–fragment reacts with the methanide to form propane and leaves the reaction. Ether cleavage is

a very well known reaction. In particular, *ipso* cleavages of non-cyclic ethers are a very common phenomenon in mass spectrometry. The appearance of cleavage reactions in zinc complexes and especially on bimetallic complexes has recently been shown by *Mulvey* and co-workers.[14,32]

In summary the appearance of the ethoxy group – although unintended – underlines the very reactive character of the new heterobimetallic complex and gives rise to hope for applicability in catalytic reactions. Since this cleavage has never been observed in any of the zinc complexes **1** and **2** as well as in the reaction of tetracarbonyl nickel with free di(*2*-benzothiazolyl)phosphane to **4** and **5** it witnesses an cooparative effect of both applied metals – one of the major goals in heterobimetallic complex research.

In solution only one type of ligand is found. Presumably, this is caused by a clevage of the P1–Zn2 bond equalizing the ligands. All signals are (at room temperature) broadened hinting to an overly of two sets of signals. Until now, it has not been possible to separate these signal lowering the recording temperature in the NMR studies.

4 Conclusion

Within this chapter, reactions of di(*2*-benzothiazolyl)phosphane with dimethyl zinc were investigated This reaction leads to two different new zinc complexes depending on the used equivalents of dimethyl zinc and the reaction procedure.
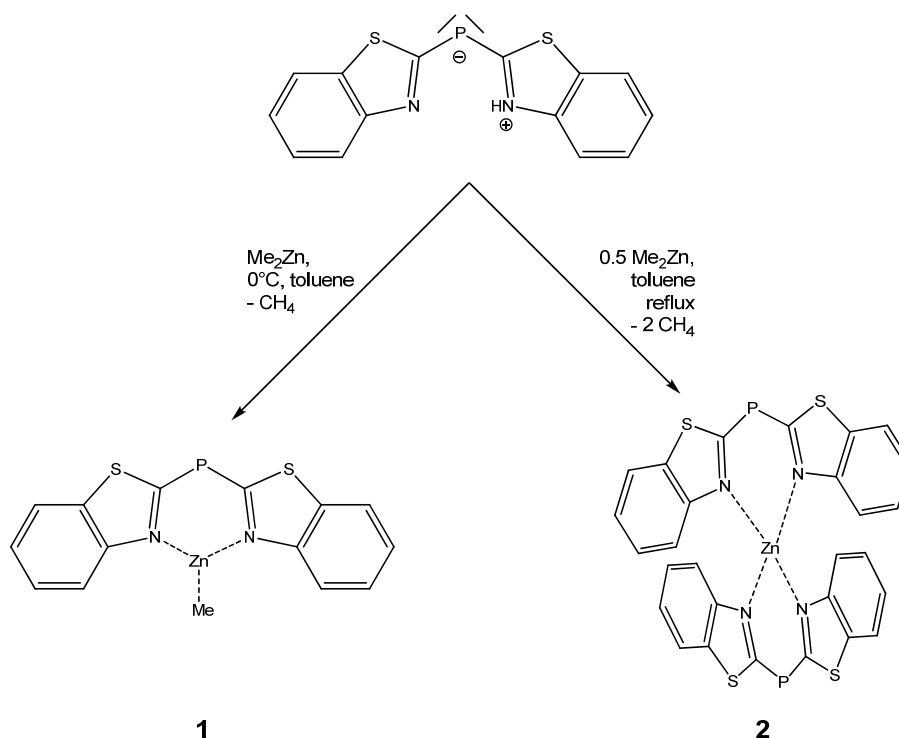
Scheme 9: novel zinc complexes of di(2-benzothiazolyl)phosphane.

Both new complexes can be prepared as a mixture or separately from each other in a good yield and a high purity. Especially compound **2** shows an improved stability and storability in comparison to the free ligand di(*2*-benzothiazolyl)phosphane. In compound **1** a methyl group remains at the zinc atom and therefore provides an additional functional group at the metal atom. In contrast to compound **1**, this methyl group is exchanged to another ligand. Both new complexes show a divalent phosphorous atom. The phosphorous atom is sp^3-hybridized and has two lone pairs like the free ligand. Hence, it acts as an 4-electron donor. These features were utilized to form heterobimetallic complexes.

Firstly, compound **2** was reacted with activated (MeCp)Mn(CO)$_2$(MeCN). An asymmetric coordinated complex with one manganese subunit on the phosohorus site and two manganese subunits on the other phosphorus site with a bis(di(*2*-benzothiazolyl)phosphanyl)zinc center coordinated by the nitrogen atoms was found.

Furthermore, compound **1** was reacted with a solution of Ni(CO)$_4$ in diethyl ether. The resulting complex combines two different arrangements of the ligand due to an diethyl ether cleavage. This result underlines the high reactivity and therefore its promising foundation for a catalytic use.
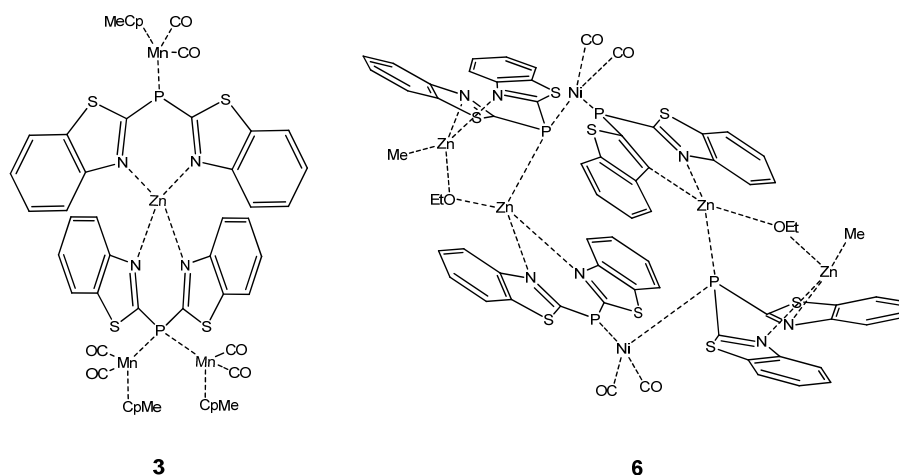
Scheme 10: derived heterobimetallic complexes from the above reported zinc complexes.

The resulting complexes were fully characterized by NMR and single crystal X-ray diffraction.

In the case of both reported heterobimetallic complexes, two different phosphorus atoms in one molecule were found. In both cases compounds the *N*-centered face of the *Janus-head* ligand is coordinated to a zinc atom. One ligand is bent while the other is twisted. Differently to the structure of compound **3**, the phosphorous atom in the bent ligand of compound **4** is fourfold coordinated while the twist is only threefold coordinated. Therefore the prospective shape of the ligand cannot be deduced from the coordination number. Both di(*2*-benzothiazolyl)phosphanide ligands show differences in the bond lengths and angles. The differences come along with a different numbers of bonds at the phosphorus atoms. Due to the rising number of bonds, charge concentration is decreased and the P–C$_{ipso}$ bonds become longer while the coordination sphere approximates the ideal tetrahedral motif of a sp^3-hybridized phosphorous atom.

Additionally, complexes **4** and **5** from the reaction of tetracarbonyl nickel and di(*2*-benzothiazolyl)phosphane were identified by NMR studies and mass spectrometry. Like in the case of compounds **1** and **2**, no evidence of ether cleavage was found within these reactions. The cleavage reaction was only detected in the heterobi-metallic species underlining the enhanced reactivity due to the corporative effects of the two different metal atoms.

5 Experimental

5.1 General

All manipulations were carried out with strict exclusion of air and moiety in nitrogen or argon atmosphere using modified *Schlenk*-techniques or in an argon dry box.[33-36] All solvents were either dried on standard laboratory procedures and were freshly distilled from sodium/potassium alloy prior to use or directly used from an *MBraun SPS* connected to the glove box. All employed reactants were commercially available or reproduced by literature known procedures.

For photolysis reactions the *HERAEUS 411 F85 UV* unit with a *Q180* lamp was used.

5.2 Spectroscopic and analytic methods

5.2.1 Nuclear Magnetic Resonance

All probes were prepared and bottled within the argon dry box into Schlenk-NMR-tubes. The NMR-tube was merged to exclude any impurities. Solvents were dried with potassium. Spectra were recorded at room temperature at a *Bruker Avance 300*, or a *Bruker Avance 500* NMR spectrometer.

All chemical shifts δ are given relative to their usual standards and coupling constants J are given in Hz. Assignments of the shifts were checked by 2d-correlation spectra. NMR shifts are assigned to the given scheme.

5.2.2 Mass spectrometry

EI-spectra were recorded with a *MAT 95* device (EI-MS: 70 eV). ESI-spectra were recorded with a Bruker HTCultra. Peaks are give according to the abundance of the main isotope as a mass to charge ratio *m/z*.

5.2.3 IR-spectroscopy

All IR-spectra were recorded at the department of chemistry at the Georg-August University on a *Varian FTS 1000*.

5.2.4 Elemental analysis

Elemental analysis was performed as a combustion analysis by the *Analytischen Labor des Institutes für Anorganische Chemie* at the Georg-August Universität Göttingen with an *elementar vario EL III*.

5.3 (Di(*2*-benzothiazolyl)phosphanyl)(methyl)zinc (1)

1.00 g (3.33 mmol) di(2-benzothiazolyl)phosphane dissolved in 100 mL toluene was added dropwise to 8.22 mL (1.2 M in toluene, 6.8 mmol) dimethyl zinc in 30 mL toluene at 0°C. After stirring 1 h all volatile compounds were removed in vacuum.

Sum formula:	$C_{15}H_{11}N_2PS_2Zn$
Molecular weight:	377.94 g/mol

^{1}H-NMR (300.13 MHz):   δ: - 0.96 (s, 3H, C*H*$_3$); 7.25 (dd, $^3J_{5,6}$ = 7.6, $^3J_{6,7}$ = 7.9, 2H, *6*); 7.38 (ddd, $^3J_{4,5}$ = 8.1, $^4J_{5,7}$ = 1.6, 2H, *5*); 7.74 (d, 2H, *7*); 7,93 (d, 2H, *4*) ppm.

^{13}C-NMR (75.468 MHz):   δ: -13.66 (s, *C*H$_3$); 116.48 (s, *4*); 120.85 (s, *7*); 123.3 (s, *6*); 125.78 (s, *5*); 132.61 (s, *7a*); 153.99 (s, *3a*); 190.27 (d, $^1J_{C,P}$ = 85.8, *2*) ppm.

^{31}P-NMR (121.495 MHz):   δ: –3.56 ppm.

EI-MS: *m/z* (%):   378 (14) [*M*], 363 (8) [*M*-Me], 299 (100) [*P(bth)$_2$*].

5.4 Bis[di(*2*-benzothiazolyl)phosphanyl]zinc (2)

1.00 g (3.33 mmol) di(2-benzothiazolyl)phosphane was dissolved in 50 mL toluene and 3.90 mL (1.2 M in toluene, 3.25 mmol) dimethyl zinc were added dropwise within 15 min. at 0°C. Reflux for 45 min. completed the reaction and storage of a saturated solution yielded single crystals suitable for an X-ray diffraction experiment after 6–8 weeks.

Sum formula:	$C_{28}H_{16}N_4P_2S_4Zn$

Molecular weight: 661.90 g/mol

^{1}H-NMR (300.13 MHz):   δ: 7.10 (ddd, $^3J_{5,6}$ = 7.4, $^3J_{6,7}$ = 7.9, $^4J_{4,6}$ = 1.3, 4H, *6*);
7.17 (ddd, $^3J_{4,5}$ = 7.5, $^4J_{5,7}$ = 1.2, 4H, *5*); 7.26 (dd, 4H, *4*);
7,70 (dd, 4H, *7*) ppm.

^{13}C-NMR (75.468 MHz):   δ: 115.37 (s, *4*); 121.22 (s, *7*); 123.91 (s, *6*); 126.76 (s, *5*);
132.02 (s, *7a*); 152.39 (s, *3a*); 191.41 (d, $^1J_{C,P}$ = 91.2, *2*)
ppm.

^{31}P-NMR (121.495 MHz): δ: –6.02 ppm.

EI-MS: *m/z* (%):   662 (20) [*M*], 527 (4) [*M*-bth], 363 (8) [*M*- P(bth)$_2$], 299
(100) [*P(bth)$_2$*].

5.5 [{(MeCp)(OC)$_2$Mn}{P(bth)$_2$Zn(bth)$_2$P} {Mn(CpMe)(CO)$_2$}]$_2$ (3)

1.00 g (1.51 mmol) **2** was dissolved in 50 mL toluene and 1.39 g (6 mmol) (MeCp)Mn(CO)$_2$(MeCN) in 30 mL toluene were added dropwise at -10°C. The temperature was allowed to rise to room temperature and the mixture stirred for 24 h. After filtration all volatile material were removed in vacuum, re-dissolved in toluene and the resulting saturated solution in toluene was stored at room temperature for crystallization. After around 3 month suitable single crystals for an X-ray diffraction experiment were obtained.

Sum formula: C$_{52}$H$_{37}$Mn$_3$N$_4$O$_6$P$_2$S$_4$Zn

Molecular weight: 1231.85 g/mol

^{1}H-NMR (300.13MHz):   δ: 1.93 (s, 6H, *H35a, H35b, H35c, H65a H65b, H65c);*
2.10 (s, 3H, H55a, H55b, H55c); 4.36 (s, 4H, *H30, H31,
H60, H61*); 4.51 (s, 2H, *H50, H51*); 4.56 (d, $^4J_{H,H}$ = 2.0, 4H,
H32, H34, H62, H64); 4.62 (dd, $^3J_{H,H}$ = 7.9, $^4J_{H,H}$ = 2.0, 2H

| | *H52, H54*); 6.44–6.59 (m, 4H); 6.62–6.78 (m, 4H); 6.88–7.02 (m, 4H); 7.32–7.44 (m, 4H) ppm. |

^{13}C-NMR (100.61 MHz): δ: 13.10 (s, Cp*CH$_3$*); 82.00 (s, Cp); 83.03 (s, Cp); 115.71 (s, *4*); 121.82 (s, *7*); 124.11 (s, *6*); 125.64 (s, *5*); 137.83 (s, *7a*); 151.87 (s, *3a*); 192.69 (s, *2*); 199.85 (s, *C*O) ppm.

^{15}N-NMR (30.423 MHz): δ: −190.18 (s) ppm.

^{31}P-NMR (121.495 MHz): δ: -3.115 (s, P1): 29.989 (s, P2) ppm.

IR (nujol, cm^{-1}):   1925, 1857.

ESI-MS: *m/z* (%):   1001 (10) [*M*- 3Cp'], 679 (38) [*M*-Pbth$_2$-MnCp'(CO)$_2$-Zn], 623 (24) [*M*-Pbth$_2$-(MnCp'(CO)$_2$)$_2$-Cp'-CO], 567 (100) [*M*$^{2+}$-Cp'-CO], 446 (4) [*M*-Pbth$_2$-2MnCp'(CO)$_2$-Cp'-CO].

Elemental analysis:

CHNS, found(calc.):   C: 51.9 %(50.60%); H: 3.32 %(3.02%);

N: 4.63 %(4.54%); S: 9.70 %(10.3%).

5.6 [Di(*2*-benzothiazolyl)phosphanyl] (tricarbonyl)nickel (4)

1.0 g (3.33 mmol) di(2-benzothazolyl)phosphane was dissolved in 50 mL diethyl ether and 4.8 mL (0.62 M in diethyl ether, 3 mmol) tetracarbonyl nickel were added drop wise at -78°C. The temperature was allowed to rise to room temperature and the mixture stirred for 24 h. After filtration all volatile compounds were removed *in vacuo*. The product was obtained as a non separable yellow powder in a 1:1 ratio according to the NMR spectra.

Sum formula: C$_{17}$H$_9$N$_2$NiO$_3$PS$_2$

Molecular weight: 445.06 g/mol

^{1}H-NMR (300.13 MHz):   δ: 7.46 (dd, $^3J_{4,5}$ = 6.9, $^3J_{5,6}$ =7.9, 2H, *5*); 7.49 (dd, $^3J_{6,7}$ = 7.5, 2H, *6*); 7.96 (d, 2H, *4*), 8.07 (d, 2H, *7*) ppm.

^{13}C-NMR (75.468 MHz):   δ: 122.40 (s, *4*); 124.28 (s, *7*); 126.63 (s, *5*); 127.09 (s, *6*); 132.49 (s, *7a*); 156.40 (s, *3a*); 187.52 (s, *2*); 196.93 (s, *CO*); 211.83 (s, *CO*) ppm.

^{31}P-NMR (121.495 MHz): δ: -18.28(s) ppm.

EI-MS: *m/z* (%):   443 (1) [*M*], 385 (8) [*M*-2CO], 299 (40) [Pbth$_2$], 135 (100) [bth].

5.7 Bis[di(*2*-benzothiazolyl)phosphanyl]   (dicarbonyl)nickel (5)

The preparation of **5** is identical to **4** since both occur always in a non separable mixture.

Sum formula: C$_{30}$H$_{18}$N$_4$NiO$_2$P$_2$S$_4$

Molecular weight: 715.39 g/mol

^{1}H-NMR (300.13 MHz):   δ: 7.24 (dd, $^3J_{4,5}$ = 7.4, $^3J_{5,6}$ =7.9, 4H, *5*); 7.41 (dd, $^3J_{6,7}$ = 7.5, 4H, *6*); 7.75 (s, 4H, *4*), 7.78 (s, 4H, *7*) ppm.

^{13}C-NMR (75.468 MHz): δ: 117.02 (s, *7*); 122.19 (s, *4*); 124.53 (s, *5*); 127.11 (s, *6*); 132.13 (s, *7a*); 163.84 (s, *3a*); 181.93 (s, *2*); 196.51 (s, *CO*) ppm.

^{31}P-NMR (121.495 MHz): δ: -15.43(s) ppm.

EI-MS: *m/z* (%):   715 (2) [*M*], 580 (18) [*M*-bth], 565 (17) [*M*-bth-CO], 415 (4) [*M*-Pbth$_2$], 299 (40) [Pbth$_2$], 135 (100) [bth].

5.8 [{(OC)₂NiP(bth)₂ZnMe)(P(bth)₂ZnOEt)}₂] (6)

1.00 g (2.64 mmol) **1** was dissolved in 50 mL toluene and 4.8 mL (0.62 M in diethyl ether, 3 mmol) tetracarbonyl nickel were added dropwise at -10°C. The temperature was allowed to rise to room temperature and the mixture stirred for 24 h. After filtration all volatile compounds were removed *in vacuo*, re-dissolved in toluene and the saturated solution in toluene was stored at room temperature for crystallization. After around 4 month suitable single crystals for an X-ray diffraction experiment were obtained.

Sum formula:	$C_{66}H_{48}N_8Ni_2O_6P_4S_8Zn_4$
Molecular weight:	1799,62 g/mol

^{1}H-NMR (300.13 MHz): δ: 0.25 (s, Zn–CH_3); 0.25 (t, Zn–CH$_2$-CH_3); 2.72 (q, Zn–CH_2-CH$_3$); 6.43 (dd, $^3J_{4,5}$ = 7.8, $^3J_{5,6}$ =7.5, 8H, *5*); 6.60 (dd, $^3J_{6,7}$ = 8.2, 8H, *6*); 6.79 (d, 8H, *4*); 7.45 (d, 8H, *7*) ppm.

^{13}C-NMR (75.468 MHz): δ: −7.90 (s, Zn–CH_3); 14.30 (s, CH$_2$–CH$_3$); 34.19 (s, CH$_2$–CH$_3$); 115.92 (s, *7*); 121.28 (s, *4*); 124.12 (s, *5*); 127.16 (s, *6*); 130.72 (s, *7a*); 131.59 (s, *3a*); 151.19(s, *2*); 191.54 (s, CO); 192.63 (s, CO) ppm.

^{31}P-NMR (121.495 MHz): δ: −4.98 (s$_{broad}$) ppm.

IR (nujol, cm^{-1}): 2010, 1945.

ESI-MS: *m/z* (%): 900 (5) [M^{2+}], 887 (12) [M^{2+}-CO], 873 (40) [M^{2+}-2CO], 859 (75) [M^{2+}-3CO], 845 (5) [M^{2+}-4CO], 831 (8) [M^{2+}-CO-OEt], 719 (12) [Zn(bth)$_2$PNiP(bth)$_2$], 441 (100) [0.5M^{2+}-CO], 300 (20) [P(bth)$_2$].

Elemental analysis:

CHNS, found(calc.): C: 40.52 %(43.83 %); H: 2.93 %(2.68 %);
                     N: 4.70 %(6.20%); S: 10.12 %(14.18%).

6 Literature

[1]   B. Cornils, W. A. Herrmann, *Applied Homogenous Catalysis with Organometallic Compounds*, VCH, Weinheim, **1996**.

[2]   S. P. Sarish, B. Nekoueishahraki, A. Jana, H. W. Roesky, T. Schulz, D. Stalke, *Chem. Eur. J.* **2010**, *submitted*.

[3]   S. Handa, V. Gnanadesikan, S. Matsunaga, M. Shibasaki, *J. Am. Chem. Soc.* **2010**, *132*, 4925-4934.

[4]   A. P. Shaw, J. R. Norton, D. Buccella, L. A. Sites, S. S. Kleinbach, D. A. Jarem, K. M. Bocage, C. Nataro, *Organometallics* **2009**, *28*, 3804-3814.

[5]   C. A. de Parrodi, P. J. Walsh, *Angew. Chem.* **2009**, *121*, 4773-4776; *Angew. Chem. Int. Ed.* **2009**, *48*, 4679-4682.

[6]   I. Kuzu, I. Krummenacher, J. Meyer, F. Armbruster, F. Breher, *Dalton Trans.* **2008**, 5836-5865.

[7]   S. Handa, K. Nagawa, Y. Sohtome, S. Matsunaga, M. Shibasaki, *Angew. Chem.* **2008**, *120*, 3274-3277; *Angew. Chem. Int. Ed.* **2008**, *47*, 3230-3233.

[8]   S.-y. Tosaki, K. Hara, V. Gnanadesikan, H. Morimoto, S. Harada, M. Sugita, N. Yamagiwa, S. Matsunaga, M. Shibasaki, *J. Am. Chem. Soc.* **2006**, *128*, 11776-11777.

[9]   G. Bai, S. Singh, H. W. Roesky, M. Noltemeyer, H.-G. Schmidt, *J. Am. Chem. Soc.* **2005**, *127*, 3449-3455.

[10]   T. I. Doukov, T. M. Iverson, J. Seravalli, S. W. Ragsdale, C. L. Drennan, *Science* **2002**, *298*, 567-572.

[11]   H. Sasai, T. Arai, S. Watanabe, M. Shibasaki, *Catal. Today* **2000**, *62*, 17-22.

[12]   M. Shibasaki, H. Sasai, T. Arai, *Angew. Chem.* **1997**, *109*, 1290-1311; *Angew. Chem. Int. Ed. Engl.* **1997**, *36*, 1235-1256.

[13]   R. E. Mulvey, *Organometallics* **2006**, *25*, 1060-1075.

[14]   A. R. Kennedy, J. Klett, R. E. Mulvey, D. S. Wright, *Science* **2009**, *326*, 706-708.

[15]   T. Stey, Ph.D. thesis, Universität Würzburg (Germany), **2004**.

[16]   P.-F. Yang, G. K. Yang, *J. Am. Chem. Soc.* **1992**, *114*, 6937-6938.

[17]   W. Strohmeier, *Angew. Chem.* **1964**, *76*, 873-881; *Angew. Chem. Int. Ed. Engl.* **1964**, *3*, 730-737.

[18]   T. Stey, D. Stalke, *Z. Anorg. Allg. Chem.* **2005**, *651*, 2931-2936.

[19]   P. P. Power, *Nature* **2010**, *463*, 171-177.

[20]   M. Bochmann, S. J. Lancaster, *Angew. Chem.* **1994**, *106*, 1715-1718; *Angew. Chem. Int. Ed. Engl.* **1994**, *33*, 1634-1637.

[21]   R. Noyori, *Angew. Chem.* **2002**, *114*, 2108-2123; *Angew. Chem. Int. Ed.* **2002**, *41*, 2008-2023.

[22]   P. v. Matt, A. Pfaltz, *Angew. Chem.* **1993**, *105*, 614-615; *Angew. Chem. Int. Ed. Engl.* **1993**, *32*, 566.

[23]   J. P. Wolfe, S. Wagaw, S. L. Buchwald, *J. Am. Chem. Soc.* **1996**, *118*, 7215-7216.

[24]   J. Henn, K. Meindl, A. Oechsner, G. Schwab, T. Koritsanszky, D. Stalke, *Angew. Chem.* **2010**, *122*, 2472-2476; *Angew. Chem. Int. Ed.* **2010**, *49*, 2422.

[25]   P. Kuhn, D. Semeril, D. Matt, M. J. Chetcuti, P. Lutz, *Dalton Trans.* **2007**, *5*, 515-528.

[26]   K. Weissermel, H.-J. Arpe, *Industrial Organic Chemistry*, Wiley-VCH, Weinheim, **1997**.

[27]   L. Mond, C. Langer, F. Quincke, *Journal of the Chemical Society, Transction* **1890**, *57*, 749-753.

[28]   W. C. Roberts-Austin, *Nature* **1898**, *59*, 63-64.

[29]   B. o. E. S. a. Toxicology., *"Nickel Carbonyl: Acute Exposure Guideline Levels"*. *Acute Exposure Guideline Levels for Selected Airborne Chemicals*, National Academies Press, **2008**, p. 213-259.

[30]   C. Elschenbroich, A. Salzer, *Organometallics – A Concise Introduction*, VCH, Weinheim, **1992**.

[31]   C. Elschenbroich, A. Salzer, *Organometallchemie - Eine kurze Einführung*, B. G. Teubner, Stuttgart, **1990**.

[32]   R. E. Mulvey, V. L. Blair, W. Clegg, A. R. Kennedy, L. Russo, *Nature Chemistry* **2010**, *2*, 588-591.

[33]   W. Schlenk, A. Thal, *Ber. Dtsch. Chem. Ges.* **1913**, *46*, 2840-2854.

[34]   W. Schlenk, J. Holtz, *Ber. Dtsch. Chem. Ges.* **1917**, *50*, 262-274.

[35]   T. T. Tidwell, *Angew. Chem.* **2001**, *113*, 343-349; *Angew. Chem. Int. Ed.* **2001**, *40*, 331-337.

[36]   W. Schlenk, *Die Methoden der Organischen Chemie* in *Die Methoden der Organischen Chemie* (Ed. J. Houben), G. Thieme, Leipzig, **1924**, p. 720.

1 Crystallographic section

1.1 Crystal Application

The crystals were taken from the mother liquor using standard *Schlenk*-techniques and placed in perfluorinated polyether oil on a microscope slide. An appropriately sized crystal of high quality was selected under a polarization microscope (for detection of twinning and the presence of satellites) with help of the *X-TEMP2* cooling device.[1,2] It was mounted on a glass fibre glued to the magnetic pin of the goniometer head in a way that it was completely coated with the perfluorinated polyether oil.[3] Oil and crystal were shock-cooled in the cold gas stream of an open flow nitrogen cooling device attached to the diffractometer. The amorphous frozen oil served as glue and protected the sensitive compounds along with the nitrogen gas stream from moisture and oxygen.

1.2 Data Collection and Processing

All compounds were measured on a *Bruker D8 goniometer* platform, equipped with a *SMART APEX II CCD* camera. The compounds were measured using either a Incoatec microfocus source with Quazar mirror optics or on a rotating anode device.[4] Both are equipped with an *APEX II CCD* detector, mounted on a three-circle D8 goniometer, and Incoatec Helios mirrors as monochromator optics, which supplies very intense and brilliant MoK_α radiation (λ = 0.71073 Å).

All crystals were centered optically using a video camera after being mounted on the diffractometer.

Data collection was controlled with the *APEX2* package.[5] A test run (usually 50 frames in ω-scan mode at φ = 0 °) was recorded prior to each experiment to check the crystal quality, to get a rough estimate of the cell parameters, and to determine the optimum exposure time. All scans of the data collections were performed in an ω-scan mode with a step-width of 0.3° or 0.5° at fixed φ-angles.

The determination of the unit cells and orientation matrices were performed with the tools supplied in the *APEX2* package. [5] The collected frames were integrated with *SAINT*[6] using the 3d profiling method described by *Kabsch*.[7]

All data sets were corrected for absorption and scaled using *SADABS*[8] or *TWINABS*.[9] *XPREP*[10] was used to determine the space group prior to the absorption correction, as this is crucial for a correct treatment. *SADABS* and *TWINABS* refine an empirical model function by symmetry-equivalent reflections.

Data merging according to the determined symmetry and setup of the files for structure solution and refinement was performed with *XPREP*.[10]

1.3 Structure Solution and Refinement

The structures were solved with direct methods using *SHELXS*.[11] All refinements were performed on F^2 with *SHELXL*.[11]

If not stated otherwise, the hydrogen atoms of the compounds were refined using a riding model. The positions were geometrically optimized and the U_{iso} were constrained to 1.2 U_{eq} of the pivot atom or 1.5 U_{eq} of the methyl carbon atom.

In all refinements the function $M(p_i, k)$ (Eq. 1) was minimized using the weights w_H defined in Eq. 2. The variables g1 and g2 are given in the crystallographic tables.

Eq. 1 :
$$M(p_i, k) = \sum_H w_H \left[k |F_{obs}(\mathbf{H})|^2 - |F_{calc}(\mathbf{H})|^2 \right]^2 = \min$$

Eq. 2 :
$$w_H^{-1} = \sigma_H^2 F_{obs}^2 + (g1 \cdot P)^2 + g2 \cdot P \text{ with } P = \left(\frac{F_{obs}^2 + 2F_{calc}^2}{3} \right)$$

The results of the refinements were verified by comparison of the calculated and the observed structure factors. Commonly used criteria are the residuals $R1$ (Eq. 3) and $wR2$ (Eq. 4). The $wR2$ is more significant, because the model is refined against F^2.

Eq. 3:
$$R1 = \frac{\sum \left(\|F_{obs}| - |F_{calc}\| \right)}{\sum |F_{obs}|}$$

Eq. 4:
$$wR2 = \frac{\sum_H w_H \left(|F_{obs}|^2 - |F_{calc}|^2 \right)^2}{\sum_H w_H |F_{obs}|^4}$$

Additionally, the goodness of fit (GoF), a figure of merit showing the relation between deviation of F_{calc} from F_{obs} and the over-determination of refined parameters is calculated.

Eq. 5:
$$GoF = \sqrt{\frac{\sum_H w_H \left(|F_{obs}| - |F_{calc}| \right)^2}{N - n}}$$

The residual densities from difference *Fourier* analysis should be low. Due to the model restrictions the residuals are normally found in the bonding regions. Higher residuals for heavy scatterers are acceptable as they arise mainly from absorption effects and *Fourier* truncation errors due to the limited recorded resolution range. The

highest peak and deepest hole from difference *Fourier* analysis are listed in the crystallographic tables.

Additionally, the orientation, size and ellipticity of the ADP's show the quality of the model. Ideally, the ADP's should be oriented perpendicular to the bonds, be equal in size and show little ellipticity. All graphics were generated and plotted with the *XShell* program at the 50 % probability level.

If not stated otherwise hydrogen atoms were refined isotropically on calculated positions using a riding model with their U_{iso} values constrained to equal to 1.5 times the U_{eq} of their pivot atoms for terminal sp^3 carbon atoms and 1.2 times for all other carbon atoms. The position of certain hydrogen atoms (*e. g.* in OH groups) were found with a difference Fourier analysis of the rest electron density. The hydrogen bond lengths were restrained to a sensible value and the U_{iso} were constrained to 1.2 times the U_{eq} of the pivot atoms.

1.4 Treatment of Disorder

Structures containing disordered fragments were refined using constraints and restraints. The geometries of chemically equivalent but crystallographically independent fragments can be fitted to each other by distance restraints. Especially the 1,2 distances (bond lengths) and 1,3 distances (bond angles) are set to be equal within their effective standard deviations. This is helpful for refining disordered positions as the averaging of equivalent fragments implements chemical information and stabilizes the refinement.

Restraints affecting the anisotropic displacement parameters are often essential for the anisotropic refinement of disordered atomic positions. The rigid bond restraints (DELU in *SHELXL*)[12] fit the components of the anisotropic displacement parameters along the bonds within esd's. Similarity restraints (SIMU in *SHELXL*)[12] adjust the ADPs of neighboring atoms within a certain radius to be equal according to their esd's. The ISOR command in *SHELXL*[12] forces the ADPs to adapt a more spherical, isotropic behavior, which is sometimes necessary to refine positions with minor occupation factors.
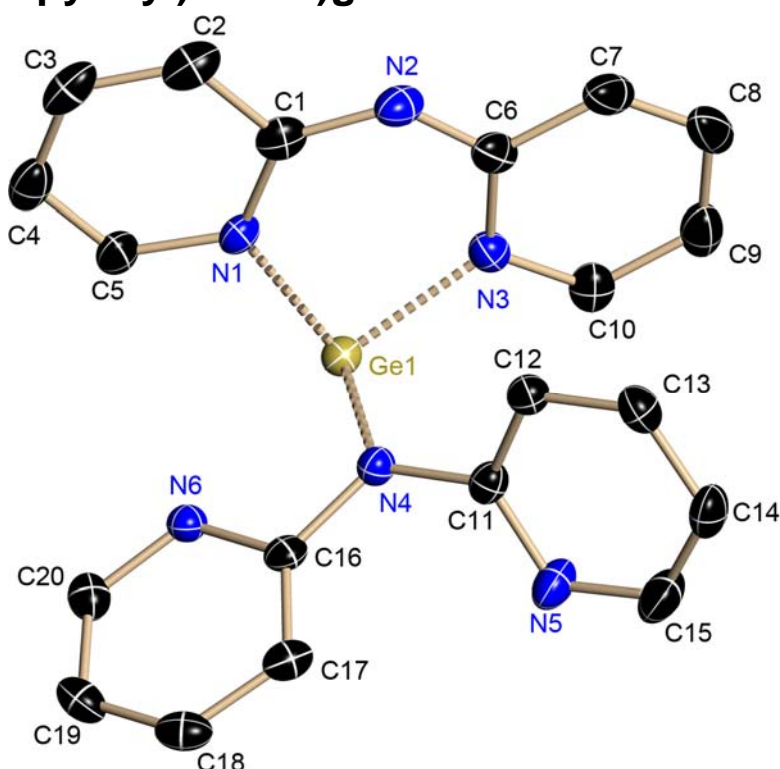
1.5 Bis(di(2-pyridyl)amido)germanium

Figure 1: Asymmetric unit of bis(di(2-pyridyl)amido)germanium. Anisotropic displacement parameters are depicted at a probability level of 50%, hydrogen atoms are omitted for clarity.

Table 1: crystallographic data for bis(di(2-pyridyl)amido)germanium .

| identification code	DPA2Ge	temperature [K]	101(2)
empirical formula	$C_{20}H_{16}GeN_6$	max./min. transmission	0.9254 / 1.0000
molecular mass [g/mol]	412.98	ρ_{calc} [g/cm^3]	1.568
crystal size [mm]	0.16 x 0.15 x 0.14	μ [mm^{-1}]	1.769
crystal system	orthorhombic	F(000)	1680
space group	$Pbca$	Θ range [°]	1.66 – 27.11
a [Å]	7.7626(2)	reflections all / unique	32420 / 4212
b [Å]	18.4215(4)	data / restraints / parameter	29485 /0 / 244
c [Å]	24.4650(6)	R1 (all data)	0.0519
α [°]	90.00	wR2 (all data)	0.0801
β [°]	90.00	g1 / g2	0.0296 / 3.2311
γ [°]	90.00	GoF	1.052
V [Å^3]	3498.46(15)	peak / hole	
Z	8	max. /min. [10^6eÅ^{-3}]	0.54 / -0.44

1.6 Bis(di(*2*-pyridyl)amido)tin
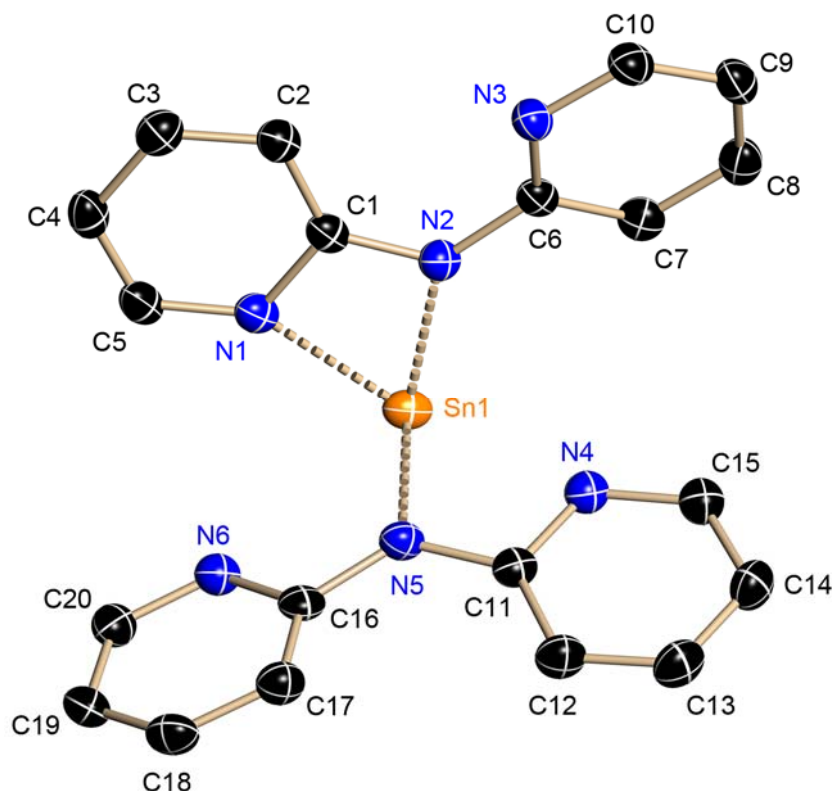
Figure 2: Asymmetric unit of bis(di(*2*-pyridyl)amido)tin. Anisotropic
displacement parameters are depicted at a probability level
of 50%, hydrogen atoms are omitted for clarity.

Table 2: crystallographic data for bis(di(*2*-pyridyl)amido)tin.

identification code	DPA2Sn	temperature [K]	108(2)
empirical formula	$C_{20}H_{16}N_6Sn$	max./min. transmission	0.8813 / 1.0000
molecular mass [g/mol]	459.08	ρ_{calc} [g/cm^3]	1.695
crystal size [mm]	0.2 x 0.2 x 0.2	μ [mm^{-1}]	1.438
crystal system	Monoclinic	$F(000)$	912
space group	$P2_1$/n	Θ range [°]	2.40 – 27.45
a [Å]	11.8184(10)	reflections all / unique	24396 / 4392
b [Å]	9.2591(8)	data / restraints / parameter	4127/ 0 / 244
c [Å]	16.9547(14)	*R*1 (all data)	0.0320
α [°]	90.00	*wR*2 (all data)	0.0561
β [°]	104.1080	g1 / g2	0.0242 / 1.0404
γ [°]	90.00	GoF	1.069
V [Å^3]	1798.6(3)	peak / hole	
Z	4	max. /min. [10^{6}eÅ^{-3}]	0.772 / -0.462

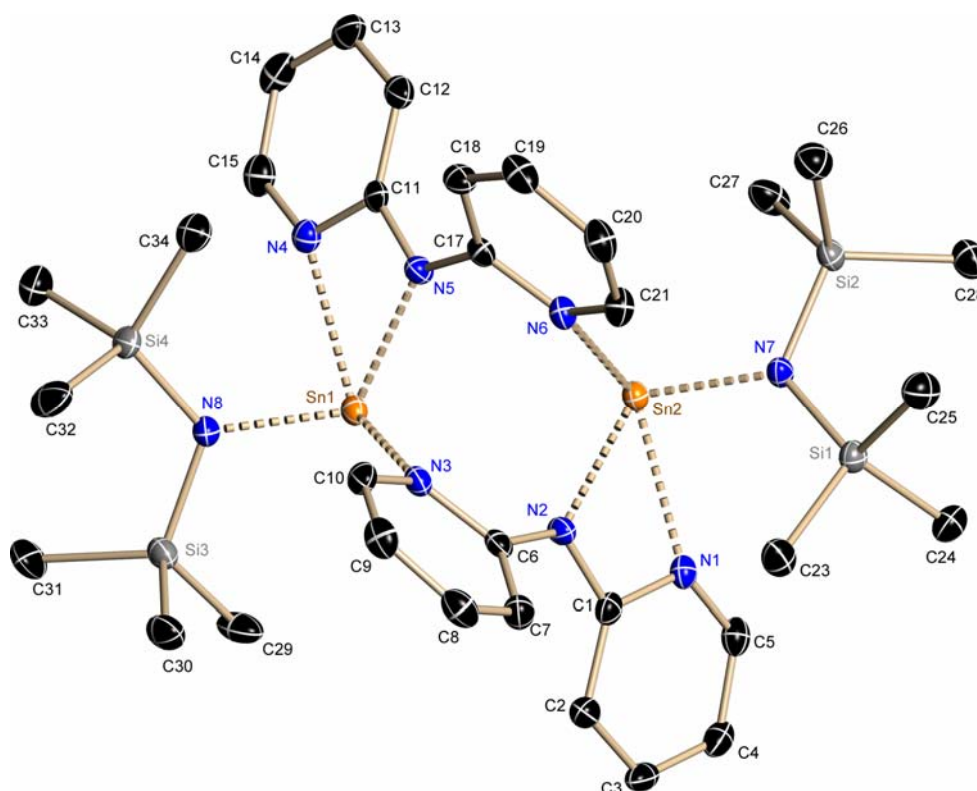# 1.7 (Di(2-pyridyl)amido)tin(hexamethyldisilazane)

Figure 3: Asymmetric unit of (di(2-pyridyl)amido)tin(hexamethyldisilazane)
(**5**). Anisotropic displacement parameters are depicted at a
probability level of 50%, hydrogen atoms are omitted for clarity.

Table 3: crystallographic data for (di(2-pyridyl)amido)tin(hexamethyldisilazane).

identification code	DPASnN(TMS)2	temperature [K]	100(2)
empirical formula	$C_{32}H_{52}N_8Si_4Sn$	max./min. transmission	0.3781 / 0.4302
molecular mass [g/mol]	900.14	ρ_{calc} [g/cm^3]	1.486
crystal size [mm]	0.2 x 0.2 x 0.2	µ [mm^{-1}]	1.401
crystal system	triclinic	F(000)	906
space group	$P\overline{1}$	Θ range [°]	1.45 – 27.09
a [Å]	11.3364(11)	reflections all / unique	50736 / 8812
b [Å]	12.5684(13)	data / restraints / parameter	8810 / 0 / 426
c [Å]	15.8152(16)	$R1$ (all data)	0.0476
α [°]	68.2410(10)	$wR2$ (all data)	0.0806
β [°]	73.334(2)	g1 / g2	0.0242 / 1.0404
γ [°]	86.94(2)	GoF	1.074
V [Å^3]	2001.2(3)	peak / hole	
Z	2	max. /min. [10^6eÅ^{-3}]	1.597 / -0.640

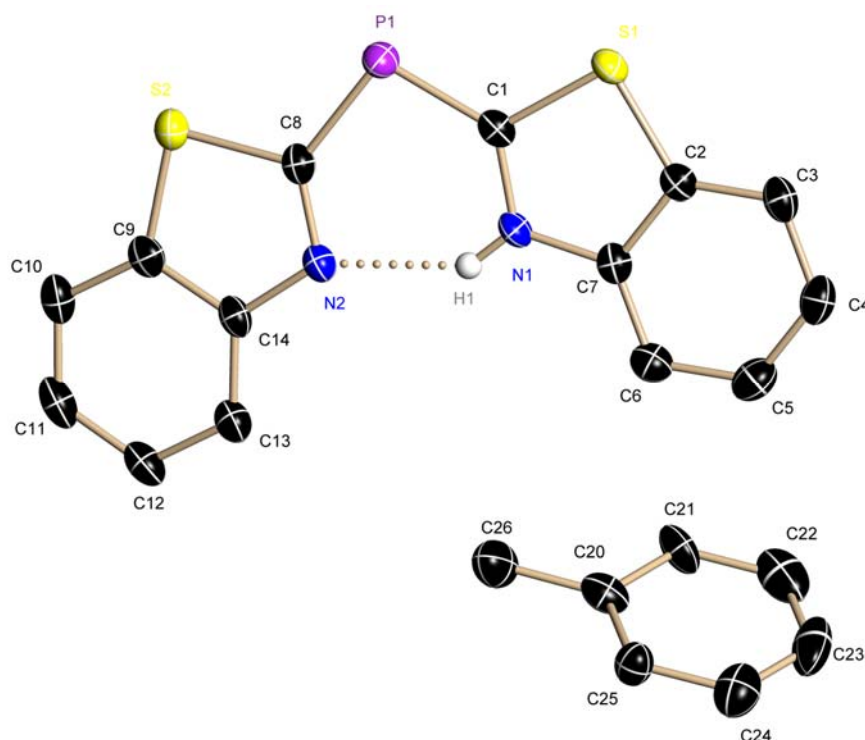# 1.8 Di(2-benzothiazolyl)phosphane with toluene

Figure 4: Asymmetric unit of di(2-benzothiazolyl)phosphane with co-crystallized toluene. Anisotropic displacement parameters are depicted at a probability level of 50%, hydrogen atoms are omitted for clarity.

Table 4: crystallographic data for di(2-benzothiazolyl)phosphane co-crystallized with toluene.

identification code	Pbth2@tol	temperature [K]	100(2)
empirical formula	$C_{17.5}H_{13}N_2PS_2$	max./min. transmission	0.6412 / 0.7454
molecular mass [g/mol]	346.39	ρ_{calc} [g/cm^3]	1.433
crystal size [mm]	0.2 x 0.2 x 0.15	µ [mm^{-1}]	0.429
crystal system	monoclinic	$F(000)$	716
space group	$P2_1/c$	Θ range [°]	2.44 – 26.46
a [Å]	6.1855(11)	reflections all / unique	18328 / 3428
b [Å]	15.540(3)	data / restraints / parameter	3292 / 2 / 228
c [Å]	16.872(3)	$R1$ (all data)	0.0356
α [°]	90.00	$wR2$ (all data)	0.0900
β [°]	97.990(2)	g1 / g2	0.0333 / 1.2359
γ [°]	90.00	GoF	1.141
V [Å^3]	1606.1(5)	peak / hole	
Z	4	max. /min. [10^{6}eÅ^{-3}]	0.384 / -0.215

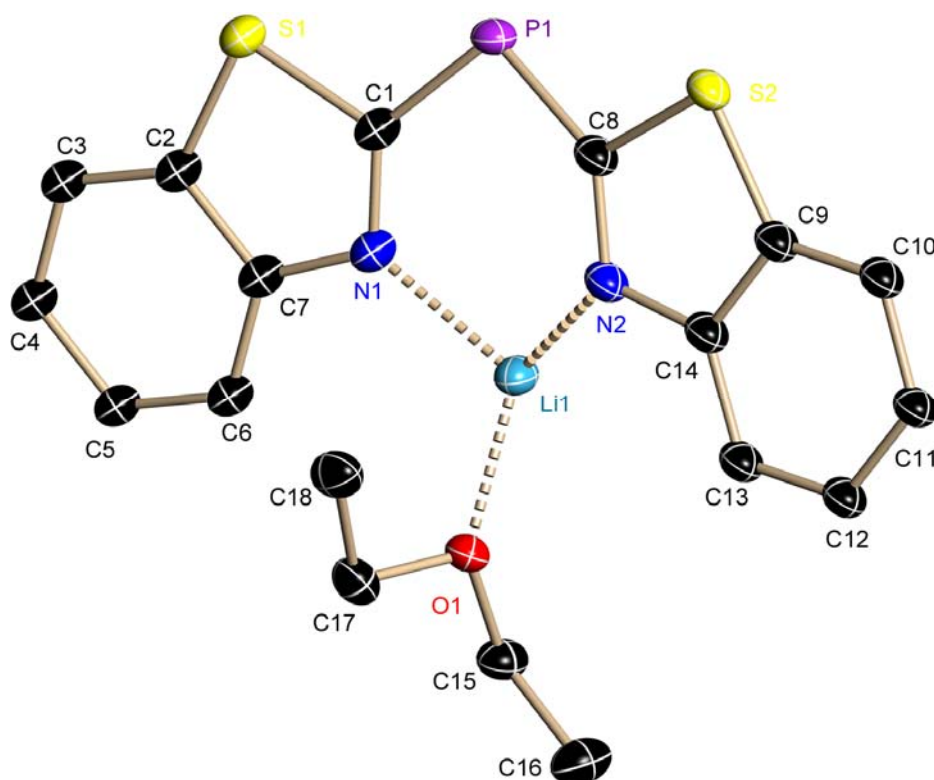## 1.9 Di(*2*-benzothiazolyl)phosphanid lithium

Figure 5: Asymmetric unit of di(*2*-benzothiazolyl)phosphanid lithium. Anisotropic displacement

parameters are depicted at a probability level of 50%, hydrogen atoms are omitted for clarity.

Table 5: crystallographic data for di(*2*-benzothiazolyl)phosphanid lithium.

identification code	(Pbth2Li*Et2O)2	temperature [K]	100(2)
empirical formula	$C_{36}H_{36}Li_2N_4O_2P_2S_4$	max./min. transmission	0.8126 / 0.9280
molecular mass [g/mol]	760.16	ρ_{calc} [g/cm^3]	1.375
crystal size [mm]	0.17 x 0.16 x 0.12	μ [mm^{-1}]	0.384
crystal system	monoclinic	F(000)	792
space group	$P2_1/n$	Θ range [°]	2.07 – 26.76
a [Å]	11.8606(8)	reflections all / unique	18365 / 4083
b [Å]	11.8643(8)	data / restraints / parameter	3879/ 54 / 190
c [Å]	13.4223(9)	R1 (all data)	0.0530
α [°]	90.00	wR2 (all data)	0.1156
β [°]	103.3020(10)	g1 / g2	0.0329 / 3.5907
γ [°]	90.00	GoF	1.075
V [Å^3]	1838.1(2)	peak / hole	
Z	4	max. /min. [10^{6}eÅ^{-3}]	0.81 / -0.65

1.10 Di(*2*-benzothiazolyl)phosphanid-bis(trimethylsilyl)amide-germanium(II)
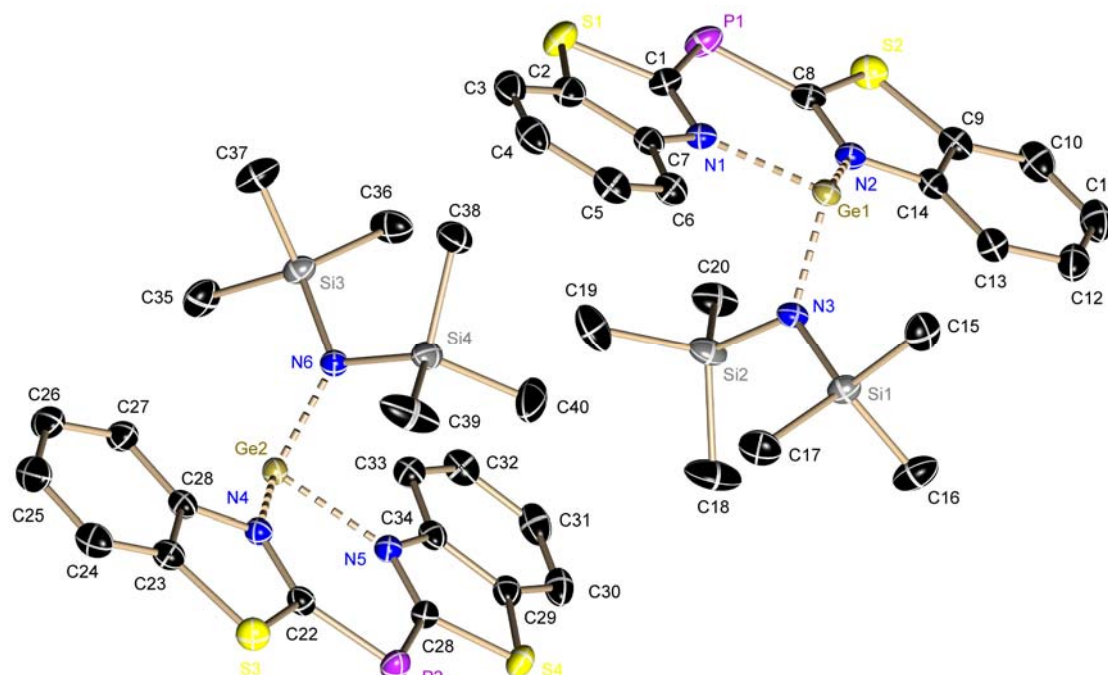

Figure 6: Asymmetric unit of di(*2*-benzothiazolyl)phosphanid-bis(trimethylsilyl)amide-germanium(II). Anisotropic displacement parameters are depicted at a probability level of 50%, hydrogen atoms are omitted for clarity.

Table 6: crystallographic data for di(*2*-benzothiazolyl)phosphanid-bis(trimethylsilyl)amide-germanium(II).

identification code	Pbth2Ge	temperature [K]	100(2)
empirical formula	$C_{20}H_{26}GeN_3PS_2Si_2$	max./min. transmission	0.6945 / 0.7455
molecular mass [g/mol]	532.36	ρ_{calc} [g/cm^3]	1.450
crystal size [mm]	0.3 x 0.3 x 0.2	μ [mm^{-1}]	1.604
crystal system	triclinic	$F(000)$	1096
space group	$P\bar{1}$	Θ range [°]	1.34 – 27.23
a [Å]	11.3756(8)	reflections all / unique	109640 / 10873
b [Å]	14.2567(10)	data / restraints / parameter	10873 / 0 / 535
c [Å]	16.1005(11)	R1 (all data)	0.0241
α [°]	108.5920(10)	wR2 (all data)	0.0556
β [°]	90.8910(10)	g1 / g2	0.0333 / 1.2359
γ [°]	98.9720(10)	GoF	1.050
V [Å^3]	1606.1(5)	peak / hole	
Z	4	max. /min. [10^6eÅ^{-3}]	0.39 / -0.30

1.11 Di(*2*-benzothiazolyl)phosphanid-bis(trimethylsilyl)amide-lead(II)oxid
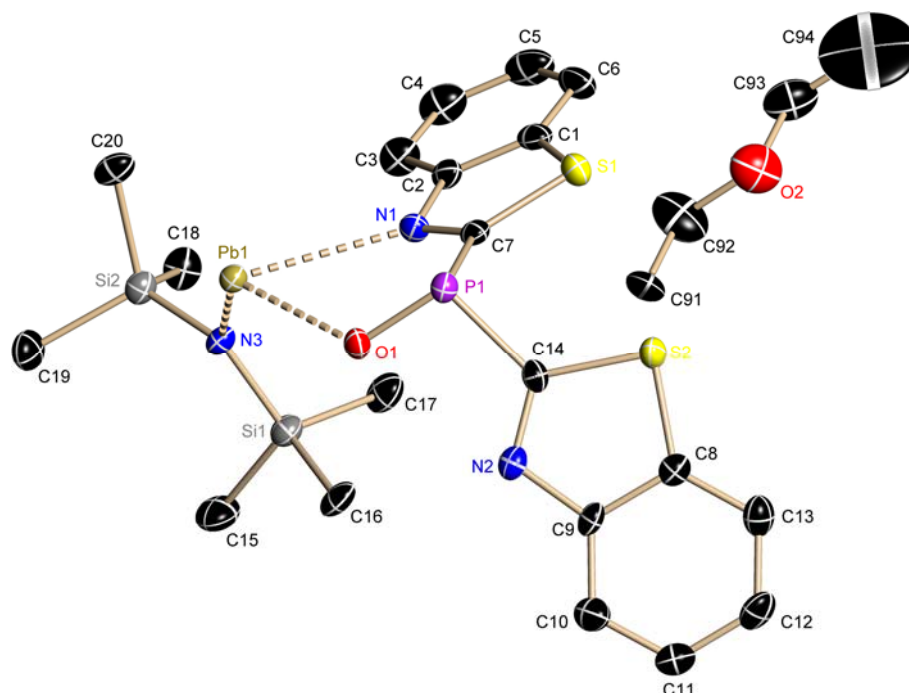

Figure 7: Asymmetric unit of di(*2*-benzothiazolyl)phosphanid-bis(trimethylsilyl)amide-lead(II)oxid. Anisotropic displacement parameters are depicted at a probability level of 50%, hydrogen atoms are omitted for clarity.

Table 7: crystallographic data for di(2-benzothiazolyl)phosphanid-bis(trimethylsilyl)amide-lead(II)oxid.

identification code	Pbth2Pb	temperature [K]	100(2)
empirical formula	$C_{22}H_{31}N_3O_{1.5}PPbS_2Si_2$	max./min. transmission	0.3338 / 0.4302
molecular mass [g/mol]	719.96	ρ_{calc} [g/cm^3]	1.744
crystal size [mm]	0.05 x 0.2 x 0.02	μ [mm^{-1}]	6.472
crystal system	Monoclinic	$F(000)$	1412
space group	$P2_1/c$	Θ range [°]	1.75 – 27.15
a [Å]	12.4754(17)	reflections all / unique	25745 / 6308
b [Å]	15.367(2)	data / restraints / parameter	6067 / 6 / 309
c [Å]	15.296(2)	R1 (all data)	0.0579
α [°]	90.00	wR2 (all data)	0.0663
β [°]	110.727(2)	g1 / g2	0.0299 / 0.000
γ [°]	90.00	GoF	0.999
V [Å^3]	2742.5(6)	peak / hole	
Z	4	max. /min. [10^{6}eÅ^{-3}]	1.362 / -1.288

1.12 [*P*-{di(*2*-benzothiazolyl)phosphanide} (cyclopentadienyl) (carbonyl)iron] dimer
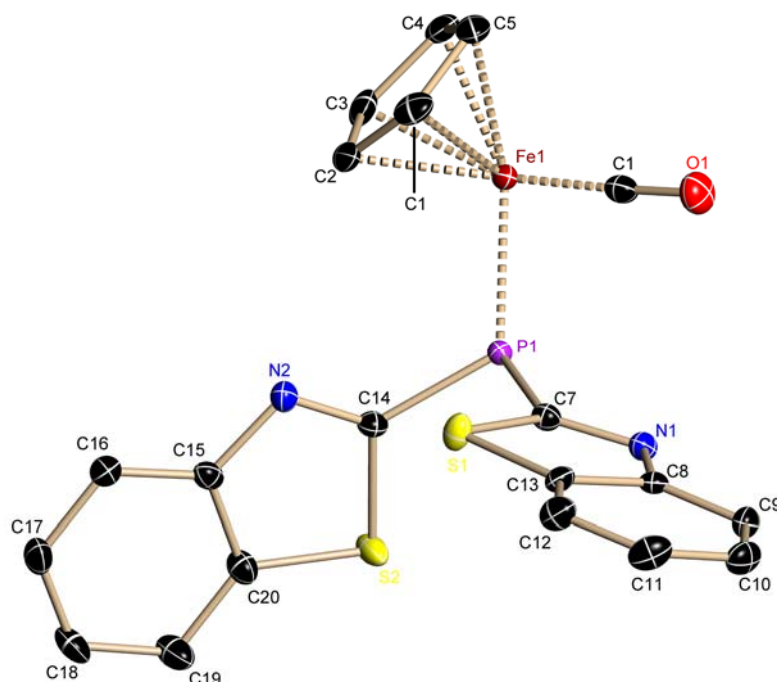

Figure 8: Asymmetric unit of [*P*-{di(*2*-benzothiazolyl)phosphanide}(cyclopentadienyl)

(carbonyl)iron] dimer. Anisotropic displacement parameters are depicted at a probability

level of 50%, hydrogen atoms are omitted for clarity.

Table 8: crystallographic data for [*P*-{di(*2*-benzothiazolyl)phosphanide}(cyclopentadienyl)

(carbonyl)iron] dimer.

identification code	[P(bth)2(FeCpCO)]2	temperature [K]	113(2)
empirical formula	$C_{20}H_{13}FeN_2OPS_2$	max./min. transmission	0.9477 / 1.000
molecular mass [g/mol]	448.26	ρ_{calc} [g/cm^3]	1.671
crystal size [mm]	0.1 x 0.08 x 0.004	µ [mm^{-1}]	1.184
crystal system	Triclinic	$F(000)$	456
space group	$P\bar{1}$	Θ range [°]	2.33 – 27.16
a [Å]	9.3115(4)	reflections all / unique	19536 / 3959
b [Å]	9.8585(4)	data / restraints / parameter	3959 / 0 / 244
c [Å]	11.8692(5)	$R1$ (all data)	0.0372
α [°]	114.3770(10)	$wR2$ (all data)	0.0807
β [°]	95.5980(10)	g1 / g2	0.0339 / 1.2725
γ [°]	110.5600(10)	GoF	1.057
V [Å^3]	890.86(6)	peak / hole	
Z	2	max. /min. [10^{6}eÅ^{-3}]	0.532 / -0.300

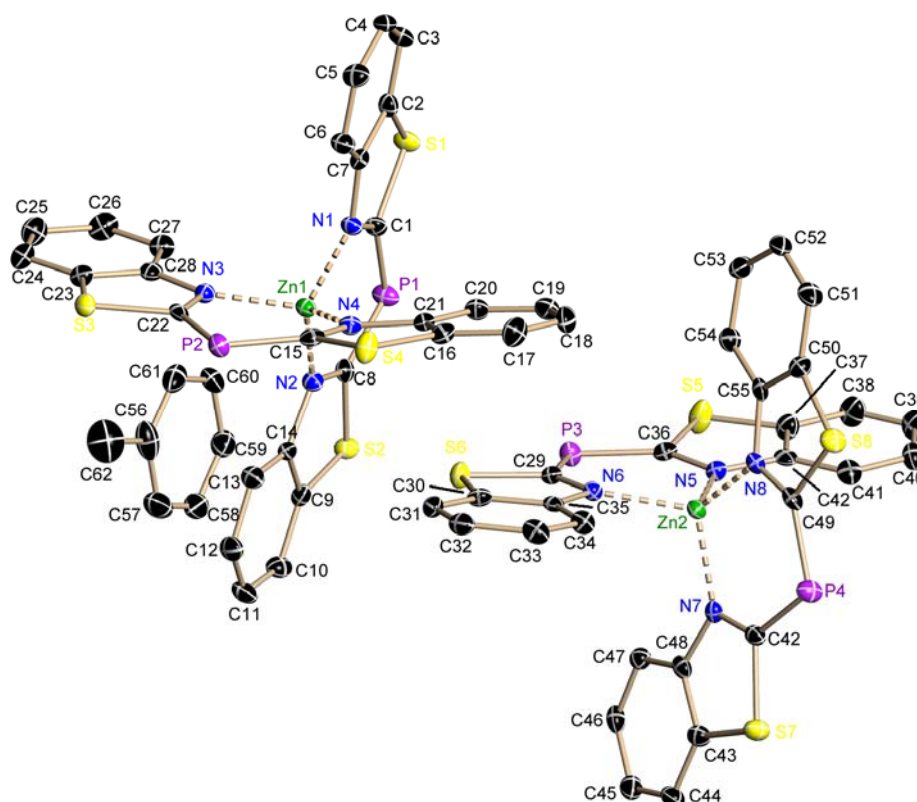## 1.13 Bis[di(*2*-benzothiazolyl)phosphanyl]zinc

Figure 9: Asymmetric unit of bis[di(*2*-benzothiazolyl)phosphanyl]zinc. Anisotropic displacement parameters are depicted at a probability level of 50%, hydrogen atoms are omitted for clarity.

Table 9: crystallographic data for bis[di(*2*-benzothiazolyl)phosphanyl]zinc.

identification code	[P(bth)2]2Zn	temperature [K]	107(2)
empirical formula	$C_{126}H_{80}N_{16}P_8S_{16}Zn_4$	max./min. transmission	0.6587 / 0.7454
molecular mass [g/mol]	2840.26	ρ_{calc} [g/cm^3]	1.538
crystal size [mm]	0.10 x 0.05 x 0.05	μ [mm^{-1}]	1.208
crystal system	triclinic	$F(000)$	1444
space group	$P\bar{1}$	Θ range [°]	1.14 – 26.46
a [Å]	10.710(2)	reflections all / unique	63224 / 12630
b [Å]	16.095(3)	data / restraints / parameter	12630 / 0 / 767
c [Å]	18.274(4)	R1 (all data)	0.0969
α [°]	80.27(3)	wR2 (all data)	0.1000
β [°]	81.19(3)	g1 / g2	0.0341 / 1.5510
γ [°]	89.72(3)	GoF	1.028
V [Å^3]	3067.2(11)	peak / hole	
Z	2	max. /min. [10^{6}eÅ^{-3}]	0.661 / -0.616

1.14 [{(MeCp)(OC)$_2$Mn}{P(bth)$_2$Zn(bth)$_2$P}{Mn(CpMe)(CO)$_2$}]$_2$
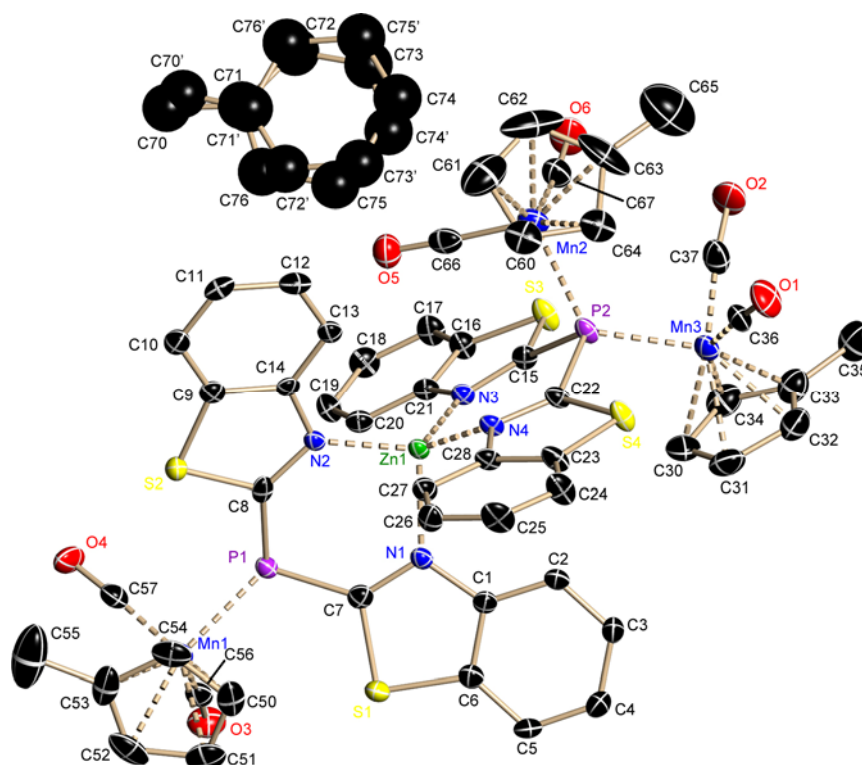
Figure 10: Asymmetric unit of [{(MeCp)(OC)$_2$Mn}{P(bth)$_2$Zn(bth)$_2$P}{Mn(CpMe)(CO)$_2$}]$_2$. Anisotropic
displacement parameters are depicted at a probability level of 50%, hydrogen atoms
are omitted for clarity. Co-crystallized toluene refined only isotropic.

Table 10: crystallographic data [{(MeCp)(OC)$_2$Mn}{P(bth)$_2$Zn(bth)$_2$P}{Mn(CpMe)(CO)$_2$}]$_2$.

|			
identification code	LMnZn	temperature [K]	100(2)
empirical formula	C$_{55.5}$H$_{41}$Mn$_3$N$_4$O$_6$P$_2$S$_4$Zn	max./min. transmission	0.9024 / 1.0000
molecular mass [g/mol]	1280.29	ρ_{calc} [g/cm^3]	1.610
crystal size [mm]	0.15 x 0.10 x 0.02	μ [mm^{-1}]	1.610
crystal system	triclinic	F(000)	1298
space group	$P\bar{1}$	Θ range [°]	2.22 – 24.99
a [Å]	12.713(2)	reflections all / unique	72603 / 9741
b [Å]	13.253(2)	data / restraints / parameter	9741 / 23 / 670
c [Å]	17.834(3)	R1 (all data)	0.0767
α [°]	108.450(5)	wR2 (all data)	0.1208
β [°]	110.826(5)	g1 / g2	0.0498 / 6.3069
γ [°]	90.253(5)	GoF	1.053
V [Å^3]	2640.9(8)	peak / hole	
Z	2	max. /min. [10^{6}eÅ^{-3}]	1.334 / -0.792

1.15 [{(OC)$_2$NiP(bth)$_2$ZnMe)(P(bth)$_2$ZnOEt)}$_2$]
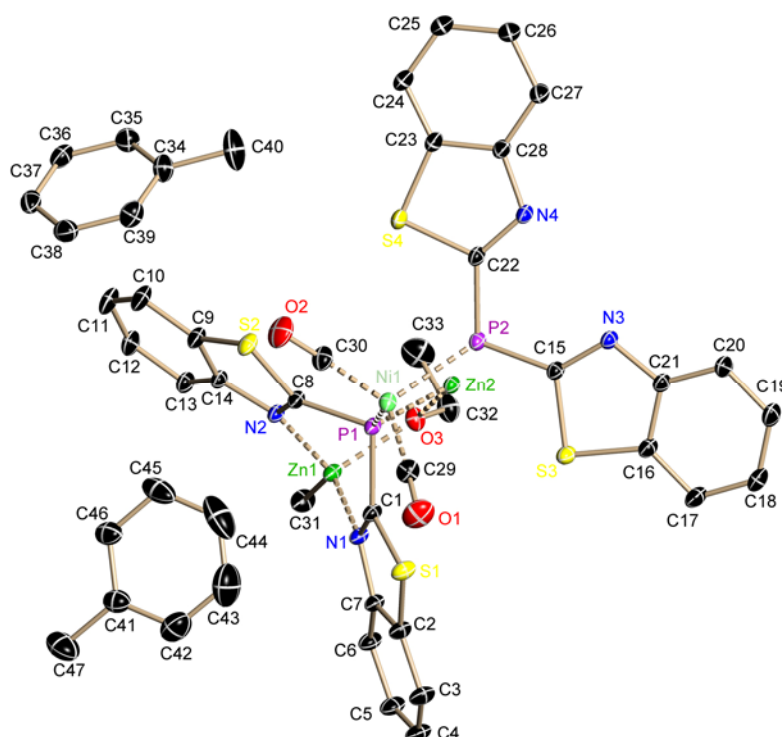
Figure 11: Asymmetric unit of [{(OC)$_2$NiP(bth)$_2$ZnMe)(P(bth)$_2$ZnOEt)}$_2$]. Anisotropic displacement parameters are depicted at a probability level of 50%, hydrogen atoms are omitted for clarity.

Table 11: crystallographic data for [{(OC)$_2$NiP(bth)$_2$ZnMe)(P(bth)$_2$ZnOEt)}$_2$].

identification code	LNiZn	temperature [K]	100(2)
empirical formula	C$_{47}$H$_{40}$N$_4$NiO$_3$P$_2$S$_4$Zn$_2$	max./min. transmission	0.6690 / 0.7730
molecular mass [g/mol]	1088.46	ρ_{calc} [g/cm^3]	1.559
crystal size [mm]	0.3 x 0.20 x 0.20	μ [mm^{-1}]	1.723
crystal system	monoclinic	F(000)	2224
space group	P2$_1$/c	Θ range [°]	1.30 – 54.31
a [Å]	17.841(3)	reflections all / unique	825073 / 58869
b [Å]	16.023(3)	data / restraints / parameter	57705 / 0 / 688
c [Å]	18.463(3)	R1 (all data)	0.0484
α [°]	90	wR2 (all data)	0.1030
β [°]	118.494(2)	g1 / g2	0.0498 / 6.3069
γ [°]	90	GoF	1.081
V [Å^3]	4638.8(14)	peak / hole	
Z	4	max. /min. [10^{6}eÅ^{-3}]	3.092 / -0.802

2 Literature

[1]   T. Kottke, D. Stalke, *J. Appl. Crystallogr.* **1993**, *26,* 615-619.

[2]   D. Stalke, *Chem. Soc. Rev.* **1998**, *27*, 171-178.

[3]   H. Hope, *Acta Crystallogr.* **1988**, *B44*, 22-26.

[4]   T. Schulz, K. Meindl, D. Leusser, D. Stern, J. Graf, C. Michaelsen, M. Ruf, G. M. Sheldrick, D. Stalke, *J. Appl. Crystallogr.* **2009**, *42*, 885-891.

[5]   Bruker APEX v2.2-0, Bruker AXS Inst. Inc., Madison (WI, USA), **2007**.

[6]   Bruker, SAINT v7.34A. , Bruker AXS Inc., Madison (WI, USA), **2005**.

[7]   W. Kabsch, *J. Appl. Crystallogr.* **1988**, *21*, 916-924.

[8]   G. M. Sheldrick, SADABS 2007/5, Göttingen, **2007**.

[9]   G. M. Sheldrick, TWINABS v1.05 in Bruker APEX v2.1-0, Bruker AXS Inst. Inc., Madison (WI, USA), **2005**.

[10]   G. M. Sheldrick, XPREP in SHELXTL v6.12, Bruker AXS Inst. Inc., Madison (WI, USA), **2000**.

[11]   G. M. Sheldrick, *Acta Crystallogr., Sect. A.* **2008**, *64*, 112-122.

[12]   P. Müller, R. Herbst-Irmer, A. L. Spek, T. R. Schneider, M. R. Sawaya, *Crystal Structure Refinement - A Crystallographer's Guide to SHELXL* in *IUCr Texts on Crystallography, Vol. 8* (Ed. P. Müller), Oxford University Press, Oxford (England), **2006**.

1 Conclusion

1.1 Metal complexes based on di(*2*-pyridyl)amine

In the first part of this thesis different metal complexes based on di(*2*-pyridyl)amine are reported. On the one hand, metal complexes of germanium, tin and lead were prepared by classical transmetalation methods.

On the other hand, another tin complex by direct metalation with of the ligand with bis(hexamethyldisilazane)tin as well as a zinc complex by direct metalation of the ligand with dimethyl zinc was achieved.

The group 14 complexes show different coordination modes. Figure 1 shows the different conformations reported in this thesis.
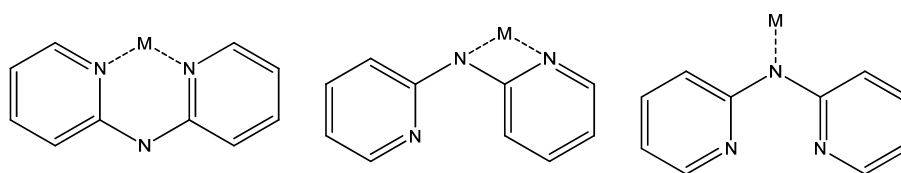

Figure 1: coordination motifs reported in this thesis.

Divalent group 14 metal atoms are coordinated by two di(*2*-pyridyl)amide ligands. The comparably small germanium atom shows two different motifs, a coordination by two pyridyl nitrogen atoms, and additionally by the bridging nitrogen atom of a amide second ligand. Furthermore, a second symmetric coordination is shown in the NMR spectra. The solid state structure of the bis[di(*2*-pyridyl)amide]tin shows two different coordination modes as well. One ligand coordinates the metal atom by the bridging nitrogen atom and by one pyridyl nitrogen atom, while the other ligand coordinates only via its bridging nitrogen atom. The dimeric metal complex originated from the direct metalation also shows a comparable coordination motif. Due to the NMR studies on the lead complex a similar structure as the tin complex from the transmetalation is presumed.

The structure of the zinc complex also shows a coordination of the metal atom by the pyridyl nitrogen atoms. The complex exhibts as linked as head to tail trimers in a ring. The change of the coordination motifs can very well be explained by the increasing radii of the metal atoms and the accompanied decrease of the hardness. While the comparable small zinc and germanium atoms still fit in the bit of the pyridyl rings the larger atoms descending group 14 are too large. Thus coordination via the bridging nitrogen atom becomes more and more favorable and the charge localization moves from the pyridyl rings to the bridge.

Due to the good accessibility and the high purity, these complexes will provide a good basis as organometallic precursors as well as fine tuning agents in metalation chemistry.

1.2 Di(*2*-benzothiazolyl)phosphane

Within this work it was possible to reproduce the di(*2*-benzothiazolyl)phosphane according to the recipe reported by *Stey* and upscale the reaction up to 80 mmol pure product.

Furthermore, first approaches to a modification were undertaken. The applied concept can easily be transferred to many other substituents and is therefore very versatile. The herein applied isopropyl substituent leaves still problems in the carbon–phosphorous coupling. These problems will be avoided using different substituents with less acidic protons.

In addition, it was possible to re-determine the structure of di(*2*-benzoiazolyl)-phosphane crystallized from toluene. This structure shows the stability of the ligand in multiple solvents. Other then assumed before, reactions not only in diethyl ether are feasible. This was directly underlined by a new structure of [di(*2*-benzothiazolyl)-phosphanyl] lithium. It shows the high donor activity of the ligand also towards hard metals, if no other donor is available. This fact underlines the versatile and flexible character of di(*2*-benzothiazolyl)phosphane.

1.3 Metal complexes based on di(*2*-benzothiazolyl)-phosphane

In this field of research different approaches were examined. First an earlier reported metal complex of tin structure was re-determined and all analytic data collected. Thus, di(*2*-benzothiazolyl)phosphane was reacted with $[Sn\{N(SiMe_3)_2\}_2]$ in a direct metalation. Other than anticipated earlier the compound is stable in solution and storable using *Schlenk*techniques. To learn more about group 14 complexes of di(*2*-benzothiazolyl)phosphane the analog reaction of di(*2*-benzothiazolyl)phosphane with germanium- and $[Pb\{N(SiMe_3)_2\}_2]$ was performed, respectively. In the case of germanium amide, a very similar metal complex as in the case of the tin complex was found. Both show a exchange of one amid residue to our ligand in an *N,N*-coordination. It was neither possible to exchange both amide residues to our ligand nor to substitute the residual amide group by another residue.

In the case of the lead amide a different result occurred. In every case an oxygen atom bonds to the phosphorous atom. Other than the first assumption it is no originated by accidental oxygen inlet to the reaction. This was excluded by many reruns of the reaction. As this reaction was always run in diethyl ether an ether cleavage reaction in presumed. This is fortified by the later findings on a heterobimetallic complex containing nickel and zinc, as well as in the recent literature.
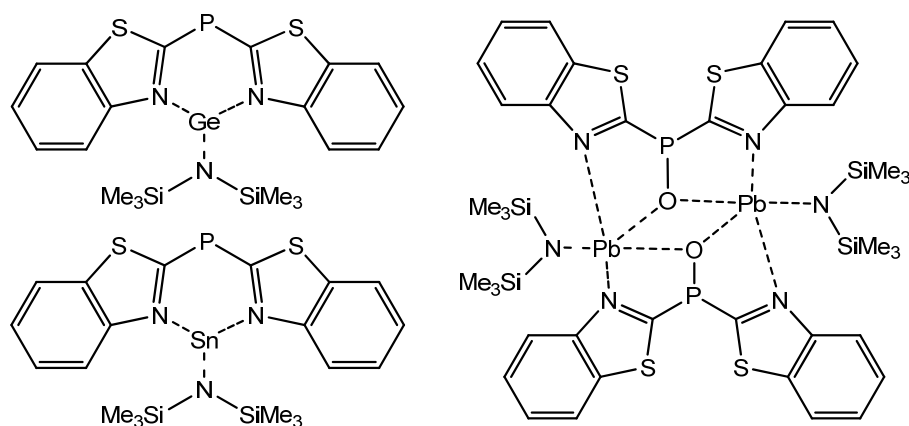

Figure 2: group 14 complexes of di(*2*-benzothiazolyl)phosphane.

Furthermore, a better storable form of the ligand was casted. Heading towards (hetero-)bimetallic complexes this form is ideally already a metal complex. A possibility is the earlier reported lithium complex, but this has neither a good yield nor is easy to purify. Also the group 14 metal complexes are well available in good yields and moderate to purify, they are not useful as it is not possible to remove the amide residue.

A good alternative is a zincation of the di(*2*-benzothiazolyl)phosphane. Using dimethyl zinc instead of [Zn{N(SiMe$_3$)$_2$}$_2$]different stable and storable products are obtainable, depending on the applied reaction conditions. Thus, a double ligand coordinated zinc atom or a zinc methyl with one ligand are available. This new zinc species allow classical transmetalation reactions as well as the introduction of a second metal.
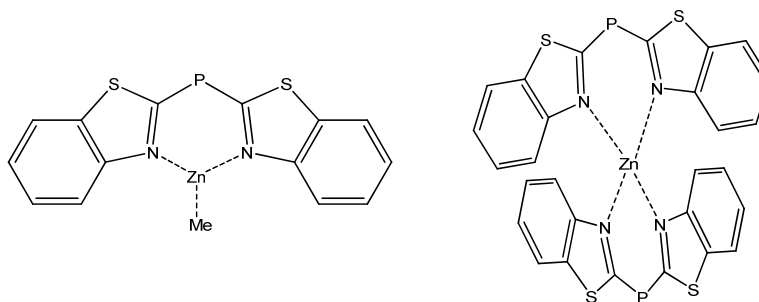
Figure 3: zincated di(*2*-benzothiazolyl)phosphanes.

To underline the use of the new zinc complexes, a classical transmetalation was performed yielding a phosphorous-only coordinated complex of the di(*2*-benzothiazolyl)phosphanid for the first time. The resulting iron complex shows a central $(P–Fe)_2$ four membered ring and therefore underlines the phosphanidic character of the ligand. In combination with an earlier reported iron complex it is additionally a good example for the versatility of the ligand. Obviously, the ligand can stabilize the same metal in the same oxidation state differently: as a 14 valence electrons complex by a *N,N*-coordination reported earlier by *Stey* and by a coordination with its phosphorous atom only in an 18 valence electrons complex. Both complexes give insights to the huge number of possibilities mixing metals, linked by the di(*2*-benzothiazolyl)phosphane.
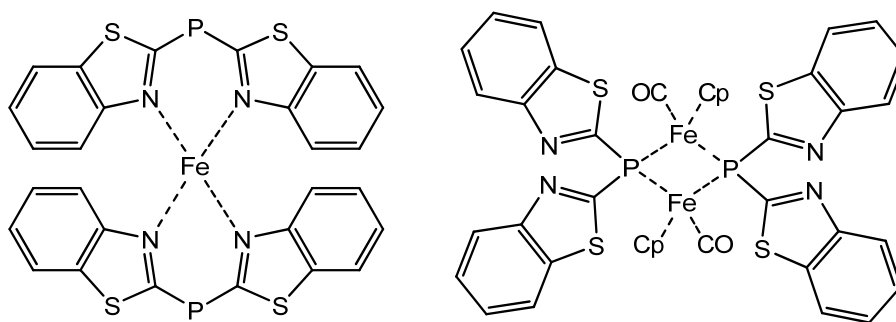

Figure 4: iron complexes of di(*2*-benzothiazolyl)phosphane.

As mentioned earlier heterobimetallic complexes are a major goal in catalysis research. To prove this ability for both zincated the di(*2*-benzothiazolyl)phosphane forms these were reacted with metal carbonyls.

Bis[di(*2*-benzothiazolyl)phosphanyl]zinc reacts with $(MeCp)Mn(CO)_2(MeCN)$ to form an asymmetric heterobimetallic complex. The complex shows the intact $[Zn\{(bth)_2P\}_2]$ subunit in the middle while the manganese units are coordinated to the phosphorous atoms.

In addition, the [di(2-benzothiazolyl)phosphanyl](methyl)zinc was reacted with tetracarbonyl nickel.
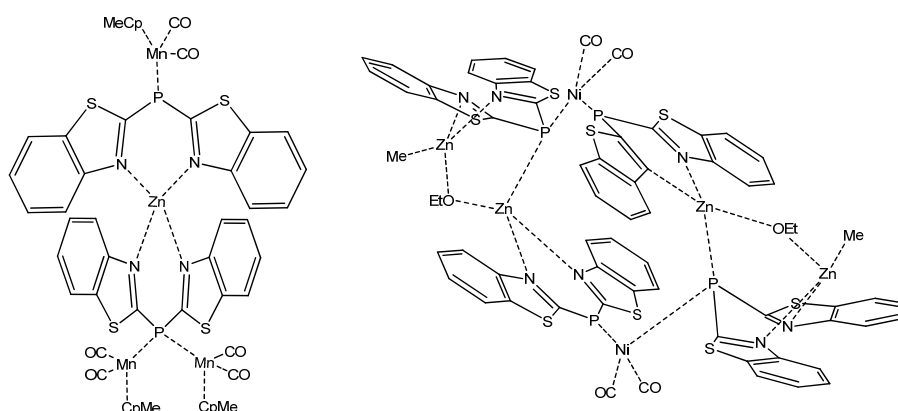

Figure 5: heterobimetallic complexes of di(2-benzothiazolyl)phosphane.

This heterobimetallic complex containing nickel and zinc is very promising since both metals on its own already find use in catalysis. The higher reactivity due to a cooperative effect shows the ether cleavage reaction. The additional characterized complexes from pure ligand and tetracarbonyl nickel as well as the complexes with zinc do not show any reactions like that.
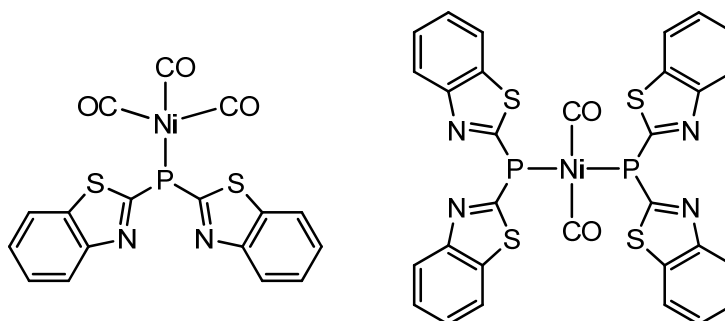

Figure 6: complexes of di(2-benzothiazolyl)phosphane and tetracarbonyl nickel

Unfortunately the latter were not characterized by single crystal X-ray structural analysis as all complexes above. Still the NMR and mass analytics underline the products.

Over all, many new and different metal complexes on the basis of di(2-benzothiazolyl)phosphane are reported. These give new insights into the chemistry of this promising ligand and indicate its versatility.

2 Outlook

Encourage by the better stability of the zincated di(*2*-benzothiazolyl)phosphane and the shown ability thereof to form heterobimetallic complexes a good access to catalysis is founded.

The newly shown heterobimetallic complexes are a good basis for further research on catalytic activities of these systems. Thus, a test in respect to their best field of application should be investigated.

The shown manipulations on the ligand itself provide a fundamentals to further functionalizing and utilization of the ligand.

Additionally, high resolution data X-ray and a subsequent multipole refinement should give even more insights into the electronic situation of the ligands complexes.

The heterobimetallic complex containing nickel and zinc already showed the necessary diffraction ability even if its crystal quality was regrettably no yet good enough to suffice the demands of experimental charge density studies.